Role of Pancreatic Delta Cells and Somatostatin in Glucose Homeostasis

By

JESSICA L HUANG

DISSERTATION

Submitted in partial satisfaction of the requirements for the degree of

DOCTOR OF PHILOSOPHY

in

Biochemistry, Molecular, Cellular, and Developmental Biology

in the

OFFICE OF GRADUATE STUDIES

of the

UNIVERSITY OF CALIFORNIA

DAVIS

Approved:

Dr. Mark Huising, Chair

Dr. John Albeck

Dr. Karen Ryan

Dr. Manuel Navedo

Committee in Charge

2022

Contents

List of Figures vii

List of Tables ix

Abstract x

Acknowledgements xi

1 Introduction 1

1.1 Preface 1

1.1.1 Authorship 1

1.2 Abstract 1

1.3 Pancreatic islets and blood glucose homeostasis 2

1.3.1 Beta cell function and maturity 3

1.3.2 Systemic and paracrine contribution of alpha cells 4

1.3.3 Discovery of delta cells and somatostatin 5

1.4 Delta cell response to paracrine, endocrine, and neural inputs 6

1.4.1 Insulin 7

1.4.2 Glucagon 7

1.4.3 Urocortin 3 7

1.4.4 Ghrelin 8

1.4.5 ATP 9

1.4.6 Acetylcholine 9

1.4.7 Epinephrine 10

1.4.8 Dopamine 10

1.5 Delta cell regulation of beta and alpha cells 11

1.5.1 Feedback modulation by delta cells on beta cells 11

1.5.2 Effects of delta cells on glucagon 12

1.6 Contribution of other SST-expressing cells to glucose homeostasis 14

1.6.1 Somatostatin-expressing cells in the CNS 14

1.6.2 Somatostatin-expressing in the gastrointestinal system 15

1.7 Conclusion 17

1.8 References 19

2 Genetic deletion of Urocortin 3 does not prevent functional maturation of beta cells 30
2.1 Preface 30
2.2 Abstract 30
2.3 Introduction 31
2.4 Results 33
2.4.1 Expression of beta cell maturity genes persists in *Ucn3*-null mice 33
2.4.2 Beta cell dedifferentiation is not increased in *Ucn3*-null mice 38
2.4.3 Virgin beta cells remain identifiable in *Ucn3*-null mice 39
2.4.4 Beta cells in *Ucn3*-null mice exhibit normal calcium response to glucose 41
2.5 Discussion 44
2.6 Funding & Acknowledgements 47
2.7 Materials and Methods 47
2.7.1 Animals 47
2.7.2 Glucose Tolerance Test 48
2.7.3 Immunofluorescence 48
2.7.4 Islet isolation 49
2.7.5 Next generation sequencing and bioinformatics 49
2.7.6 Western blotting 50
2.7.7 Functional imaging 50
2.7.8 Antibodies 50
2.7.9 Statistical Analysis 51
2.8 Supplemental Materials 52
2.9 References 58
3 Effect of somatostatin on beta and alpha cell gene expression 63
3.1 Preface 63
3.2 Abstract 63
3.3 Introduction 64
3.4 Results 66
3.4.1 FACS-purification of beta and alpha cells 66
3.4.2 Effect of SST and SSTR antagonists on beta cell gene expression 68
3.4.3 Effect of SST and SSTR antagonists on alpha cell gene expression 70
3.5 Discussion 72
3.6 Funding & Acknowledgements 73

3.7 Materials and Methods 74
3.7.1 Animals 74
3.7.2 Islet isolation and FACS sorting 74
3.7.4 RNA isolation and library prep 75
3.7.5 Next generation sequencing and bioinformatics 75
3.7.6 Statistical analysis 76
3.8 Supplemental Information 76
3.9 References 84
4 Paracrine signaling by pancreatic delta cells determines the glycemic set point 88
4.1 Preface 88
4.1.1 Authorship 88
4.4 Results 92
4.4.1 Absence of somatostatin lowers the glycemic set point 92
4.4.2 Delta cell ablation lowers the glycemic set point 95
4.4.3 Delta cell ablation increases glucose tolerance and glucose-stimulated insulin secretion 99
4.4.4 Alpha cell ablation does not affect basal glycemia 102
4.4.5 Delta cell ablation decreases the glucose threshold for beta cell response 105
4.5 Discussion 109
4.6 Funding and Acknowledgements 113
4.7 Materials and Methods 113
4.7.1 Animals 113
4.7.2 DT, tamoxifen, and STZ treatments 114
4.7.3 Glucose tolerance test and plasma insulin collection 115
4.7.4 Islet isolation 115
4.7.5 Static insulin secretion assays 116
4.7.6 Calcium imaging and dynamic insulin secretion assays 116
4.7.7 Hormone measurements 116
4.7.8 Immunofluorescence and cell counting 116
4.7.9 RNA Extraction and qPCR 117
4.7.10 Continuous Glucose Monitoring 117
4.7.11 Statistical Analysis 118
4.8 Supplemental Information 119

4.9 References 122
5 The Difference Delta Cells Make in Glucose Control 130
5.1 Preface 130
5.2 Abstract 130
5.3 Introduction 130
5.4 The pancreatic islet is home to more than beta cells 131
5.5 Discovery of delta cells 133
5.6 Paracrine crosstalk within pancreatic islets 134
5.7 The delta cell provides paracrine feedback within the islet 135
5.8 Urocortin3 is required for normal glucose-stimulated somatostatin secretion 136
5.9 Bidirectional exchange of paracrine signals within the islet 137
5.10 The beta cell as a blueprint for the delta cell 139
5.11 The delta cell as a modulating hub that shapes islet cell activity 140
5.12 Local feedback inhibition by delta cells determines the set point for plasma glucose 141
5.13 The benefit of feedback inhibition by delta cells 143
5.14 Loss of UCN3 from beta cells early in diabetes increases glycemic volatility 145
5.15 Summary and Conclusions 147
5.16 Acknowledgements 148
5.17 References 149
6 Transcriptomic comparison of beta and alpha cells in lean and *ob/ob* mice 159
6.1 Preface 159
6.1.1 Authorship 159
6.2 Abstract 159
6.3 Introduction 160
6.4 Results 162
6.4.1 Phenotypic comparison between lean and *ob/ob* mice 162
6.4.2 Transcriptomic comparison between beta cells from lean and *ob/ob* mice 165
6.4.3 Transcriptomic comparison between alpha cells from lean and *ob/ob* mice 168
6.5 Discussion 169
6.6 Funding and Acknowledgements 171
6.7 Materials and Methods 171
6.7.1 Animals 171
6.7.2 Islet Isolation and FACS Sorting 172

6.7.3 Nucleic Acid Isolation and Library Prep 172
6.7.4 Statistical analysis and bioinformatics 173
6.8 Supplemental Information 173
6.9 References 175
7 Conclusions and Future Work 180
7.1 Abstract 180
7.2 Summary of Work 180
7.3 Future Directions 184
7.3.1 Regulation of actin dynamics in beta and alpha cells by SST 184
7.3.2 Alpha cell contribution to beta cell activity in the absence of delta cells 185
7.3.3 Effect of delta cell ablation during diabetes 185
7.3.4 Contribution of delta cells to the glycemic set point in humans 186
7.4. Conclusions 187
7.5 References 188

List of Figures

1.1 Paracrine and systemic actions of the pancreatic islet

1.2 Pancreatic islet hormone secretion in non-diabetic vs. diabetic circumstances.

2.1 Genes encoding beta cell maturity markers are not differentially regulated between *Ucn3*-null mice and wild-type littermates

2.2 UCN3 expression is not necessary for beta cells to express maturity markers

2.3 The absence of UCN3 expression does not lead to beta cell dedifferentiation

2.4 Virgin beta cells are maintained at the islet periphery in the absence of UCN3

2.5 Beta cell calcium response remains unaltered in mice that do not express UCN3

2.6 S1, related to Figure 2.1

2.7 S2, related to Figure 2.2

2.8 S3, related to Figure 2.4

2.9 S4, related to Figure 2.5

3.1 Schematic of islet incubation and cell sorting strategy

3.2 Changes in beta cell gene expression in response to SST and SSTR antagonists

3.3 Changes in alpha cell gene expression in response to SST and SSTR antagonists

4.1 Homozygous *Sst*-Cre mice exhibit loss of *Sst* and a decreased glycemic set point

4.2 Delta cell ablation leads to a lasting decrease in the glycemic set point

4.3 Delta cell ablation increases glucose tolerance and insulin secretion

4.4 Alpha cell ablation does not affect basal glycemia

4.5 Beta cells exhibit calcium response at a lower glucose threshold in the absence of delta cells

4.6 Simultaneous collection of calcium dynamics in islets and insulin secretion

4.7 S1, related to Figure 4.2: Effect of DT-mediated ablation on other SST-expressing tissue

4.8 S2, related to Figure 4.2: Effect of delta cell ablation on body weight and food intake

4.9 S3, related to Figure 4.4: Glucagon secretion increases in the absence of delta cells

5.1 Paracrine interactions in the islet

5.2 Differential delta cell morphology between human and mouse

5.3 Glucose set point in newborn and adult mice

5.4 SST feedback in healthy and pre-diabetic conditions

6.1 Phenotypic comparison of lean and *ob/ob* mice

6.2 Transcriptomic comparison of lean and *ob/ob* beta cells

6.3 Transcriptomic comparison of lean and *ob/ob* alpha cells

6.4 S1, related to Figure 6.1

6.5 S2, related to Figure 6.2

List of Tables

2.1 Significantly enriched genes in wild-type (22 genes) and *Ucn3*-null (7 genes) mouse islets.

3.1 Top 40 differentially expressed genes in SST-treated beta cells

3.2 Top 40 differentially expressed genes in SSTR Antagonist-treated beta cells

3.3 Overlap of genes between SST-treated and SSTR Antagonist treated beta cells

3.4 Differentially expressed genes in SST + SSTR Antagonist-treated beta cells

3.5 Differentially expressed genes in SST-treated alpha cells

3.6 Top 40 differentially expressed genes in SSTR Antagonist-treated alpha cells

3.7 Differentially expressed genes in SST + SSTR Antagonist-treated alpha cells

Abstract

Blood glucose homeostasis is the maintenance of blood glucose levels within a narrow range. The tight regulation of blood glucose levels is critical, as hypoglycemia can be acutely fatal and hyperglycemia leads to diabetes and its associated complications. Pancreatic islets play an essential role in maintaining normoglycemia. They are composed of insulin-secreting beta cells, glucagon-secreting alpha cells, and somatostatin-secreting delta cells, which coordinate to regulate blood glucose levels through paracrine interactions. Breakdown of these interactions contributes to the development of diabetes.

This dissertation focuses on how beta, alpha, and delta cells are affected by changes in paracrine interactions and disease, with a focus on how delta cells contribute to the regulation of beta cells as well as alpha cells. Chapter 1 provides an overview of the beta, alpha and delta cells within the pancreatic islet and how their interactions shape glucose homeostasis, as well as a section on other known somatostatin-secreting cells. Chapter 2 focuses on UCN3 and its role as a marker but not a driver of beta cell maturity. Chapter 3 investigates how SST signaling affects gene expression in beta and alpha cells. Chapter 4 presents work on the contribution of delta cells and SST signaling to the glycemic set point and how this occurs through paracrine interaction with beta cells. Chapter 5 further discusses the role of delta cells in the control of blood glucose levels. Chapter 6 returns to the topic of beta cell and alpha cell gene expression and what changes occur in a model of obesity. Chapter 7 provides a summary of the work and potential future directions.

Acknowledgements

I would first like to thank my PI and mentor Dr. Mark Huising for all his guidance throughout the last 6 years. From the very beginning, he has been a great role model and leader. By allowing me to drive my project independently while also providing constant feedback, he has helped me develop as a scientist. I will always appreciate his words of encouragement throughout every step of my PhD and his unwavering support as I began to explore a career in teaching. I would also like to thank my committee members- Dr. John Albeck, Dr. Karen Ryan, and Dr. Manuel Navedo- for their support and advice in both my science and my career goals.

I would like to thank all the members of the Huising Lab, with a shout out to soon-to-be Dr. Sharon Lee for being with me this entire time. She has been a wonderful friend and has also been instrumental to several of my projects. I greatly admire how she always makes sure everyone in the lab feels included, how amazing of a mentor she is for every single one of our undergraduates, and how dedicated she is to achieving the high standards she has set for herself. Thank you also to Dr. Alex Mawla, our amazing bioinformatician who always patiently helps us with our -Seq analyses, and Dr. Glyn Noguchi, who set a great example for all of us and looked out for us in his own way.

A big thank you to all the undergraduates who have dedicated several hours each week to helping us in the lab. Special mention to Justin Huynh, Jaresley Guillen, Jodie Stroeve, Jerice Banola, Ariana Momen, and Paola Aniceto for helping me and being patient with me as their mentor.

And of course, thank you to Mohammad Pourhosseinzadeh, my partner both in and outside of lab. He has given me never-ending care and support throughout the last several years of my PhD, the pandemic, and this entire dissertation writing process. I hope we will continue to support each other for the rest of our lives.

Chapter 1

Introduction

1.1 Preface

Sections 1.4-1.6 contains text that is planned to be part of a review article co-written with another graduate student in the lab.

1.1.1 Authorship

Jessica L Huang, Mohammad S Pourhosseinzadeh, Mark Huising

The article has been modified to satisfy the formatting requirements of this dissertation.

1.2 Abstract

The pancreas contains clusters of hormone-secreting cells known as the islets of Langerhans. There are several different cell types found within the islet, including beta, alpha, and delta cells. The paracrine interactions between these cells help shape glucose homeostasis. This introductory chapter begins with an overview of the pancreatic islet and the three major cell types. The focus then shifts to focus on delta cells and the major inputs that they receive, followed by a review of how they regulate both beta and alpha cells. At the end, a comparison between delta cells and other somatostatin-expressing cells within the body is drawn, with a focus on somatostatin-expressing neurons within the hypothalamus and D cells within the stomach and duodenum. At the very end, a summary of the introduction and a preview for the remaining dissertation chapters is provided.

1.3 Pancreatic islets and blood glucose homeostasis

The islets of Langerhans are clusters of hormone-secreting cells that comprise the endocrine portion of the pancreas (Steiner *et al.* 2010). They are primarily composed of beta cells, alpha cells, and delta cells. Beta cells are the sole producers of insulin, the hormone necessary for lowering blood glucose levels. Alpha cells produce glucagon, one of the counterregulatory hormones that increases blood glucose levels. Delta cells produce somatostatin (SST), which acts in a paracrine manner to regulate insulin and glucagon secretion from beta and alpha cells respectively. Coordination between these cell types within the islet provide precise regulation of blood glucose homeostasis (Figure 1.1). This section provides an overview on each of these three cell types.

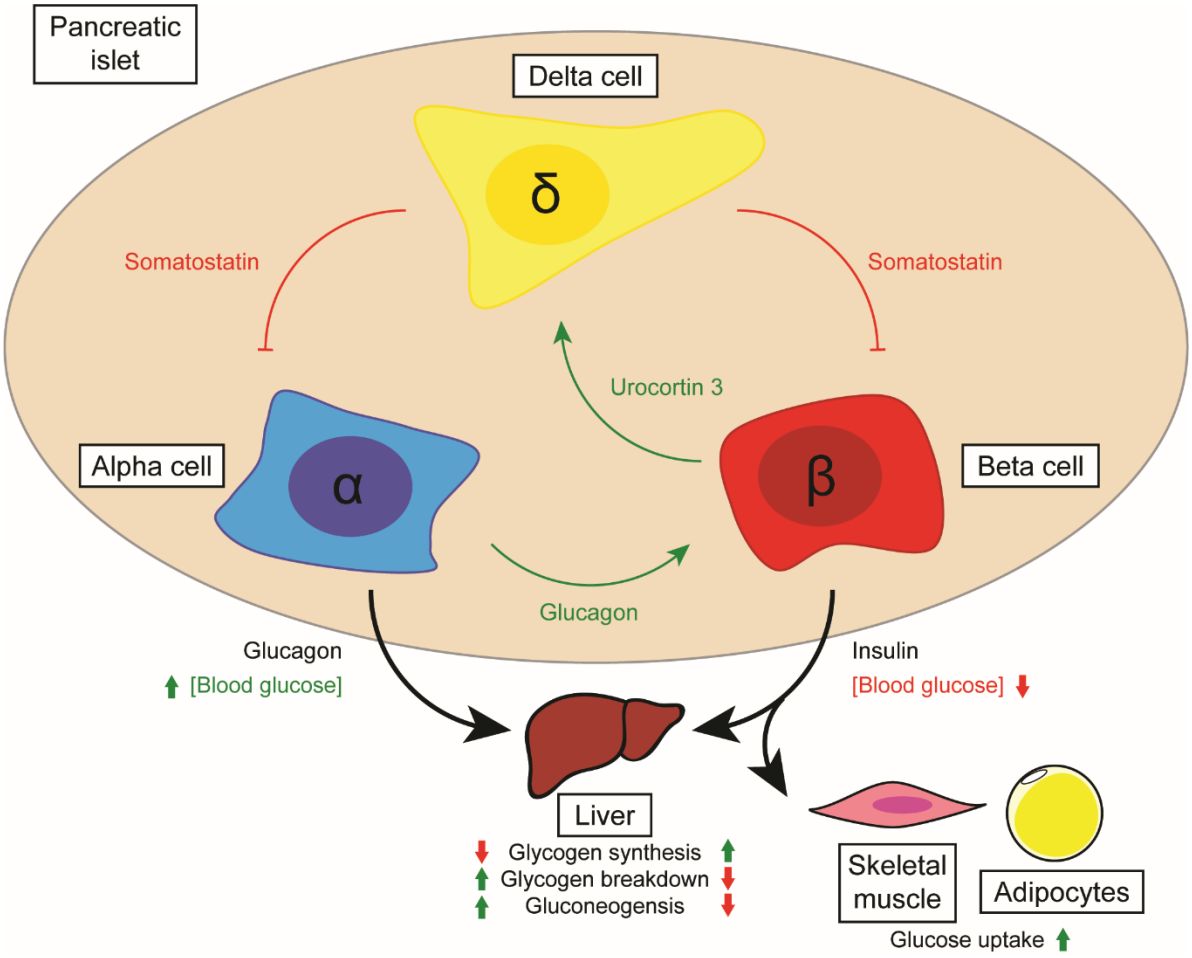

Figure 1.1: Paracrine and systemic actions of the pancreatic islet.

1.3.1 Beta cell function and maturity

Among the islet cells, beta cells are by far the most studied due to their essential role in secreting insulin to lower glycemia under prandial conditions. Insulin signals to several other peripheral organs within the body, including the liver, skeletal muscle, and adipose tissue (Dimitriadis *et al.* 2011). The primary action of insulin in the liver is to promote storage of glucose as glycogen, while in skeletal muscle and adipose tissue it promotes glucose uptake (Figure 1.1). Insulin also signals to the brain, where it acts as one of many nutritional signals to regulate brain metabolism (Duarte *et al.* 2012). Type I Diabetes manifests when there is loss of beta cell mass due to immune attack, while Type II Diabetes

occurs when there is insufficient beta cell mass to meet increasing insulin demand due to insulin resistance of insulin-responding tissues.

Many beta cell maturity markers are involved in driving beta cell maturity or function. For example, *Mafa* encodes a transcription factor that marks beta cells in later differentiation stages and is required for beta cell identity (Artner *et al.* 2010). The gene *Slc2a2* encodes GLUT2, the primary glucose transporter on mouse beta cells that allows the beta cells to sense and uptake glucose (Berger & Zdzieblo 2020). After entering the cell, glucose is metabolized by glucokinase. Another beta cell maturity marker, *G6pc2*, encodes the catalytic subunit of the glucose phosphatase that opposes glucokinase action, providing additional internal modulation of beta cell activity (Pound *et al.* 2013). During the process of glucose metabolism, ATP is produced and closes ATP-sensitive potassium channels, leading to depolarization. This then opens voltage-gated calcium channels, allowing for influx of calcium and subsequent secretion of insulin. The peptide hormone Urocortin 3 (UCN3) is another known marker of beta cell maturity and is packaged in vesicles with insulin (van der Meulen *et al.* 2015). UCN3 goes on to stimulate SST secretion from delta cells, allowing for negative feedback on beta cells that prevent excess insulin secretion. Proper expression of these proteins allows beta cells to have proper insulin response to glucose and help define a mature, functional beta cell. Indeed, many of the genes encoding these proteins are downregulated in diabetes. Thus, there is a need to investigate these markers of beta cell state and how they contribute to maintaining beta cell function.

1.3.2 Systemic and paracrine contribution of alpha cells

Alpha cells are known for their role in secreting glucagon during post-prandial conditions to increase glycemia. They primarily signal to the liver to promote gluconeogenesis and the breakdown of glycogen to allow for release of glucose into the bloodstream (Briant *et al.* 2016) (Figure 1.1). There is increasing focus on the contribution of alpha cells to diabetes. It has been shown that in patients with

Type 2 Diabetes that alpha cells inappropriately secrete excess glucagon even under hyperglycemic conditions, leading to exacerbated hyperglycemia (Shah *et al.* 2000). On the other hand, alpha cells have also been demonstrated to have impaired counterregulatory response in Type 1 Diabetes, leading to higher incidences of hypoglycemia (Ma *et al.* 2018).

In more recent years, alpha cells have also been established to have an important paracrine contribution within the pancreatic islet, in addition to their systemic counterregulatory role. Mice in which glucagon signaling is disrupted specifically in beta cells have alpha cells were inhibited, absent, or lacking expression of glucagon have impaired insulin secretion (Chambers *et al.* 2017; Svendsen *et al.* 2018; Capozzi *et al.* 2019a; Zhu *et al.* 2019), and restoring glucagon expression specifically in alpha cells has been shown to rescue the phenotype (Chambers *et al.* 2017). Mice in which the glucagon receptor (Gcgr) and glucagon-like peptide receptor (Glp1r) were knocked out in beta cells specifically also had impaired insulin secretion (Capozzi *et al.* 2019b). Thus, alpha cells appear to play a more complementary role to beta cells, rather than the opposing role they are generally though to play systemically.

1.3.3 Discovery of delta cells and somatostatin

SST was initially discovered in sheep hypothalamic extracts (Brazeau *et al.* 1973), and SST-expressing cells in the pancreatic islet were discovered soon after (Dubois 1975). Since then, the secretion of SST from pancreatic delta cells has been established as an important paracrine regulator within the cell, in contrast to the systemic actions of insulin and glucagon (Hauge-Evans *et al.* 2009). Somatostatin is initially translated as a prohormone before being cleaved into a smaller peptide. SST can be processed into two different lengths, SST-14 and SST-28. Pancreatic delta cells secrete the SST-14 isoform (Strowski & Blake 2008), and so that is the form we will be referring to throughout the text unless otherwise stated. There are five different SST receptors, SSTR1-SSTR5, with SSTR2 having two

isoforms in humans (Braun 2014). It is likely that these different somatostatin receptors allow for differential SST action on different cell types throughout the body, including beta and alpha cells.

While beta cells are known to be active only past a specific glucose threshold and alpha cells are thought to be primarily active under high glucose conditions, delta cells appear to be active across all glucose levels, albeit with increased activity under high glucose (Arrojo e Drigo *et al.* 2019). This property is in line with their role in inhibiting both beta and alpha cells. How delta cells are affected in diabetes is still not very well studied. There are mixed reports on how delta cell number changes, although most report that there is no difference between non-diabetic and diabetic patients (Saito *et al.* 1979; Rahier *et al.* 1983). However, there is evidence that delta cell function is impaired in diabetes. Under high glucose conditions, beta cells simultaneously release insulin and UCN3 (van der Meulen *et al.* 2015). Insulin goes on to signal to other tissue throughout the body, while UCN3 stimulates delta cells. Thus, when UCN3 expression is lost in diabetes, somatostatin secretion under high glucose is also reduced (van der Meulen *et al.* 2015). Reduced delta cell activity has also been observed in high fat diet-induced diabetic mice (Arrojo e Drigo *et al.* 2019). The loss of communication between beta and delta cells in turn leads to reduced communication between delta cells and alpha cells, and this leads to impaired alpha cell response in diabetes (Briant *et al.* 2016; Huising *et al.* 2018; Kellard *et al.* 2020). Thus, delta cell signaling plays an important role in maintaining blood glucose homeostasis.

1.4 Delta cell response to paracrine, endocrine, and neural inputs

Delta cells respond to many inputs. The paracrine role of delta cells, their activity throughout a large range of glucose levels, and the presence of several different SST receptors within the islet position delta cells as central regulators within the pancreatic islet. This section covers several of the inputs that have been proposed to act on delta cells.

1.4.1 Insulin

A subset of pancreatic delta cells in humans have been reported to express the insulin receptor (*Insr*) (Muller *et al.* 2007), and more recent transcriptomes suggest that delta cells express *Insr* in mice as well (DiGruccio *et al.* 2016). Immunoneutralization experiments with insulin suggest that endogenous insulin stimulates SST secretion under high glucose in the human pancreas (Brunicardi *et al.* 2001). More recent data in isolated human islets also support a stimulatory role of insulin in SST secretion from delta cells (Vergari *et al.* 2019). However, reports on the effect of insulin on delta cells in mice are mixed. Previously, it was shown that insulin does not stimulate SST secretion from delta cells within intact mouse islets, regardless of glucose level, and that treatment with insulin receptor antagonists also did not have an effect on SST secretion (Hauge-Evans *et al.* 2012). This is supported by a more recent study in which treatment with insulin or an insulin receptor antagonist did not have a significant effect on SST secretion (Svendsen & Holst 2021). Thus, while insulin may stimulate SST in humans, it does not appear to be necessary for basal SST secretion in mice.

1.4.2 Glucagon

Mouse delta cells express *Gcgr* and it has been demonstrated that exogenous glucagon stimulates SST secretion in a dose-dependent manner under both low and high glucose levels (Svendsen & Holst 2021). Furthermore, ablation of alpha cells led to blunted SST secretion in isolated islets under high glucose, suggesting an important paracrine role of alpha cells in mediating SST response to glucose. However, immunoneutralization of glucagon in the human pancreas had no significant effect on SST secretion in basal or high glucose conditions, suggesting little contribution from endogenous glucagon to SST secretion in humans (Brunicardi *et al.* 2001).

1.4.3 Urocortin 3

UCN3 is a member of the corticotropin-releasing factor (CRF) family of hormones and selectively binds to the $G_{\alpha s}$-coupled receptor CRHR2 (Lewis *et al.* 2001). When UCN3 was first discovered in beta cells, it was initially believed to act directly on beta cells in an autonomous manner (Li *et al.* 2003). However, we have since demonstrated that the α isoform of CRHR2 is selectively expressed in delta cells within the pancreatic islet (van der Meulen *et al.* 2015). Under hyperglycemic conditions, Ucn3 is co-secreted with insulin and acts in a paracrine manner to stimulate SST secretion from delta cells. When UCN3 is knocked out, pharmacologically inhibited, or reduced in expression during diabetes, SST secretion under high glucose is significantly blunted (van der Meulen *et al.* 2015). This leads to increased insulin secretion from beta cells. Thus, UCN3 plays an important role in enabling SST secretion and mediating the negative feedback it provides to beta cells. In humans, UCN3 is also expressed in alpha cells (van der Meulen *et al.* 2012). This likely helps mediate negative feedback on alpha cells in humans as well.

1.4.4 Ghrelin

While ghrelin has long been known to inhibit insulin secretion, it was thought to act directly on beta cells. Transcriptomic analysis of purified alpha, beta and delta cells from mouse islets revealed that the ghrelin receptor (*Ghsr*) is in fact specifically expressed in delta cells (Adriaenssens *et al.* 2016; DiGruccio *et al.* 2016). Indeed, further experiments showed that exogenous administration of ghrelin selectively activates delta cell activity within intact mouse islets. This is in line with GHSR being a $G_{\alpha q}$-coupled receptor, which would stimulate secretion. Thus, ghrelin acts indirectly on beta cells by stimulating SST secretion from delta cells, which goes on to inhibit insulin secretion from beta cells. Since ghrelin is released as a signal for hunger, this is important for ensuring that beta cell activity is inhibited during this time when nutrient availability is low.

1.4.5 ATP

ATP is produced by beta cells during the course of glucose metabolism and has been shown to be secreted with insulin granules (Richards-Williams *et al.* 2008). Both ADP and ATPyS, a non-hydrolyzable version of ATP, have been shown to have an effect on SST secretion in human islets (Cabrera *et al.* 2008). These effects appear to be at least partially mediated through the purinergic receptor P2Y1, as knockout of the receptor changes the pattern of SST secretion (Salehi *et al.* 2009) and blocking P2Y1 with the antagonist MRS 2179 inhibits SST secretion (Salehi *et al.* 2007). Delta cells have also been proposed to express P2X1 (Ji *et al.* 2018), and transcriptomic data suggests expression of PX4 (DiGruccio *et al.* 2016).

1.4.6 Acetylcholine

Acetylcholine is a neurotransmitter that plays a major role in the parasympathetic nervous system, in which acetylcholine action is primarily mediated through G-protein coupled muscarinic receptors. delta cells predominantly express the M4 subtype of muscarinic receptors (*Chrm4*), which is $G_{\alpha i}$-coupled, and also exhibit some expression of the M3 subtype, which is $G_{\alpha q}$-coupled (DiGruccio *et al.* 2016). The expression of both a stimulatory and inhibitory muscarinic receptor may explain why there have been mixed reports of the effect of cholinergic signaling on delta cells. While treatment of delta cells with the cholinergic agonist carbachol consistently inhibits SST secretion under high glucose (Hauge-Evans *et al.* 2009; Stone *et al.* 2014), there is evidence that it is actually stimulatory under basal glucose (Zhang *et al.* 2007). It is therefore possible that the M3 receptor predominantly mediates cholinergic signaling in delta cells under basal glucose conditions, while M4 is the predominant mediator under high glucose conditions. Human delta cells, on the other hand, have only been reported to express the $G_{\alpha q}$-coupled M1 receptor, and blocking the receptor decreases SST secretion

to allow for increased insulin secretion (Molina *et al.* 2014). Overall, the differential effects of acetylcholine on delta cells suggest that delta cells help mediate parasympathetic input into the islet.

1.4.7 Epinephrine

Epinephrine and norepinephrine are neurotransmitters that play a major role in the sympathetic nervous system. Like beta cells, delta cells express *Adra2a*, which encodes the $G_{\alpha i}$-coupled Alpha-2A adrenergic receptor. This is supported by a study showing that norepinephrine inhibits SST secretion (Hauge-Evans *et al.* 2010). There is little to no expression of the other adrenergic receptors in mice. Experiments performed on the human pancreas have shown that directly stimulating splanchnic nerves under high glucose decreases SST secretion, suggesting that there is an overall inhibitory effect from adrenergic signaling in humans as well (Brunicardi *et al.* 1994). Interestingly, blocking the alpha-adrenergic receptors with an antagonist under high glucose with nerve stimulation led to higher SST secretion than high glucose alone, and blocking the beta-adrenergic receptors further inhibited secretion, suggesting a potential weaker stimulatory effect on delta cells from beta-adrenergic receptors in humans. Regardless, there is a consistent inhibition of delta cells through sympathetic input.

1.4.8 Dopamine

While there is little to no expression of dopamine receptors in the mouse islet, it has been suggested that the D2 receptor, encoded by *Drd2*, is expressed in human delta cells and enables inhibition of SST secretion (Lawlor *et al.* 2017; Bucolo *et al.* 2019). There are immunofluorescent stains supporting the expression of the D2 receptor in delta cells, as well as of selective D5 receptor expression (Zhang *et al.* 2015). As the D2 receptor is inhibitory and the D5 receptor is stimulatory, it remains to be seen whether there are differential effects from these two types of receptors in delta cells.

1.5 Delta cell regulation of beta and alpha cells

The capability of exogenous SST to inhibit beta and alpha cells is well-established. In this section we will discuss how endogenous SST secretion from delta cells regulates beta and alpha cells throughout the range of glucose levels under physiological conditions.

1.5.1 Feedback modulation by delta cells on beta cells

Delta cells are active throughout a wide range of glucose levels, while beta cells activate only above a specific glucose threshold (Figure 1.2). Thus, tonic SST secretion from delta cells likely contributes to restraining beta cell insulin secretion under lower glucose levels. However, under high glucose conditions, beta cell and delta cell activity become coordinated. Both are secreted in a pulsatile manner, with somatostatin secretion following the pattern of insulin secretion closely but with a 30 second delay in perfused pancreas (Salehi *et al.* 2007). This illustrates the importance of delta cells to beta cell function: insulin is first released in response to glucose, and soon after delta cells secrete somatostatin to attenuate insulin secretion (Huising *et al.* 2018). The attenuation of insulin secretion is critical for preventing the hypersecretion of insulin, which could lead to hypoglycemia and be acutely fatal.

Reports on the somatostatin receptors expressed on beta cells have been conflicting, which can be partially attributed to species differences. In human beta cells, expression of SSTR1 (Kumar *et al.* 1999), 2 (Atiya *et al.* 1997; Kailey *et al.* 2012), 3 (Taniyama *et al.* 2005), and 5 (Strowski & Blake 2008; Braun 2014) have been reported, with general consensus that Sstr4 is not expressed in the islet at all. This is supported by transcriptomic data from purified human beta cells (Benner *et al.* 2014). In mice, pharmacological and knockout studies have suggested that SSTR5 is the predominant receptor in beta cells (Rohrer & Schaeffer 2000; Strowski *et al.* 2000, 2003). However, transcriptomic data suggest that SSTR3 is the only receptor with any meaningful expression, and blocking SSTR3 has been shown to

prevent delta cell-mediated inhibition of beta cell activity (DiGruccio *et al.* 2016). SSTR3 has also been demonstrated to localize specifically to the primary cilia of beta cells (Iwanaga *et al.* 2011).

Endogenous somatostatin secreted by pancreatic delta cells plays an important role in preventing excess glucose-stimulated insulin secretion. Immunoneutralization of SST in perfused human pancreas led to increased insulin secretion under both low and high glucose conditions, suggesting a tonic inhibitory role for SST (Brunicardi *et al.* 2001). Studies in $Sst^{-/-}$ mice demonstrated that while basal plasma insulin levels were comparable to levels in control mice, glucose administration led to significantly higher insulin levels (Hauge-Evans *et al.* 2009). As pancreatic delta cells are the sole source of somatostatin in isolated islets, these experiments confirmed that delta cell-secreted somatostatin provides negative feedback to beta cells in a paracrine manner.

As noted above, paracrine factors secreted by the beta cell such as UCN3 play a role in stimulating somatostatin secretion from neighboring delta cells. This likely allows for the fine-tuning of insulin secretion such that there is enough to establish normoglycemia, but not so much as to induce hypoglycemia (Huising *et al.* 2018).

1.5.2 Effects of delta cells on glucagon

There is uniform agreement that SSTR2 is the predominant somatostatin receptor expressed on alpha cells in both humans and rodents (Strowski *et al.* 2000; Cejvan *et al.* 2003; Kailey *et al.* 2012). Knocking out SSTR2 or using SSTR2-selective antagonists consistently leads to increases in glucagon secretion (Strowski *et al.* 2000; Cejvan *et al.* 2003). However, alpha cells in human islets have been proposed to express Sstr1 (Kumar *et al.* 1999) as well. In mice, some expression of SSTR3 has also been demonstrated (DiGruccio *et al.* 2016; Lai *et al.* 2018).

Like beta cells, alpha cells are regulated by endogenous SST secreted by neighboring delta cells. Immunoneutralization of SST in human perfused pancreas increased glucagon secretion under

low glucose, although there was no significant change under high glucose (Brunicardi *et al.* 2001). In *Sst*$^{-/-}$ mice, there is increased arginine-stimulated glucagon secretion (Hauge-Evans *et al.* 2009) as well as decreased suppression of glucagon secretion under high glucose (Hauge-Evans *et al.* 2009; Lai *et al.* 2018). Experiments performed on rat islets under more physiological glucose levels demonstrated that inhibition of glucagon secretion under increasing glucose levels is mediated by SST (Xu *et al.* 2020). Furthermore, SST appears to maximally inhibit glucagon secretion at 7 mM glucose (Lai *et al.* 2018).

Since SST both tonically inhibits glucagon under low glucose and mediates high glucose-induced inhibition of glucagon secretion, how changes in SST signaling during diabetes affects alpha cell activity can vary (Figure 1.2). Reduced somatostatin signaling in high fat diet-induced diabetic mice has been shown to lead to disinhibition of glucagon secretion (Kellard *et al.* 2020), providing evidence that loss of SST signaling contributes to aggravation of hyperglycemia by glucagon. Blocking SSTR2 does not further increase glucagon secretion in these mice, suggesting total loss of SST-mediated repression. On the other hand, blocking SST signaling through applying a SSTR2-specific antagonist in streptozotocin-induced diabetic mice increases glucagon secretion under low glucose conditions (Yue *et al.* 2012). This suggests that there is excess SST secretion under low glucose conditions that contributes to impair alpha cell counterregulatory response. These two different effects of SST on alpha cell activity illustrate the complexity of paracrine interactions within the islet and the importance of investigating these interactions in both healthy and diseased states.

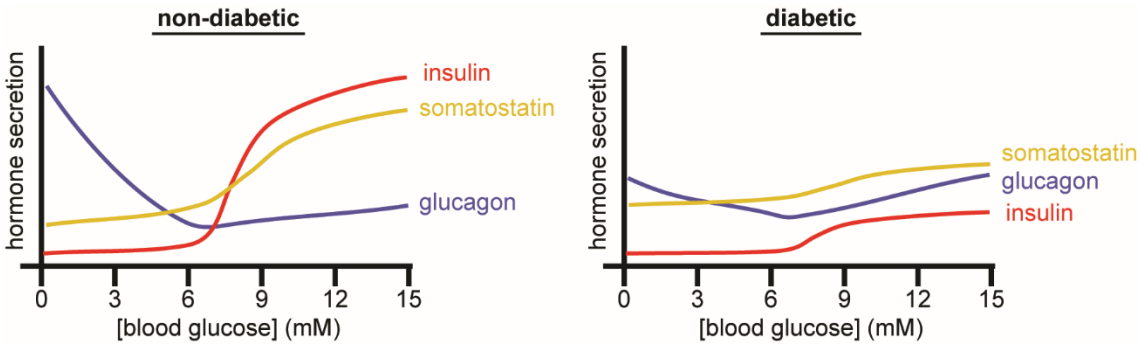

Figure 1.2: Pancreatic islet hormone secretion in non-diabetic vs. diabetic circumstances.

1.6 Contribution of other SST-expressing cells to glucose homeostasis

SST is widely expressed throughout the body as a potent paracrine inhibitor. It has been found in the thyroid, adrenal glands, kidney, and immune cells (Kumar & Singh 2020). In this section, we draw comparisons between the pancreatic delta cell and the somatostatin-expressing cells within these systems. While SST is found throughout the entire central nervous system (CNS), the focus will be on SST-expressing neurons within the hypothalamus, which plays a central role in the regulation of energy homeostasis. We will also discuss the SST-expressing D cells in the stomach and the duodenum.

1.6.1 Somatostatin-expressing cells in the CNS

SST was originally discovered as an inhibitor of growth hormone release in the hypothalamus (Brazeau *et al.* 1973). Since then, SST has been found to be expressed throughout several regions within the hypothalamus; while the majority of SST+ neurons are found in the periventricular nucleus (Patel 1977; Kumar & Singh 2020), SST+ neurons are also found in the ventromedial nucleus, hypothalamic arcuate, lateral nucleus, paraventricular nucleus, tuberal nucleus, and nucleus of the solitary tract (Stengel & Taché 2019). Most hypothalamic SST+ neurons project into the median eminence, where they secrete SST to the anterior pituitary to regulate growth hormone levels. In addition to inhibition

of growth hormone, endogenous SST also inhibits ACTH and ghrelin levels, as both increase in the absence of SST (Luque *et al.* 2006). Like pancreatic delta cells, the primary isoform of SST released from neurons is SST-14.

SST in the hypothalamus has been implicated in regulation of energy homeostasis through modulating food intake and water intake. Chemogenetic activation of SST neurons in the tuberal nucleus as well as the arcuate nucleus increased food intake, while inhibition in the tuberal nucleus decreased feeding (Luo *et al.* 2018). Both inhibition and ablation of SST neurons specifically in the tuberal nucleus also decreased feeding. Interestingly, these SST neurons are activated by ghrelin, demonstrating a signaling pathway that is parallel to ghrelin activation of pancreatic delta cells.
ICV injection of a SST analog has also been shown to stimulate food intake (Stengel *et al.* 2010a), while administration of a SSTR2-specific antagonist decreased food intake (Stengel *et al.* 2010b). Thus, hypothalamic SST appears to primarily promote food intake. Similarly, SST analogs promote water intake through SSTR2 (Karasawa *et al.* 2014). SST is also capable of inhibiting leptin signaling, further suggesting that in the hypothalamus, it plays a role in opposing satiety signals (Stepanyan *et al.* 2007).

1.6.2 Somatostatin-expressing in the gastrointestinal system

Within the gastrointestinal system, somatostatin is secreted by D cells found both in the stomach and the small intestine. In the stomach, D cells are found in both the corpus and the pylorus, with higher numbers observed in the antrum of the pylorus (Penman *et al.* 1983). In the small intestine, D cells are predominantly found in the duodenum, with decreasing numbers found further down in the jejunum and ileum (Penman *et al.* 1983). Interestingly, humans appear to have more D cells within the duodenum, while rodents have higher numbers in the antrum (Arimura *et al.* 1975). Like pancreatic delta cells, the D cells in the stomach primarily secrete SST-14, while D cells in the mucosal glands of the small intestine secrete SST-28 (Penman *et al.* 1983). SST-28 is also the predominant form of SST

circulating in the plasma and is derived from D cells in the small intestine (Patel 1977; Gunawardene *et al.* 2011).

Like pancreatic delta cells, gastrointestinal D cells release SST in response to high glucose (Gutniak *et al.* 1987). In the stomach, D cells inhibit gastrin release (Bloom *et al.* 1974; Holst *et al.* 1992), which leads to inhibition of gastric acid secretion. SST also decreases gastric motility (Johansson *et al.* 1981) and gastric emptying (Holst *et al.* 2016), which lead to a decrease in rate of nutrient absorption. Supporting this is an observation that when rats are infused with SST, glucose directly injected into the duodenum takes more time to appear in the blood (Daumerie & Henquin 1982).

Interestingly, early on it was observed that some gastric somatostatin-expressing cells had one or two long, slender processes that formed contacts with glandular epithelial cells, in particular gastrin-secreting G cells (Larsson *et al.* 1979). This is similar to what has been noted in mouse pancreatic delta cells, which are known to form projections that have been demonstrated to increase contact with other cells within the islet (Huising *et al.* 2018; Arrojo e Drigo *et al.* 2019). In humans, some gastric D cells did not have processes, and the ones that did had shorter, thicker, and blunter ones (Larsson *et al.* 1979). Likewise, human delta cells have fewer projections and have a more circular morphology (Huising *et al.* 2018). While projections have since been observed in other enteroendocrine cell types (Latorre *et al.* 2016), these processes likely promote paracrine interactions between D cells and other enteroendocrine cells.

Overall, SST-secreting D cells within the stomach and the intestine are similar to pancreatic delta cells in that they are stimulated by glucose and largely act in a paracrine manner. However, while pancreatic delta cells may oppose satiety through SST-mediated inhibition of insulin secretion, D cells appear to promote satiety through SST secretion.

1.7 Conclusion

This introductory chapter provides a primer on pancreatic islets and the beta, alpha, and delta cells, with a focus on delta cells, how they are regulated, and how they regulate beta and alpha cells. It ends with a comparison of pancreatic delta cells to SST-expressing neurons in the hypothalamus and gastrointestinal D cells.

The majority of the pancreatic islet is comprised of beta, alpha, and delta cells, and the coordination between these three different cell types contributes to the regulation of blood glucose homeostasis. Beta cells are critical for insulin secretion to lower glycemia after feeding, and loss of functional beta cell mass contributes to the development of diabetes. Thus, there is a lot of research dedicated to determining the factors that define and drive beta cell maturity. In **Chapter 2** of my dissertation, I will demonstrate that while UCN3 is an excellent marker of beta cell maturity, its expression is not required for beta cell maturation.

Alpha cells are most known for their secretion of glucagon and action on the liver to increase glycemia. However, alpha cell-derived glucagon also plays a paracrine role by stimulating insulin secretion under fed conditions. There is also evidence that alpha cells contribute to diabetes through excess secretion under high glucose and impaired counterregulatory response under low glucose. Thus, regulation of alpha cell activity is also important for the treatment of diabetes.

Delta cells mediate inhibition of both beta and alpha cells. The negative feedback they provide to beta cells helps prevent excess insulin secretion and therefore also helps prevent insulin-induced hypoglycemia. The feedback they provide to alpha cells is critical for preventing systemic glucagon action under high glucose, which would increase hyperglycemia. Thus, delta cells are an important central regulator within the islet. In **Chapter 3** of my dissertation, I will investigate the effect of somatostatin signaling on beta and alpha cell gene expression and discuss how these changes in gene expression may reflect function.

Somatostatin is expressed throughout many other tissues in the body. There is evidence that it also contributes to glucose and energy homeostasis within the brain, stomach, and intestines. However, the physiological contribution of SST released by pancreatic delta cells to the glycemic set point has never been demonstrated. In **Chapter 4**, I will provide evidence that pancreatic delta cells specifically play a key role in determining the glycemic set point in mice. In **Chapter 5**, I will review the importance of delta cells in maintaining blood glucose homeostasis.

In **Chapter 6**, I will return to discussing changes in beta and alpha cell gene expression, now in the context of obesity, and show sex-specific differences in the correlation between transcriptomic changes and glycemic changes. **Chapter 7** will end with a summary of my dissertation, conclusions, and future directions. Overall, this dissertation focuses on the importance of delta cells and somatostatin to pancreatic islet function and blood glucose homeostasis.

1.8 References

Adriaenssens AE, Svendsen B, Lam BYH, Yeo GSH, Holst JJ, Reimann F & Gribble FM 2016 Transcriptomic profiling of pancreatic alpha, beta and delta cell populations identifies delta cells as a principal target for ghrelin in mouse islets. *Diabetologia* **59** 2156–2165. (doi:10.1007/s00125-016-4033-1)

Arimura A, Sato H, Dupont A, Nishi N & Schally A V. 1975 Somatostatin: Abundance of immunoreactive hormone in rat stomach and pancreas. *Science* **189** 1007–1009. (doi:10.1126/science.56779)

Arrojo e Drigo R, Jacob S, García-Prieto CF, Zheng X, Fukuda M, Nhu HTT, Stelmashenko O, Peçanha FLM, Rodriguez-Diaz R, Bushong E *et al.* 2019 Structural basis for delta cell paracrine regulation in pancreatic islets. *Nature Communications* **10** 3700. (doi:10.1038/s41467-019-11517-x)

Artner I, Hang Y, Mazur M, Yamamoto T, Guo M, Lindner J, Magnuson MA & Stein R 2010 MafA and MafB regulate genes critical to β-cells in a unique temporal manner. *Diabetes* **59** 2530–2539. (doi:10.2337/db10-0190)

Atiya AW, Moldovan S, Adrian TE, Coy D, Walsh J & Brunicardi FC 1997 Intraislet Somatostatin Inhibits Insulin (Via a Subtype-2 Somatostatin Receptor) but Not Islet Amyloid Polypeptide Secretion in the Isolated Perfused Human Pancreas. *Journal of Gastrointestinal Surgery* **1** 251–256. (doi:10.1016/S1091-255X(97)80117-5)

Benner C, van der Meulen T, Cacéres E, Tigyi K, Donaldson CJ & Huising MO 2014 The transcriptional landscape of mouse beta cells compared to human beta cells reveals notable species differences in long non-coding RNA and protein-coding gene expression. *BMC Genomics* **15** 620. (doi:10.1186/1471-2164-15-620)

Berger C & Zdzieblo D 2020 Glucose transporters in pancreatic islets. *Pflugers Archiv European Journal*

of Physiology. (doi:10.1007/s00424-020-02383-4)

Bloom SR, Mortimer CH, Thorner MO, Besser GM, Hall R, Gomez-Pan A, Roy VM, Russell RCG, Coy DH, Kastin AT *et al.* 1974 Inhibition of Gastrin and Gastric-Acid Secretion By Growth-Hormone Release-Inhibiting Hormone. *The Lancet* **304** 1106–1109. (doi:10.1016/S0140-6736(74)90869-1)

Braun M 2014 *The Somatostatin Receptor in Human Pancreatic β-Cells*. Elsevier Inc. (doi:10.1016/B978-0-12-800174-5.00007-7)

Brazeau P, Vale W, Burgus R, Ling N, Butcher M, Riviver J & Guillemin R 1973 Hypothalamic polypeptide that inhibits the secretion of immunoreactive pituitary growth hormone. *Science* **179** 77–79.

Briant L, Salehi A, Vergari E, Zhang Q & Rorsman P 2016 Glucagon secretion from pancreatic α-cells. *Upsala Journal of Medical Sciences* **121** 113–119. (doi:10.3109/03009734.2016.1156789)

Brunicardi FC, Elahi D & Andersen DK 1994 Splanchnic neural regulation of somatostatin secretion in the isolated perfused human pancreas. *Annals of Surgery* **219** 258–266. (doi:10.1097/00000658-199403000-00005)

Brunicardi FC, Kleinman R, Moldovan S, Nguyen THL, Watt PC, Walsh J & Gingerich R 2001 Immunoneutralization of somatostatin, insulin, and glucagon causes alterations in islet cell secretion in the isolated perfused human pancreas. *Pancreas* **23** 302–308. (doi:10.1097/00006676-200110000-00012)

Bucolo C, Leggio GM, Drago F & Salomone S 2019 Dopamine outside the brain: The eye, cardiovascular system and endocrine pancreas. *Pharmacology and Therapeutics* **203**. (doi:10.1016/j.pharmthera.2019.07.003)

Cabrera O, Jacques-Silva MC, Berman DM, Fachado A, Echeverri F, Poo R, Khan A, Kenyon NS, Ricordi C, Berggren PO *et al.* 2008 Automated, high-throughput assays for evaluation of

human pancreatic islet function. *Cell Transplantation* **16** 1039–1048. (doi:10.3727/000000007783472408)

Capozzi ME, Svendsen B, Encisco SE, Lewandowski SL, Martin MD, Lin H, Jaffe JL, Coch RW, Haldeman JM, MacDonald PE *et al.* 2019a β Cell tone is defined by proglucagon peptides through cAMP signaling. *JCI Insight* **4**. (doi:10.1172/jci.insight.126742)

Capozzi ME, Wait JB, Koech J, Gordon AN, Coch RW, Svendsen B, Finan B, D'Alessio DA & Campbell JE 2019b Glucagon lowers glycemia when β cells are active. *JCI Insight* **4**. (doi:10.1172/jci.insight.129954)

Cejvan K, Coy DH & Efendic S 2003 Intra-islet somatostatin regulates glucagon release via type 2 somatostatin receptors in rats. *Diabetes* **52** 1176–1181. (doi:10.2337/diabetes.52.5.1176)

Chambers AP, Sorrell JE, Haller A, Roelofs K, Hutch CR, Kim KS, Gutierrez-Aguilar R, Li B, Drucker DJ, D'Alessio DA *et al.* 2017 The Role of Pancreatic Preproglucagon in Glucose Homeostasis in Mice. *Cell Metabolism* **25** 927-934.e3. (doi:10.1016/j.cmet.2017.02.008)

Daumerie C & Henquin JC 1982 Somatostatin and the intestinal transport of glucose and other nutrients in the anaesthetised rat. *Gut* **23** 140–145. (doi:10.1136/gut.23.2.140)

DiGruccio MR, Mawla AM, Donaldson CJ, Noguchi GM, Vaughan J, Cowing-Zitron C, van der Meulen T & Huising MO 2016 Comprehensive alpha, beta and delta cell transcriptomes reveal that ghrelin selectively activates delta cells and promotes somatostatin release from pancreatic islets. *Molecular Metabolism* **5** 449–458. (doi:10.1016/j.molmet.2016.04.007)

Dimitriadis G, Mitron P, Lambadiari V, Maratou E & Raptis SA 2011 Insulin effects in muscle and adipose tissue. *Diabetes Research and Clinical Practice* **93** 52–59. (doi:10.1016/S0168-8227(11)70014-6)

Duarte AI, Moreira PI & Oliveira CR 2012 Insulin in central nervous system: More than just a peripheral hormone. *Journal of Aging Research* **2012**. (doi:10.1155/2012/384017)

Dubois MP 1975 Immunoreactive somatostatin is present in discrete cells of the endocrine pancreas. *Proceedings of the National Academy of Sciences of the United States of America* **72** 1340–1343. (doi:10.1073/pnas.72.4.1340)

Gunawardene AR, Corfe BM & Staton CA 2011 Classification and functions of enteroendocrine cells of the lower gastrointestinal tract. *International Journal of Experimental Pathology* **92** 219–231. (doi:10.1111/j.1365-2613.2011.00767.x)

Gutniak M, Grill V, Wiechel KL & Efendic S 1987 Basal and meal-induced somatostatin-like immunoreactivity in healthy subjects and in IDDM and totally pancreatectomized patients. Effects of acute blood glucose normalization. *Diabetes* **36** 802–807. (doi:10.2337/diab.36.7.802)

Hauge-Evans AC, King AJ, Carmignac D, Richardson CC, Robinson ICAF, Low MJ, Christie MR, Persaud SJ & Jones PM 2009 Somatostatin secreted by islet δ-cells fulfills multiple roles as a paracrine regulator of islet function. *Diabetes* **58** 403–411. (doi:10.2337/db08-0792)

Hauge-Evans AC, King AJ, Fairhall K, Persaud SJ & Jones PM 2010 A role for islet somatostatin in mediating sympathetic regulation of glucagon secretion. *Islets* **2** 341–344. (doi:10.4161/isl.2.6.13858)

Hauge-Evans AC, Anderson RL, Persaud SJ & Jones PM 2012 Delta cell secretory responses to insulin secretagogues are not mediated indirectly by insulin. *Diabetologia* **55** 1995–2004. (doi:10.1007/s00125-012-2546-9)

Holst JJ, Orskov C & Seier-Poulsen S 1992 Somatostatin is an essential paracrine link in acid inhibition of gastrin secretion. *Digestion* **51** 95–102. (doi:10.1159/000200882)

Holst JJ, Gribble F, Horowitz M & Rayner CK 2016 Roles of the gut in glucose homeostasis. *Diabetes Care* **39** 884–892. (doi:10.2337/dc16-0351)

Huising MO, van der Meulen T, Huang JL, Pourhosseinzadeh MS & Noguchi GM 2018 The Difference δ-Cells Make in Glucose Control. *Physiology* **33** 403–411.

(doi:10.1152/physiol.00029.2018)

Iwanaga T, Miki T & Takahashi-Iwanaga H 2011 Restricted expression of somatostatin receptor 3 to primary cilia in the pancreatic islets and adenohypophysis of mice. *Biomedical Research* **32** 73–81. (doi:10.2220/biomedres.32.73)

Ji R, Zhu J, Wang D, Sui QQ, Knight GE, Burnstock G, Yuan H & Xiang Z 2018 Expression of P2X1 receptors in somatostatin-containing cells in mouse gastrointestinal tract and pancreatic islets of both mouse and human. *Purinergic Signalling* **14** 285–298. (doi:10.1007/s11302-018-9615-6)

Johansson C, Wisen O, Efendic S & Uvnäs-Wallensten K 1981 Effects of Somatostatin on Gastrointestinal Propagation and Absorption of Oral Glucose in Man. *Digestion* **22** 126–137. (doi:https://doi.org/10.1159/000198619)

Kailey B, van de Bunt M, Cheley S, Johnson PR, MacDonald PE, Gloyn AL, Rorsman P & Braun M 2012 SSTR2 is the functionally dominant somatostatin receptor in human pancreatic β- and α-cells. *AJP: Endocrinology and Metabolism* **303** E1107–E1116. (doi:10.1152/ajpendo.00207.2012)

Karasawa H, Yakabi S, Wang L, Stengel A, Rivier J & Taché Y 2014 Brain somatostatin receptor 2 mediates the dipsogenic effect of central somatostatin and cortistatin in rats: Role in drinking behavior. *American Journal of Physiology - Regulatory Integrative and Comparative Physiology* **307** R793–R801. (doi:10.1152/ajpregu.00248.2014)

Kellard JA, Rorsman NJG, Hill TG, Armour SL, van de Bunt M, Rorsman P, Knudsen JG & Briant LJB 2020 Reduced somatostatin signalling leads to hypersecretion of glucagon in mice fed a high-fat diet. *Molecular Metabolism* **40** 101021. (doi:10.1016/j.molmet.2020.101021)

Kumar U & Singh S 2020 Role of Somatostatin in the Regulation of Central and Peripheral Factors of Satiety and Obesity. *International Journal of Molecular Sciences* **21** 2568. (doi:10.3390/ijms21072568)

Kumar U, Sasi R, Suresh S, Patel A, Thangaraju M, Metrakos P, Patel SC & Patel YC 1999 Subtype-selective expression of the five somatostatin receptors (hSSTR1- 5) in human pancreatic islet cells: A quantitative double-label immunohistochemical analysis. *Diabetes* **48** 77–85. (doi:10.2337/diabetes.48.1.77)

Lai BK, Chae H, Gómez-Ruiz A, Cheng P, Gallo P, Antoine N, Beauloye C, Jonas JC, Seghers V, Seino S *et al.* 2018 Somatostatin is only partly required for the glucagonostatic effect of glucose but is necessary for the glucagonostatic effect of KATP channel blockers. In *Diabetes*, pp 2239–2253. (doi:10.2337/db17-0880)

Larsson LI, Goltermann N, De Magistris L, Rehfeld JF & Schwartz TW 1979 Somatostatin cell processes as pathways for paracrine secretion. *Science* **205** 1393–1395. (doi:10.1126/science.382360)

Latorre R, Sternini C, De Giorgio R & Greenwood-Van Meerveld B 2016 Enteroendocrine cells: A review of their role in brain-gut communication. *Neurogastroenterology and Motility* **28** 620–630. (doi:10.1111/nmo.12754)

Lawlor N, George J, Bolisetty M, Kursawe R, Sun L, Sivakamasundari V, Kycia I, Robson P & Stitzel ML 2017 Single-cell transcriptomes identify human islet cell signatures and reveal cell-type-specific expression changes in type 2 diabetes. *Genome Research* **27** 208–222. (doi:10.1101/gr.212720.116)

Lewis K, Li C, Perrin MH, Blount A, Kunitake K, Donaldson C, Vaughan J, Reyes TM, Gulyas J, Fischer W *et al.* 2001 Identification of urocortin III, an additional member of the corticotropin-releasing factor (CRF) family with high affinity for the CRF2 receptor. *Proceedings of the National Academy of Sciences of the United States of America* **98** 7570–7575. (doi:10.1073/pnas.121165198)

Li C, Chen P, Vaughan J, Blount A, Chen A, Jamieson PM, Rivier J, Smith MS & Vale W 2003 Urocortin III is expressed in pancreatic β-cells and stimulates insulin and glucagon secretion.

Endocrinology **144** 3216–3224. (doi:10.1210/en.2002-0087)

Luo SX, Huang J, Li Q, Mohammad H, Lee CY, Krishna K, Kok AMY, Tan YL, Lim JY, Li H *et al.* 2018 Regulation of feeding by somatostatin neurons in the tuberal nucleus. *Science* **361** 76–81. (doi:10.1126/science.aar4983)

Luque RM, Gahete MD, Hochgeschwender U & Kineman RD 2006 Evidence that endogenous SST inhibits ACTH and ghrelin expression by independent pathways. *American Journal of Physiology - Endocrinology and Metabolism* **291** 395–403. (doi:10.1152/ajpendo.00038.2006.)

Ma Y, Wang Q, Joe D, Wang M & Whim MD 2018 Recurrent hypoglycemia inhibits the counterregulatory response by suppressing adrenal activity. *Journal of Clinical Investigation* **128** 3866–3871. (doi:10.1172/JCI91921)

van der Meulen T, Xie R, Kelly OG, Vale WW, Sander M & Huising MO 2012 Urocortin 3 Marks Mature Human Primary and Embryonic Stem Cell-Derived Pancreatic Alpha and Beta Cells. *PLoS ONE* **7** 1–12. (doi:10.1371/journal.pone.0052181)

van der Meulen T, Donaldson CJ, Cáceres E, Hunter AE, Cowing-Zitron C, Pound LD, Adams MW, Zembrzycki A, Grove KL & Huising MO 2015 Urocortin3 mediates somatostatin-dependent negative feedback control of insulin secretion. *Nature Medicine* **21** 769–776. (doi:10.1038/nm.3872)

Molina J, Rodriguez-Diaz R, Fachado A, Jacques-Silva MC, Berggren PO & Caicedo A 2014 Control of insulin secretion by cholinergic signaling in the human pancreatic islet. *Diabetes* **63** 2714–2726. (doi:10.2337/db13-1371)

Muller D, Huang GC, Amiel S, Jones PM & Persaud SJ 2007 Gene expression heterogeneity in human islet endocrine cells in vitro: The insulin signalling cascade. *Diabetologia* **50** 1239–1242. (doi:10.1007/s00125-007-0671-7)

Patel YC 1977 General Aspects of the Biology and Function of Somatostatin. *The Role of Somatostatin.*

Basic and Clinical Aspects of Neuroscience **Springer,** 1–16.

Penman E, Wass JAH, Butler MG, Penny ES, Price J, Wu P & Rees LH 1983 Distribution and characterisation of immunoreactive somatostatin in human gastrointestinal tract. *Regulatory Peptides* **7** 53–65. (doi:10.1016/0167-0115(83)90281-1)

Pound LD, Oeser JK, O'Brien TP, Wang Y, Faulman CJ, Dadi PK, Jacobson DA, Hutton JC, McGuinness OP, Shiota M *et al.* 2013 G6PC2: A negative regulator of basal glucose-stimulated insulin secretion. *Diabetes* **62** 1547–1556. (doi:10.2337/db12-1067)

Rahier J, Goebbels RM & Henquin JC 1983 Cellular composition of the human diabetic pancreas. *Diabetologia* **24** 366–371. (doi:10.1007/BF00251826)

Richards-Williams C, Contreras JL, Berecek KH & Schwiebert EM 2008 Extracellular ATP and zinc are co-secreted with insulin and activate multiple P2X purinergic receptor channels expressed by islet beta-cells to potentiate insulin secretion. *Purinergic Signalling* **4** 393–405. (doi:10.1007/s11302-008-9126-y)

Rohrer SP & Schaeffer JM 2000 Identification and characterization of subtype selective somatostatin receptor agonists. *Journal of Physiology Paris* **94** 211–215. (doi:10.1016/S0928-4257(00)00215-1)

Saito K, Yaginuma N & Takahashi T 1979 Differential Pancreatic Subjects Volumetry of A , B and D Cells in the Islets of Diabetic and Nondiabetic The First Department of Pathology , Tohoku University School In our foregoing paper , diabetic cases were subjected to islet morphometry , in which t. *Jorunal of Experimental Medicine* **129** 273–283.

Salehi A, Qader SS, Grapengiesser E & Hellman B 2007 Pulses of somatostatin release are slightly delayed compared with insulin and antisynchronous to glucagon. *Regulatory Peptides* **144** 43–49. (doi:10.1016/j.regpep.2007.06.003)

Salehi A, Parandeh F, Fredholm BB, Grapengiesser E & Hellman B 2009 Absence of adenosine A1 receptors unmasks pulses of insulin release and prolongs those of glucagon and somatostatin.

Life Sciences **85** 470–476. (doi:10.1016/j.lfs.2009.08.001)

Shah P, Vella A, Basu A, Basu R, Schwenk WF & Rizza RA 2000 Lack of suppression of glucagon contributes to postprandial hyperglycemia in subjects with type 2 diabetees mellitus. *Journal of Clinical Endocrinology and Metabolism* **85** 4053–4059. (doi:10.1210/jc.85.11.4053)

Steiner DJ, Kim A, Miller K & Hara M 2010 Pancreatic islet plasticity: Interspecies comparison of islet architecture and composition. *Islets* **2** 135–145. (doi:10.4161/isl.2.3.11815)

Stengel A & Taché Y 2019 Central somatostatin signaling and regulation of food intake. *Annals of the New York Academy of Sciences* **1455** 98–104. (doi:10.1111/nyas.14178)

Stengel A, Coskun T, Goebel M, Wang L, Craft L, Alsina-Fernandez J, Rivier J & Taché Y 2010a Central injection of the stable somatostatin analog ODT8-SST induces a somatostatin2 receptor-mediated orexigenic effect: Role of neuropeptide Y and opioid signaling pathways in rats. *Endocrinology* **151** 4224–4235. (doi:10.1210/en.2010-0195)

Stengel A, Goebel M, Wang L, Rivier J, Kobelt P, Monnikes H & Tache Y 2010b SELECTIVE CENTRAL ACTIVATION OF SOMATOSTATIN RECEPTOR 2 INCREASES FOOD INTAKE, GROOMING BEHAVIOR AND RECTAL TEMPERATURE IN RATS. *Journal of Physiology and Pharmacology* **61** 399–407.

Stepanyan Z, Kocharyan A, Behrens M, Koebnick C, Pyrski M & Meyerhof W 2007 Somatostatin, a negative-regulator of central leptin action in the rat hypothalamus. *Journal of Neurochemistry* **100** 468–478. (doi:10.1111/j.1471-4159.2006.04219.x)

Stone VM, Dhayal S, Brocklehurst KJ, Lenaghan C, Sörhede Winzell M, Hammar M, Xu X, Smith DM & Morgan NG 2014 GPR120 (FFAR4) is preferentially expressed in pancreatic delta cells and regulates somatostatin secretion from murine islets of Langerhans. *Diabetologia* **57** 1182–1191. (doi:10.1007/s00125-014-3213-0)

Strowski MZ & Blake AD 2008 Function and expression of somatostatin receptors of the endocrine

pancreas. *Molecular and Cellular Endocrinology* **286** 169–179. (doi:10.1016/j.mce.2008.02.007)

Strowski MZ, Parmar RM, Blake AD & Schaeffer JM 2000 Somatostatin Inhibits Insulin and Glucagon Secretion via Two Receptor Subtypes: An in Vitro Study of Pancreatic Islets from Somatostatin Receptor 2 Knockout Mice. *Endocrinology* **141** 111–117. (doi:10.1210/endo.141.1.7263)

Strowski MZ, Kohler M, Chen HY, Trumbauer ME, Li Z, Szalkowski D, Gopal-Truter S, Fisher JK, Schaeffer JM, Blake AD *et al.* 2003 Somatostatin receptor subtype 5 regulates insulin secretion and glucose homeostasis. *Molecular Endocrinology* **17** 93–106. (doi:10.1210/me.2001-0035)

Svendsen B & Holst JJ 2021 Paracrine regulation of somatostatin secretion by insulin and glucagon in mouse pancreatic islets. *Diabetologia* **64** 142–151. (doi:10.1007/s00125-020-05288-0)

Svendsen B, Larsen O, Gabe MBN, Christiansen CB, Rosenkilde MM, Drucker DJ & Holst JJ 2018 Insulin Secretion Depends on Intra-islet Glucagon Signaling. *Cell Reports* **25** 1127-1134.e2. (doi:10.1016/j.celrep.2018.10.018)

Taniyama Y, Suzuki T, Mikami Y, Moriya T, Satomi S & Sasano H 2005 Systemic distribution of somatostatin receptor subtypes in human: An immunohistochemical study. *Endocrine Journal* **52** 605–611. (doi:10.1507/endocrj.52.605)

Vergari E, Knudsen JG, Ramracheya R, Salehi A, Zhang Q, Adam J, Asterholm IW, Benrick A, Briant LJB, Chibalina M V. *et al.* 2019 Insulin inhibits glucagon release by SGLT2-induced stimulation of somatostatin secretion. *Nature Communications* **10**. (doi:10.1038/s41467-018-08193-8)

Xu SFS, Andersen DB, Izarzugaza JMG, Kuhre RE & Holst JJ 2020 In the rat pancreas, somatostatin tonically inhibits glucagon secretion and is required for glucose-induced inhibition of glucagon secretion. *Acta Physiologica.* (doi:10.1111/apha.13464)

Yue JTY, Burdett E, Coy DH, Giacca A, Efendic S & Vranic M 2012 Somatostatin receptor type 2

antagonism improves glucagon and corticosterone counterregulatory responses to hypoglycemia in streptozotocin-induced diabetic rats. *Diabetes* **61** 197–207. (doi:10.2337/db11-0690)

Zhang Q, Bengtsson M, Partridge C, Salehi A, Braun M, Cox R, Eliasson L, Johnson PRV, Renström E, Schneider T *et al.* 2007 R-type Ca2+-channel-evoked CICR regulates glucose-induced somatostatin secretion. *Nature Cell Biology* **9** 453–460. (doi:10.1038/ncb1563)

Zhang Y, Zheng R, Meng X, Wang L, Liu L & Gao Y 2015 Pancreatic endocrine effects of dopamine receptors in human islet cells. *Pancreas* **44** 925–929. (doi:10.1097/MPA.0000000000000357)

Zhu L, Dattaroy D, Pham J, Wang L, Barella LF, Cui Y, Wilkins KJ, Roth BL, Hochgeschwender U, Matschinsky FM *et al.* 2019 Intraislet glucagon signaling is critical for maintaining glucose homeostasis. *JCI Insight* **4**. (doi:10.1172/jci.insight.127994)

Chapter 2

Genetic deletion of Urocortin 3 does not prevent functional maturation of beta cells

2.1 Preface

This chapter was originally published in *Journal of Endocrinology*:

Huang JL, Lee S, Hoek P, van der Meulen T, Van R, Huising MO. (2020) Genetic deletion of Urocortin 3 does not prevent functional maturation of beta cells. Journal of Endocrinology. 246(1):69-78.

I performed the experiments for all figures except Figure 2.1, 2.2A, 2.5, and 2.6. Figures 2.1 and 2.6 are derived from data previously published by the lab in *Nature Medicine* (van der Meulen et al., 2015). I analyzed the data and wrote the paper. The article has been modified to satisfy the formatting requirements of this dissertation.

2.2 Abstract

There is great interest in generating functionally mature beta cells from stem cells, as loss of functional beta cell mass contributes to the pathophysiology of diabetes. Identifying markers of beta cell maturity is therefore very helpful for distinguishing stem cells that have been successfully differentiated into fully mature beta cells from stem cells that did not. Urocortin 3 (UCN3) is a peptide hormone whose

expression is associated with the acquisition of functional maturity in beta cells. The onset of its expression occurs after other beta cell maturity markers are already expressed and its loss marks the beginning of beta cell dedifferentiation. Its expression pattern is therefore tightly correlated with beta cell maturity. While this makes UCN3 an excellent marker of beta cell maturity, it is not established whether UCN3 is required for beta cell maturation. Here, we compared gene expression and function of beta cells from *Ucn3*-null mice relative to wild-type mice to determine whether beta cells are functionally mature in the absence of UCN3. Our results show that genetic deletion of *Ucn3* does not cause a loss of beta cell maturity or an increase in beta cell dedifferentiation. Furthermore, virgin beta cells, first identified as insulin-expressing, UCN3-negative beta cells, can still be detected at the islet periphery in *Ucn3*-null mice. Beta cells from *Ucn3*-null mice also exhibit normal calcium response when exposed to high glucose. Collectively, these observations indicate that UCN3 is an excellent mature beta cell marker that is nevertheless not necessary for beta cell maturation.

2.3 Introduction

Beta cells are the sole source of insulin in the body. Thus, there is much interest in finding ways to generate new beta cells. One of the current methods of regenerating beta cells is differentiating stem cells *in vitro* (Pagliuca *et al.* 2014; Rezania *et al.* 2014; Russ *et al.* 2015; Nair *et al.* 2019; Velazco-Cruz *et al.* 2019; Veres *et al.* 2019). However, although much progress has been made towards generating beta cells from stem cells, clinically meaningful generation of functionally mature beta cells *in vitro* has yet to be achieved. Markers that can guide the maturation of beta cells *in vitro* are therefore of great utility.

The maturation of beta cells *in vivo* is driven by several key transcription factors such as PDX1, NKX6-1, and MAFA, among others. In mice, insulin-expressing cells first appear around E9.5, with a second, larger wave appearing around E13.5, which corresponds to the onset of MAFA expression

(Artner *et al.* 2010). However, most beta cells do not express MAFA at this early age and remain largely functionally immature. Additional markers, such as the peptide hormone Urocortin 3 (UCN3), have emerged as late beta cell maturity markers in recent years.

UCN3 is a member of the corticotropin-releasing factor (CRF) family that selectively binds the G-protein coupled receptor CRFR2 (Lewis *et al.* 2001). Shortly after its discovery, it was found to be expressed in beta cells (Li *et al.* 2003). UCN3 is co-released with insulin under high glucose conditions and stimulates somatostatin secretion from delta cells, which are the primary cells within the islet that express CRHR2 (van der Meulen *et al.* 2015). This creates a negative feedback loop that leads to the repression of insulin.

During development, UCN3 is first expressed by some beta cells in the later stages of mouse embryonic development at E17.5, and is not expressed by the majority of beta cells until 2 weeks after birth (Blum *et al.* 2012; van der Meulen *et al.* 2012). The late onset of UCN3 expression in beta cells places it well after that of commonly used maturity markers such as MAFA and PDX1 (van der Meulen & Huising 2014; Hunter & Stein 2017). This makes UCN3 a useful marker to distinguish between immature insulin-positive cells and fully functional, stem cell-derived beta cells. Furthermore, the expression of UCN3 coincides with the acquisition of functional maturity by mouse beta cells that is marked by a notable uptick in blood glucose values (Blum *et al.* 2012). Indeed, prematurely inducing the expression of UCN3 in beta cells of mice under 2 weeks old directly leads to a premature increase in blood glucose levels (van der Meulen *et al.* 2015). This demonstrates that UCN3 expression is sufficient to trigger the increase in blood glucose levels that thus sets the higher blood glucose set point that is associated with the acquisition of functional beta cell maturity.

More recently, we identified a novel sub-population of 'virgin' beta cells specifically located at the periphery of the islet, that was discovered by virtue of their lack of UCN3 expression (van der

Meulen *et al.* 2017). These beta cells express insulin, but do not express beta cell maturity markers, including UCN3, MAFA, ERO1LB, G6PC2, and GLUT2. These virgin beta cells are functionally immature and unable to sense glucose, in part because of their lack of cell-surface expression of GLUT2. On the other side of the spectrum, loss of UCN3 has also been established as a hallmark of beta cell dedifferentiation in diabetes (Blum *et al.* 2014; van der Meulen *et al.* 2015). In leptin-deficient *ob/ob* mice, UCN3 expression is initially indistinguishable from controls until the onset of diabetes, at which point UCN3 expression markedly decreases, which continues as diabetes progresses. The return of UCN3 expression has thus been used to demonstrate re-differentiation of beta cells (Blum *et al.* 2014). More recently, UCN3 expression has also been reported to be decreased in senescent beta cells in Type 1 Diabetes (Thompson *et al.* 2019).

The fact that UCN3 expression tracks closely with beta cell function across different beta cell states raises the question if UCN3 is merely a marker of mature beta cells, or whether beta cells directly require UCN3 for their maturation and normal function. Although the receptor for UCN3 is selectively expressed on delta cells and thus cannot affect beta cell maturity in a cell-autonomous or autocrine fashion, Ucn3 could indirectly affect beta cell maturity via paracrine, somatostatin-mediated crosstalk within the islet, analogous to its effects on insulin secretion (van der Meulen *et al.* 2015). Indeed, given the strong correlation of Ucn3 with beta cell maturity, the question of causation is regularly raised. To investigate this question, we used genetic ablation of *Ucn3* to demonstrate whether beta cells can reach functional maturity in the absence of UCN3.

2.4 Results

2.4.1 Expression of beta cell maturity genes persists in *Ucn3*-null mice

We first evaluated our previously published whole islet transcriptomes of *Ucn3*-null mice versus *Ucn3*-wt littermates (van der Meulen *et al.* 2015). Several genes are differentially regulated between *Ucn3*-wt and *Ucn3*-null mice, with 22 genes enriched in *Ucn3*-wt mice and 7 genes enriched in *Ucn3*-null mice (Figure 2.1A, Table 2.1, Figure 2.6A). *Ucn3*-null islets demonstrate a loss of UCN3, confirming successful knockout of *Ucn3*, with no observable compensation in UCN1, which is completely indetectable in both *Ucn3*-wt and *Ucn3*-null mice (Figure 2.6B), and UCN2, which has little to no expression (Figure 2.6C) and does not change significantly in *Ucn3*-null mice (Figure 2.1A). CRHR2, the receptor for UCN3, remains expressed in *Ucn3*-null mice (Figure 2.6D). Of the 22 genes with lower expression in *Ucn3*-null mice, several are known delta cell markers such as *Sst*, *Hhex*, and *Rbp4*, which was previously reported and caused by a significant reduction in delta cells in the absence of UCN3 (van der Meulen *et al.* 2015). However, there was no significant difference in the expression of *Ins1* or *Ins2* expression in *Ucn3*-null mice relative to their wild-type littermates (Figure 2.1B). To further confirm that there is no difference in beta cell maturity at the transcriptional level, we examined the gene expression of several established beta cell maturity markers, including *MafA*, *Pdx1*, *Ero1lb*, *G6pc2*, and *Slc2a2*. All of these were expressed at similar levels between *Ucn3*-null and wild-type mice (Figure 2.1C-1G).

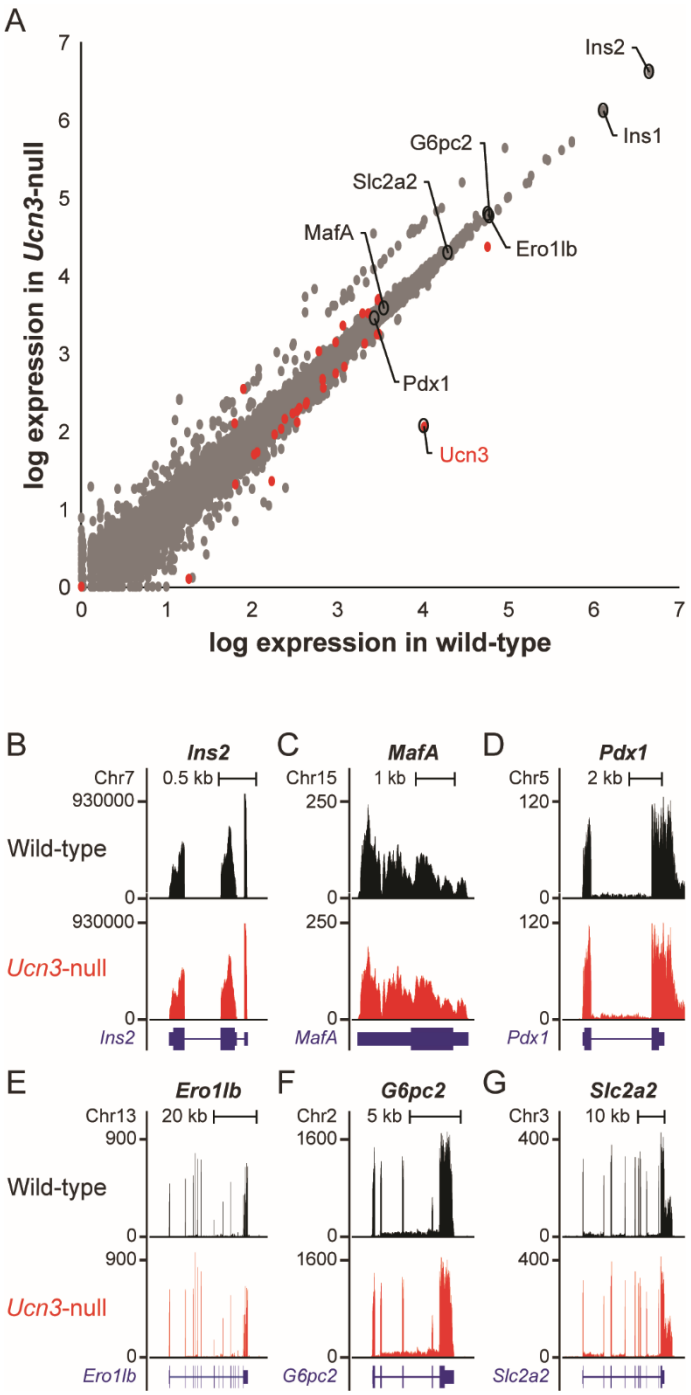

Figure 2.1: Genes encoding beta cell maturity markers are not differentially regulated between *Ucn3*-null mice and wild-type littermates. (A) Volcano plot showing global gene expression in wild-type vs *Ucn3*-null mice. Differentially expressed genes are denoted as red circles. Select markers of beta cell maturity are circled and labeled. *Ucn3* is depleted in *Ucn3*-null mice, confirming knockout, while other beta cell maturity markers are not affected at the transcript level. There is no compensation by *Ucn* or *Ucn2* within the islet. (B-G) Visualization of relative reads of different transcripts in *Ucn3*-null mice (red) compared to wild-type (black). (B) *Ins2*, (C) *MafA*, (D) *Pdx1*, (E) *Ero1lb*, (F) *G6pc2*, (G) *Slc2a2*.

Western blotting confirmed that UCN3 is no longer expressed in *Ucn3*-null mice but is retained in both *Ucn3*-wt and *Ucn3*-het mice (Figure 2.2A). Thus, both *Ucn3*-wt and *Ucn3*-het were used as controls in further experiments unless otherwise designated. Immunofluorescence also confirmed that there is no UCN3 immunoreactivity in *Ucn3*-null mice, while there is near-complete overlap between UCN3 and insulin in the controls (Figure 2.2B). The transcription factor MAFA, which is required for mature beta cell identity, is expressed in the nuclei of most beta cells in both wild-type and *Ucn3*-null mice (Figure 2.2C). Similarly, PDX1 is expressed in the nucleus of beta cells as well (Figure 2.2D). ERO1LB and G6PC2 both have strong overlap with insulin in both wild-type and *Ucn3*-null mice (Figure 2.2E-F, Figure 2.7). Immunoreactivity of the glucose transporter GLUT2, encoded by *Slc2a2*, is detected on the surface of beta cells in both *Ucn3*-null and control mice (Figure 2.2G). Overall, these results indicate that the expression of a panel of established beta cell maturity markers is unperturbed in the absence of UCN3.

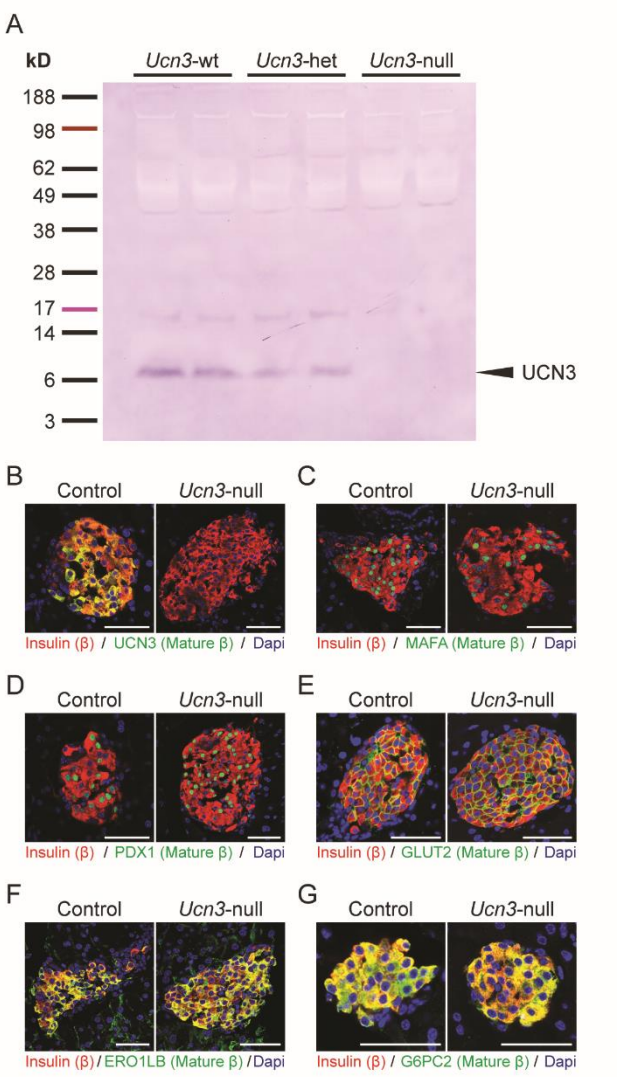

Figure 2.2: UCN3 expression is not necessary for beta cells to express maturity markers. (A) UCN3 remains expressed in *Ucn3*-wt and *Ucn3*-het mice, but not in *Ucn3*-null mice. (B-G) Co-localization of insulin and select beta cell maturity markers in islets of *Ucn3*-null mice and littermate controls. Insulin is stained in red, the marker of interest is in green, and nuclei stained by DAPI are in blue. (B) UCN3, (C) MAFA, (D) PDX1, (E) ERO1LB, (F) G6PC2, (G) GLUT2. Scale bars indicate 50 μm.

2.4.2 Beta cell dedifferentiation is not increased in *Ucn3*-null mice

The preservation of the expression of beta cell maturity markers in *Ucn3*-null compared to wild-type mice established that UCN3 expression is not necessary for beta cell maturation. Conversely, the loss of UCN3 expression in beta cells is also a sensitive and early marker of beta cell dedifferentiation (Blum *et al.* 2014; van der Meulen *et al.* 2015). To investigate if the genetic deletion of UCN3 increases beta cell dedifferentiation, we assessed the expression of several beta cell dedifferentiation markers. Aldehyde dehydrogenase 1 family, member A3 (ALDH1A3) is an established marker of dedifferentiated beta cells (Kim-Muller *et al.* 2016). As expected, ALDH1A3 was absent from the majority of beta cells in lean, wild-type mice at 0.28% ± 0.24% (Figure 2.3). However, the genetic deletion of *Ucn3* in *Ucn3*-null mice by itself did not cause a significant increase in the number of ALDH1A3-expressing beta cells (0.50% ± 0.43%). In contrast, beta cells expressed ALDH1A3 in *ob/ob* mice, which are known to exhibit beta cell dedifferentiation, consistent with published observations (Kim-Muller *et al.* 2016). We observed that almost half of the beta cells expressed ALDH1A3 at 46.70% ± 1.93% (Figure 2.3A-B). Moreover, while UCN3 immunoreactivity is also weaker and detected in fewer beta cells in *ob/ob* mice (50.17% ± 34.63%), UCN3 is completely absent in *Ucn3*-null mice. This suggests that the loss of UCN3 by itself does not cause beta cell dedifferentiation. Other dedifferentiation markers such as *Neurog3* (NGN3) and *Vim* (vimentin) also do not exhibit a significant change (Figure 2.6E-F).

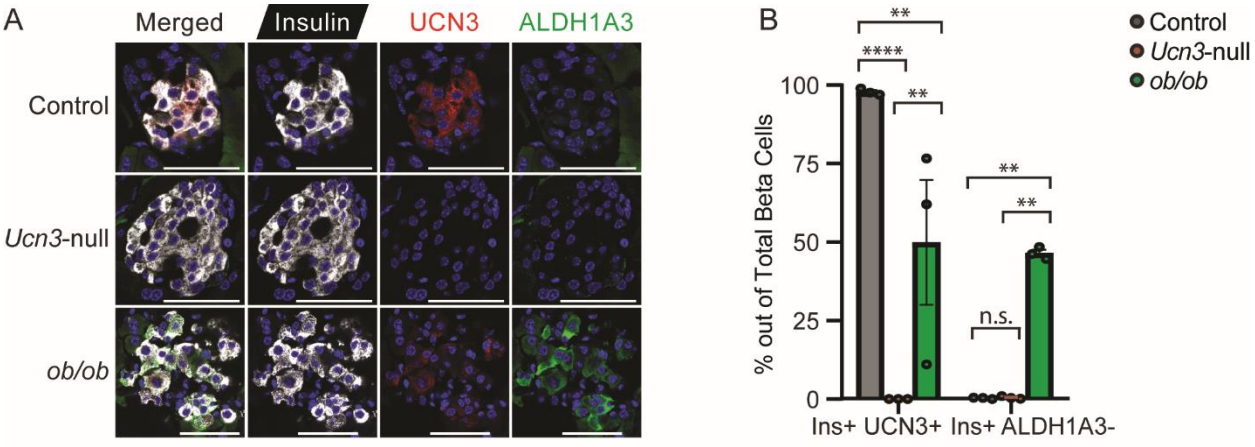

Figure 2.3: The absence of UCN3 expression does not lead to beta cell dedifferentiation. (A) Immunofluorescence of insulin, UCN3, and ALDH1A3 in islets from wild-type, *Ucn3*-null, and *ob/ob* mice. Control mice co-express insulin and UCN3 in beta cells, but express little to no ALDH1A3. In contrast, more insulin-positive beta cells in *ob/ob* islets express ALDH1A3 and exhibit weaker immunoreactivity of UCN3. *Ucn3*-null mice, like their control littermates, express little to no ALDH1A3 in beta cells but lack expression of UCN3. Scale bars indicate 50 μm. (B) Quantification of insulin-positive, UCN3-positive and insulin-positive, ALDH1A3-positive cells in control, *Ucn3*-null, and *ob/ob* mice, as percentage of total beta cells. n = 3 animals per group, at least 10 islets and 500 cells counted per animal. Error bars reflect SEM. **p<0.01, ****p<0.001

2.4.3 Virgin beta cells remain identifiable in *Ucn3*-null mice

Recently, our lab discovered virgin beta cells as a novel beta cell type that is found at the periphery of the mouse islet and is recognized by its lack of UCN3, as well as other beta cell maturity markers. As we originally identified virgin beta cells based on their absence of UCN3 expression, we wanted to determine whether they remained detectable upon genetic ablation of *Ucn3*, and if they maintained their characteristic location at the periphery of the islet. Staining for insulin, UCN3, and GLUT2 readily revealed virgin beta cells in control mice expressing UCN3, most of which also lacked cell-surface GLUT2 (csGLUT2) expression as previously shown (van der Meulen *et al.* 2017) (Figure 2.4A). Insulin-expressing cells lacking csGLUT2 expression was also found in *Ucn3*-null mice (Figure 2.4B). While the fraction of Insulin+ UCN3- virgin beta cells is similar to what we have previously established (1.21% ± 0.81%), the fraction of Insulin+ csGLUT2- beta cells is higher (3.13% ± 1.27%

in control mice, 2.96% ± 0.32% in *Ucn3*-null mice) (Figure 2.4C), similarly to what we previously published (van der Meulen *et al.* 2017). In control mice, this is due to the presence of several mature Insulin+ UCN3+ cells without csGLUT2 expression. As the fraction of Insulin+ csGLUT2- is similar in the *Ucn3*-null mice, it is likely that these cells similarly represent both virgin and mature beta cells. Nevertheless, we conclude that many of the Insulin+ csGLUT2- cell identified in the *Ucn3*-null mice are virgin beta cells, as they remain at their characteristic location of the islet periphery. We also looked at G6PC2 expression as another marker (Figure 2.4D-E). Here the data also show the expected fraction of Insulin+ UCN3- cells (1.46% ± 0.25%), with fewer Insulin+ G6PC2- cells (0.50% ± 0.16%) (Figure 2.4F). These numbers are in agreement with our previously published data (van der Meulen *et al.* 2017). The fraction of Insulin+ G6PC2- was not significantly different in Ucn3-*null* mice (0.49% ± 0.21%). All Insulin+ UCN3- and Insulin+ G6PC2- cells localize to the islet periphery in both Ucn3-*null* mice and littermate controls. The presence of MAFB, a marker more highly expressed in virgin beta cells, in cells at the periphery (Figure 2.8) further supports that continued presence of virgin beta cells in the absence of Ucn3.

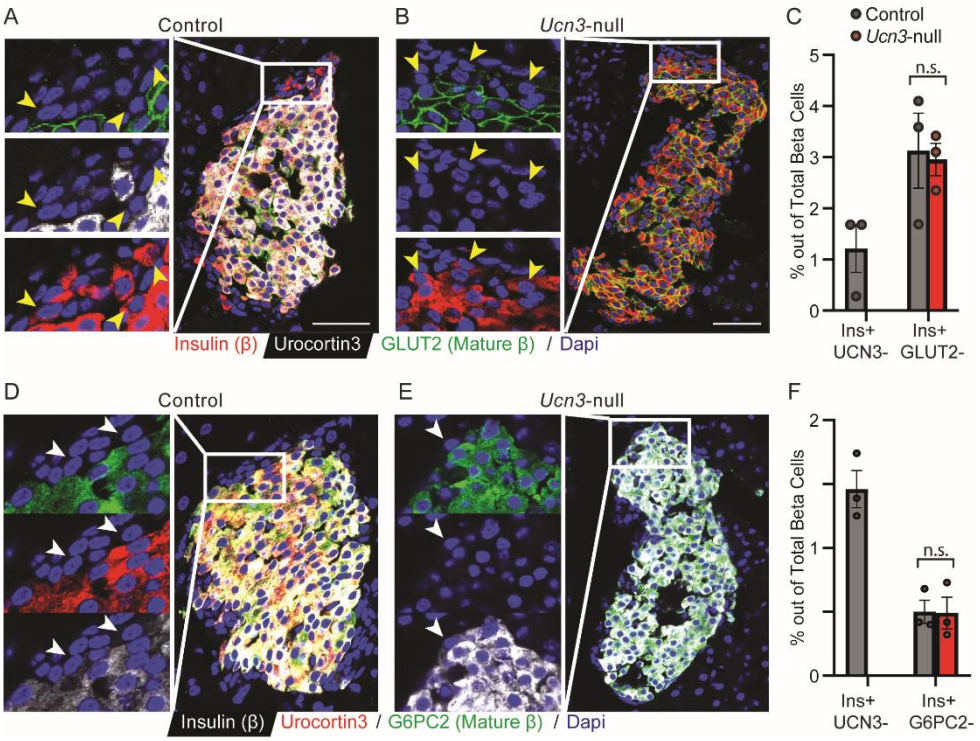

Figure 2.4: Virgin beta cells are maintained at the islet periphery in the absence of UCN3. (A-B) Immunofluorescence of insulin, UCN3, and GLUT2 in islets from (A) control and (B) *Ucn3*-null mice. Insulin and UCN3 co-localize in beta cells, while GLUT2 is expressed on the membrane of the beta cells. Arrows point to virgin beta cells, which are insulin-positive but UCN3-negative and GLUT2-negative in control mice and insulin-positive but GLUT2-negative in *Ucn3*-null mice. Scale bars indicate 50 μm. (C) Quantification of insulin-positive, UCN3-negative cells in control mice and insulin-positive, csGLUT2-negative cells in control and *Ucn3*-null mice, as percentage of total beta cells. (D-E) Immunofluorescence of insulin, UCN3, and G6PC2 in islets from (D) control and (E) *Ucn3*-null mice. Insulin, UCN3, and G6PC2 are co-expressed in the majority of beta cells in control mice. Arrows point to virgin beta cells that are insulin-positive but UCN3- and G6PC2-negative. (F) Quantification of insulin-positive, UCN3-negative cells in control mice and insulin-positive, G6PC2-negative cells in control and *Ucn3*-null mice. For both C and F, there is no quantification for insulin+ UCN3- cells in the *Ucn3*-null mice as all cells are UCN3- and thus not representative of the virgin beta cell population. n = 3 animals per group, at least 10 islets and 500 cells counted per animal. Error bars reflect SEM.

2.4.4 Beta cells in *Ucn3*-null mice exhibit normal calcium response to glucose

We established that beta cells maintain the expression of beta cell maturity markers despite the absence of UCN3. This implies that these beta cells remained functionally mature. To interrogate the functional maturity of beta cells directly, we crossed *Ucn3*-null mice to mice that express the calcium

reporter GCaMP6s (Madisen *et al.* 2015) specifically in beta cells using *MIP-Cre/ERT* (Wicksteed *et al.* 2010). Mindful of the potential confounds of the *MIP-Cre/ERT* mouse line (Carboneau et al., 2016), we used mice that were wild-type for *Ucn3* but transgenic for *MIP-Cre/ERT* as controls, thus eliminating any confounds owing to the differential presence of *MIP-Cre/ERT*. This strategy enabled the resolution of the kinetics of beta cell calcium response, which closely match the kinetics of insulin secretion (Bergsten et al., 1994), at single-cell resolution. Upon stimulation by high glucose, beta cells from both *Ucn3*-null mice and their wild-type controls respond with an increase in intracellular calcium, as represented by an increase in fluorescence (Figure 2.5). Although there is islet to islet variation in calcium response, beta cells within the same islet all respond in unison. The calcium response is also pulsatile in both *Ucn3*-null and wild-type mice, with the first phase response exhibiting a longer duration than the remaining pulses. This confirms that beta cells within each islet from *Ucn3*-null mice remain capable of sensing and responding to high glucose in a pulsatile and synchronized manner.

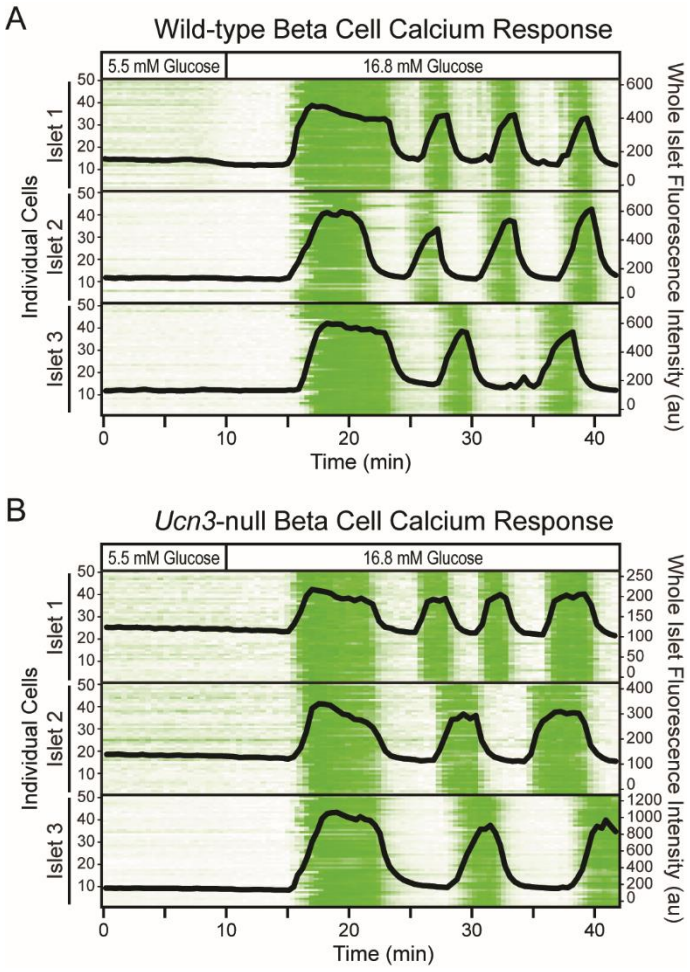

Figure 2.5: Beta cell calcium response remains unaltered in mice that do not express UCN3. Calcium responses of several intact islets were obtained simultaneously over time. All islets expressed the calcium sensor GCaMP6s selectively in beta cells (*MIP-Cre/ERT x lsl-GCaMP6s*) with or without *Ucn3*-null in the background. The trace began with low glucose and was switched to high glucose at the indicated timepoint. The calcium traces of beta cells within 3 representative islets from (A) wild-type mice and (B) *Ucn3*-null mice are shown as intensity plots. Each line represents the activity of an individual beta cell over time, and green represents an increase in fluorescence intensity. A line graph of the fluorescence intensity at the whole islet level is overlaid over each intensity plot.

2.5 Discussion

The peptide hormone UCN3 is one of the last hormones to appear during the postnatal maturation of beta cells (Blum *et al.* 2012; van der Meulen *et al.* 2012). The onset of UCN3 expression trails expression of other established beta cell maturity markers such as MAFA (van der Meulen & Huising 2014), coincides with the acquisition of functional maturity in beta cells (Blum *et al.* 2012), and has been reported to be expressed in functional beta cells derived from transplanted stem cells that were allowed to mature over time *in vivo* (van der Meulen *et al.* 2012; Xie *et al.* 2013). While these observations have helped to establish UCN3 as a very useful marker to identify functionally mature beta cells, both in the pancreas and in differentiated stem cells, the question of whether UCN3 merely marks mature beta cells or is required for beta cells to mature comes up regularly. Here, we resolve this question by demonstrating that genetic deletion of *Ucn3* does not lead to loss of other beta cell maturity markers, nor does it increase the level of expression of beta cell dedifferentiation markers, as determined by RNA-sequencing and validated by immunofluorescence. These observations indicate that beta cells continue to express other maturity markers upon *Ucn3* deletion. This suggests that UCN3 is a maturity marker, but may not directly act on the beta cell to promote beta cell maturation. This is in agreement with reports that treatment of fetal beta cells with UCN3 was insufficient to accelerate beta cell maturation (Blum *et al.* 2012; Liu & Hebrok 2017). This also agrees closely with the fact that the UCN3 receptor Crhr2 is not expressed in beta cells, but is instead selectively expressed by delta cells (DiGruccio *et al.* 2016), which respond to UCN3 with increased somatostatin release (van der Meulen *et al.* 2015).

Furthermore, beta cells from *Ucn3*-null mice exhibit synchronized, pulsatile calcium responses to high glucose comparable to the responses of beta cells from wild-type mice. The rise in intracellular calcium is required for the mobilization of insulin secretory granules, and synchronized, oscillatory

calcium response has been demonstrated to be critical for the secretion of insulin (Rorsman & Renström 2003). Our data therefore suggests that beta cells in *Ucn3*-null mice retain proper insulin secretion capabilities. However, while the kinetics of beta cell calcium responses are similar between wild-type and *Ucn3*-null mice, GCaMP6s is not calibrated to detect absolute calcium concentrations and instead detects relative changes in intracellular calcium. These are known to track the kinetics (Bergsten et al., 1994; Ravier et al., 2002), but not necessarily the magnitude of insulin secretion. Furthermore, increases in intracellular calcium levels may not represent a proportional increase in secretion. Indeed, we have previously demonstrated that beta cells in *Ucn3*-null mice exhibit exaggerated first and second phase insulin secretion that can be normalized acutely by addition of synthetic UCN3 peptide (van der Meulen *et al.* 2015). These mice also display increased glucose tolerance (van der Meulen *et al.* 2015) (Figure 2.9), setting up the interesting paradox that UCN3 is a marker for functional maturity that restrains glucose-stimulated insulin secretion. We have proposed that such feedback inhibition maintained by UCN3-dependent, somatostatin-mediated restraint on insulin secretion prevents reactive hypoglycemia (Huising et al., 2018).

We also demonstrate that beta cell states that are normally marked by the absence of UCN3, such as immature 'virgin' beta cells, can still be detected despite the genetic ablation of the *Ucn3* gene. Virgin beta cells were still readily identifiable at the islet periphery using alternative maturity markers such as csGLUT2 instead of UCN3 (Beamish *et al.* 2016). Conversely, the loss of UCN3 expression is an early hallmark of beta cell dedifferentiation (Blum *et al.* 2014; van der Meulen *et al.* 2015) that coincides with an increase in the expression of the dedifferentiation marker ALDH1A3 (Kim-Muller *et al.* 2016). Indeed, we confirmed the increase of ALDH1A3 expression in beta cells from *ob/ob* mice and demonstrate that there is a corresponding decrease in UCN3 in beta cells. However, the genetic deletion of UCN3 did not by itself cause an increase in ALDH1A3 expression in beta cells. This is similar to how the dedifferentiation marker ALDH1A3 did not induce beta cell dedifferentiation when

over expressed (Kim-Muller *et al.* 2016). Therefore, the expression of ALDH1A3 and the loss of UCN3 expression are both strong markers of dedifferentiation, but do not drive beta cell dedifferentiation. Our experiment establishes that loss of UCN3 expression is in fact an effect of beta cell dedifferentiation that occurs reliably and early on. Interestingly, *Ucn3*-null mice have been previously reported to be protected from metabolic dysfunction associated with a high-fat diet or old age (Li *et al.* 2007). This is likely due to the decreased somatostatin tone seen in *Ucn3*-null mice (van der Meulen *et al.* 2015), which would allow them to maintain increased insulin secretion to compensate for growing insulin resistance. Indeed, restoration of Ucn3 expression in moderately glycemic *ob/ob* mice at a disease stage where endogenous Ucn3 has been downregulated immediately aggravates hyperglycemia (van der Meulen *et al.* 2015), suggesting that the downregulation in effect is protective under these conditions of increased peripheral insulin resistance.

Collectively, our observations here indicate that although the onset of the endogenous expression of UCN3 marks the point at which beta cells acquire functional maturity, beta cells will express other common maturity markers and develop the capability for synchronized, pulsatile calcium responses to high glucose despite the lack of UCN3. These observations that UCN3 is not necessary for beta cell maturation should not distract from the utility of endogenous UCN3 as an excellent beta cell maturity marker under circumstances other than the genetic manipulation of the *Ucn3* gene. Furthermore, although UCN3 does not directly signal to beta cells, the possibility that the somatostatin secretion triggered by endogenous UCN3 contributes indirectly to mature beta cell identity and function remains. The onset of UCN3 expression around 2 weeks after birth in mice is correlated with a distinct rise in the glycemic setpoint (Blum *et al.* 2012), which has long been attributed to the maturation of beta cells (Rozzo *et al.* 2009; Jermendy *et al.* 2011). We have previously shown that premature induction of UCN3 specifically in beta cells causes a premature increase in the glycemic set point in mice (van der Meulen *et al.* 2015). This suggests that UCN3-stimulated somatostatin secretion

is the underlying mechanism responsible for the rise in glycemic set point by attenuating insulin secretion, underscoring the importance of paracrine pathways for normal islet function. Whether somatostatin contributes to beta cell maturation beyond this direct attenuation of insulin secretion is an important question that remains unresolved.

2.6 Funding & Acknowledgements

This work was supported by the National Institute of Diabetes and Digestive and Kidney Disease (NID DK-110276), the Juvenile Diabetes Research Foundation (CDA-2-2013-54 and 2-SRA-2019-700-S-B), and the American Diabetes Association (#1-19-IBS-078). JLH was supported by a National Institute of General Medical Sciences-funded Pharmacology Training Program (T32 GM-099608). SL was supported by the NSF Graduate Research Fellowship (1650042), the UC Davis Training Program in Molecular and Cellular Biology (T32 GM-007377), and the UC Davis NSF Bridge to Doctorate Program (1612490). We thank Jerice Banola, Ariana Momen, and Mohammad Pourhosseinzadeh for assistance with cell quantifications.

2.7 Materials and Methods

2.7.1 Animals

Mice were maintained in group housing on a 12-hour light/12-hour dark cycle with free access to water and standard rodent chow. *Ucn3*-null mice were described previously (Li et al., 2007). For all experiments, mice heterozygous for the *Ucn3*-null allele (*Ucn3*$^{+/-}$, referred to as *Ucn3*-het) were used to produce knockout mice (*Ucn3*$^{-/-}$, referred to as *Ucn3*-null) and control littermates (*Ucn3*$^{+/+}$, referred to as *Ucn3*-wt, or *Ucn3*-het). *Ucn3*-het mice were crossed to mice expressing *Tg(Ins1-cre/ERT)1Lph*,

henceforth referred to as *MIP-Cre/ERT* (Wicksteed *et al.* 2010), and *Gt(ROSA)26Sor*$^{tm96(CAG-GCaMP6s)Hze}$, henceforth referred to as *lsl-GCaMP6s* (Madisen *et al.* 2015), to produce *Ucn3*-het mice that express either *MIP-Cre/ERT* or *lsl-GCaMP6s*. They were then crossed together to produce *Ucn3*-null mice hemizygous for both *MIP-Cre/ERT* and *lsl-GCaMP6s*. These mice selectively and efficiently expressed GCaMP6s in beta cells upon oral administration of tamoxifen (Sigma-Aldritch, T5648) dissolved in sunflower seed oil (Trader Joe's) at 20 mg/mL for 5 consecutive days. Euthanization and islet isolation were carried out after a 3-day washout period. Heterozygous B6.Cg-Lep^{ob}/J breeders were bought from The Jackson Laboratories to produce homozygous mice, referred to as *ob/ob* (Coleman 1978).

Mice were used between 4-6 months of age unless otherwise indicated. All mouse experiments were approved by the UC Davis Institutional Animals Care and Use Committee and were performed in compliance with the Animal Welfare Act and the Institute for Laboratory Animal Research (ILAR) Guide to the Care and Use of Laboratory Animals.

2.7.2 Glucose Tolerance Test

Mice were weighed after an overnight fast, then given a bolus of 2g/kg glucose (dextrose; Sigma-Aldritch, D9559) via intraperitoneal injection. Blood glucose levels were collected over a 2 hour time period using tail vein blood by the OneTouch Ultra glucometer.

2.7.3 Immunofluorescence

Immunofluorescence was conducted as follows: slides were washed for 5 minutes 3 times in KPBS, then incubated with antibodies diluted in KPBS supplemented with 2% donkey serum and 0.4% Triton X-100 overnight at 4°C. Slides were then washed 3 more times in KPBS, incubated with secondary antibodies and DAPI (1 μg/mL) diluted in donkey block for 45 minutes at room

temperature, and washed 3 more times before embedding in Prolong Gold Antifade (Thermo Fisher Scientific, Waltham, MA). Images were obtained on a Nikon A1R+ confocal microscope.

2.7.4 Islet isolation

Islets were isolated by injecting 2 mL collagenaseP (0.8 mg/mL, Invitrogen) dissolved in HBSS (Roche Diagnostics) into the pancreas via the common bile duct while the ampulla of Vater was clamped. The pancreas was then collected and submerged with an additional 2 mL of collagenase solution, incubated at 37°C for 13 minutes, then dissociated through gentle manual shaking. The dissociated pancreas was then washed 3 times with cold HBSS containing 5% NCS, then passed through a nylon mesh (pore size 425 um, Small Parts) and isolated by density gradient centrifugation on a Histopaque gradient (1.077 g/mL, Sigma) for 20 min at 1400 x g without brake. Islets were collected from the interface, washed once with cold HBSS containing 5% NCS, then hand-picked several times under a dissecting microscope before culturing in RPMI (Roche Diagnostics) containing 5.5 mM glucose, 10% FBS, and pen/strep.

2.7.5 Next generation sequencing and bioinformatics

RNA isolation, library preparation, sequencing, and alignment were performed as previously described (van der Meulen *et al.* 2015). Briefly, RNA was isolated from Trizol by a chloroform extraction, then precipitated by isopropanol and cleaned up over an RNEasy microcolumn (Qiagen, Valencia, CA) per the manufacturer's instructions. RNA quality was determined by BioAnalyzer (Agilent, Santa Clara, CA). Libraries were generated using the TruSeq RNA Sample Prep Kit v2 (Illumina Inc., San Diego, CA) and sequenced at 50 cycles, single read on an Illumina HiSeq 2000 platform. Reads were aligned to mouse genome version mm9 using STAR.

2.7.6 Western blotting

50 islets were lysed using 30 μL sample treatment buffer (50 mM Tris (pH 7.5), 100 mM dithiothreitol, 2% (weight/volume) sodium dodecyl sulfate, 0.1% (weight/volume) bromophenol blue, and 10% (weight/volume) glycerol). Lysates were run on a SDS/PAGE gel and transferred nitrocellulose membranes (Whattman). Immunoblotting was done using rabbit anti-UCN3 (#7218) (gift from Dr. Wylie Vale, 1:1000) and the secondary antibody donkey anti-rabbit conjugated to HRP (GE Healthcare U.K. Ltd., 1:5000).

2.7.7 Functional imaging

After isolation, islets were placed in 35 mm dishes with a glass bottom (#1.5, MatTek Corporation) and allowed to adhere by culturing overnight. Islets were imaged over time in 3D on a Nikon A1R+ confocal microscope using a 20x lens. Continuous perfusion of islets with Krebs Ringer Buffer was done using a Masterflex peristaltic pump at 2.5 mL per minute. Islets were perfused with low glucose for 10 minutes to obtain baseline fluorescence, then switched to high glucose at the indicated time point. Regions of interest were drawn around single cells or single islets to obtain fluorescence intensity using Nikon Elements software.

2.7.8 Antibodies

Primary antibodies used were chicken polyclonal anti-insulin (Abcam ab14042, 1:1000), rat monoclonal anti-insulin (R&D Systems, 1:500), guinea pig polyclonal anti-insulin (Dako #A0564; 1:500), rabbit (#7218) or guinea pig (#044) polyclonal anti-UCN3 (gift from Dr. Wylie Vale, 1:1000), rabbit polyclonal anti-MAFA (Bethyl Laboratories IHC-00352, 1:100), rabbit polyclonal anti-MafB (Bethyl Laboratories IHC-00351, 1:100), rabbit polyclonal anti-PDX1 (Abcam ab47267, 1:500), rabbit polyclonal anti-ERO1LB (gift from Dr. David Ron, 1:300), rabbit polyclonal anti-G6PC2 (Gift from

Drs. Jay Walters and Howard Davidson, 1:200), rabbit polyclonal anti-GLUT2 (EMD Millipore #07-1402I, 1:1000), rabbit polyclonal anti-ALDH1A3 (Novus Biologicals NBP2-15339, 1:500). Secondary antibodies were obtained from Jackson ImmunoResearch and used at a 1:600 dilution.

2.7.9 Statistical Analysis

Data were analyzed by Student's t-test, corrected for multiple comparisons using the Holm-Sidak method where appropriate, and represented as mean ± SEM, with n representing number of animals in each group. Differences were considered significant when $p < 0.05$. Statistics were computed using Prism (GraphPad Software, La Jolla, CA).

2.8 Supplemental Materials

Table 2.1: Significantly enriched genes in wild-type (22 genes) and *Ucn3*-null (7 genes) mouse islets.

Gene name	Expression in WT	Expression in *Ucn3*-null	Fold change	Enriched in	p-value
Ucn3	10330.43	115.88	6.48	WT	4.19E-154
Marcksl1-ps4	170.04	22.64	2.91	WT	7.78E-21
Hhex	681.66	356.48	0.94	WT	4.21E-07
Ehf	1202.57	671.04	0.84	WT	2.79E-06
Akr1c19	1150.20	2274.55	0.98	*Ucn3*-null	3.06E-06
Ptprz1	426.84	223.80	0.93	WT	2.50E-05
Rbp4	2917.68	1723.14	0.76	WT	3.04E-05
Sst	56869.92	23561.20	1.27	WT	0.00016
Akr1c14	2085.59	1359.16	0.62	WT	0.00017
Efnb3	433.82	239.72	0.86	WT	0.00024
Mest	337.44	182.04	0.89	WT	0.00051
Oit1	220.92	107.88	1.03	WT	0.00084
Spock3	355.35	199.41	0.83	WT	0.00120
Cacna1h	301.89	168.85	0.84	WT	0.00290
Prom1	2974.07	4871.46	0.71	*Ucn3*-null	0.00325
F5	185.77	92.54	1.01	WT	0.00341
Net1	612.59	1059.56	0.79	*Ucn3*-null	0.00390
Sdk2	2320.57	3276.15	0.50	*Ucn3*-null	0.00458
Arg1	952.77	551.88	0.79	WT	0.02419
Rasgrf2	959.72	1399.87	0.54	*Ucn3*-null	0.02446
Akr1c21	18.28	1.28	3.83	WT	0.03432
Lgals3	115.68	54.23	1.09	WT	0.03432
AW551984	242.24	142.27	0.77	WT	0.03432
Reg2	79.72	346.54	2.12	*Ucn3*-null	0.03432
Vipr2	62.52	126.79	1.02	*Ucn3*-null	0.04133
Tmsb10	669.07	456.44	0.55	WT	0.04166
Fn1	336.97	131.98	1.35	WT	0.04181
Gap43	106.83	49.92	1.10	WT	0.04339
Aldh1a2	63.46	20.56	1.63	WT	0.04967

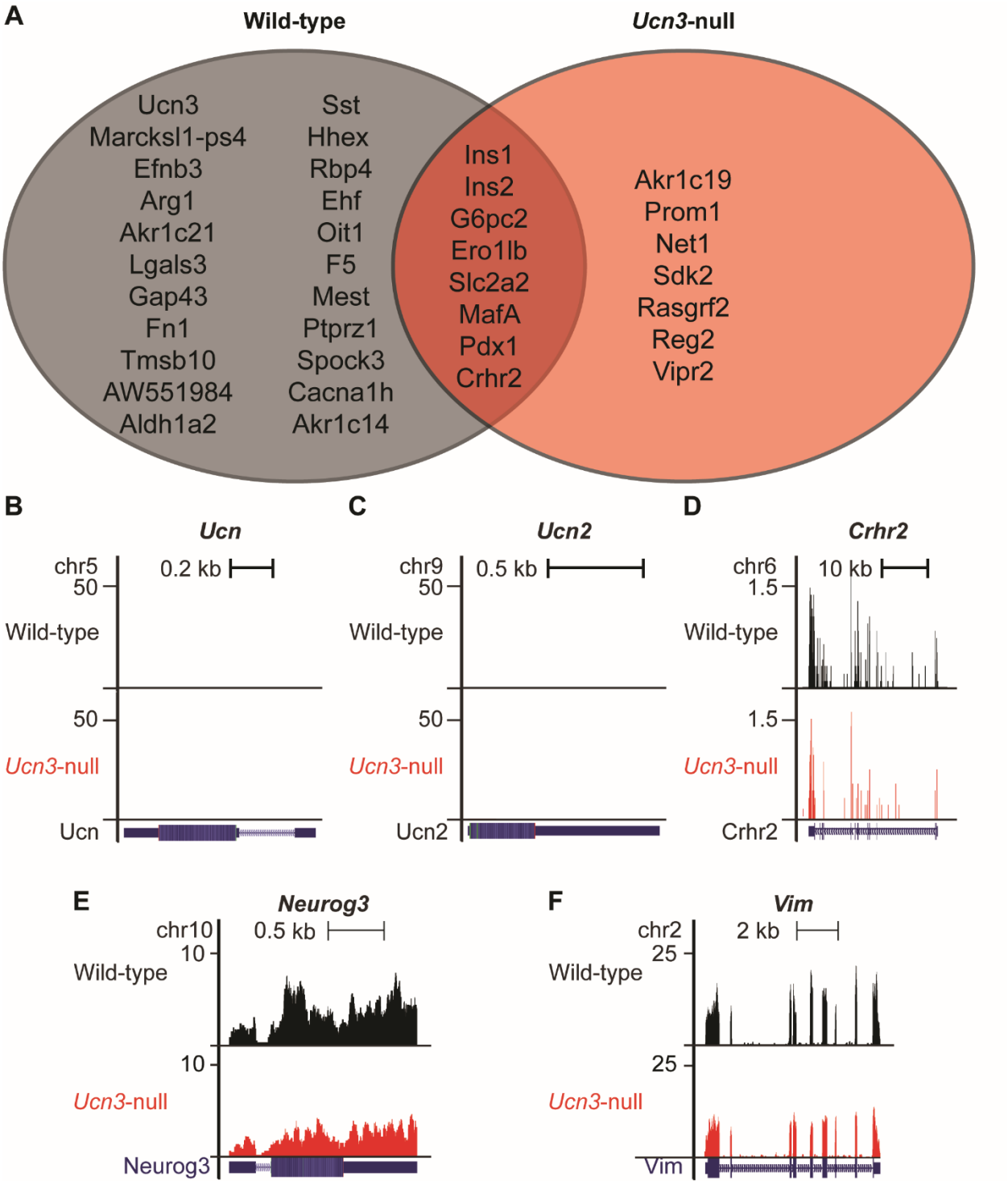

Figure 2.6: S1, related to Figure 2.1.

Figure 2.6: (continued) (A) Venn diagram showing genes enriched in wild-type and *Ucn3*-null islets, and a subset of genes that are not differentially expressed in either. (B) Browser plot for *Ucn* in wild-type and *Ucn3*-null islets. No reads are detected. (C) Browser plot for *Ucn2* in wild-type and *Ucn3*-null islets. No reads are detected in wild-type mice. There are detectable but minimal reads for *Ucn2* in *Ucn3*-null mice, but as the reads do not span the entire exon and are low in expression, this is likely background. (D) *Crfr2* remains expressed in *Ucn3*-null mice. (E and F) Browser plots showing no difference in expression for *Neurog3* (E) and *Vim* (F), which encode NGN3 and VIMENTIN, respectively.

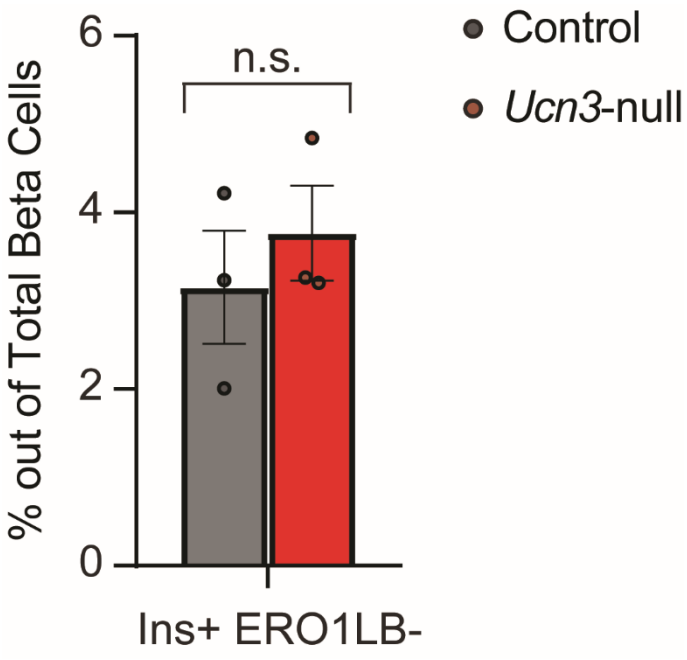

Figure 2.7: S2, related to Figure 2.2. Quantification of insulin- and ERO1LB-expressing cells in control and *Ucn3*-null mice. There is no significant difference in expression of ERO1LB in beta cells between control (3.15% ± 1.11%) and *Ucn3*-null mice (3.77% ± 0.93%). n = 3 animals per group, at least 10 islets and 500 cells counted per animal. Error bars reflect SEM.

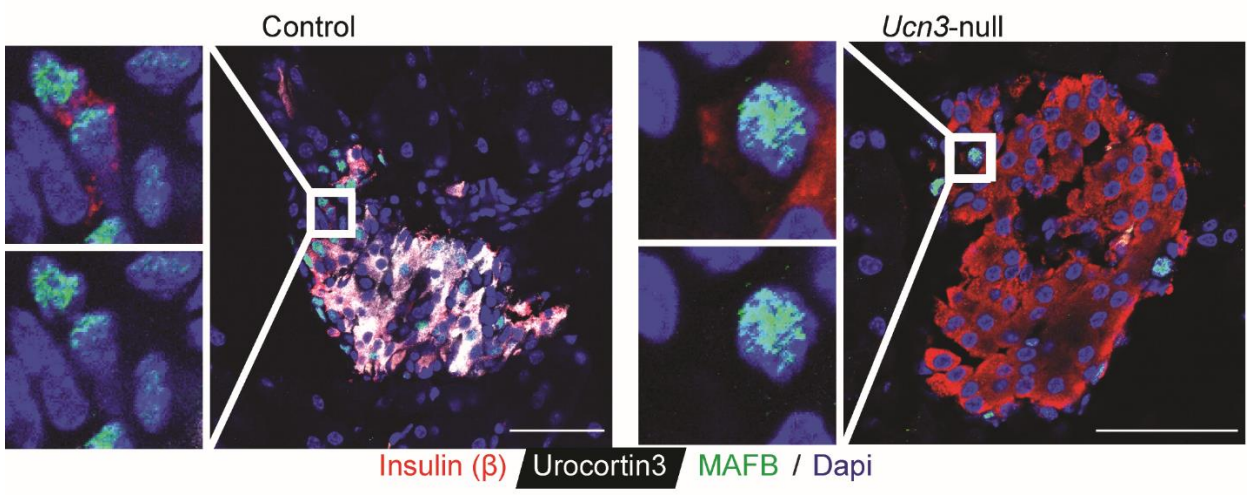

Figure 2.8: S3, related to Figure 2.4. Immunofluorescent stain for insulin, UCN3, and MAFB in a control and *Ucn3*-null mouse. Close-ups (red and green overlap and white and green overlay) show a UCN3-negative beta cell expressing MAFB.

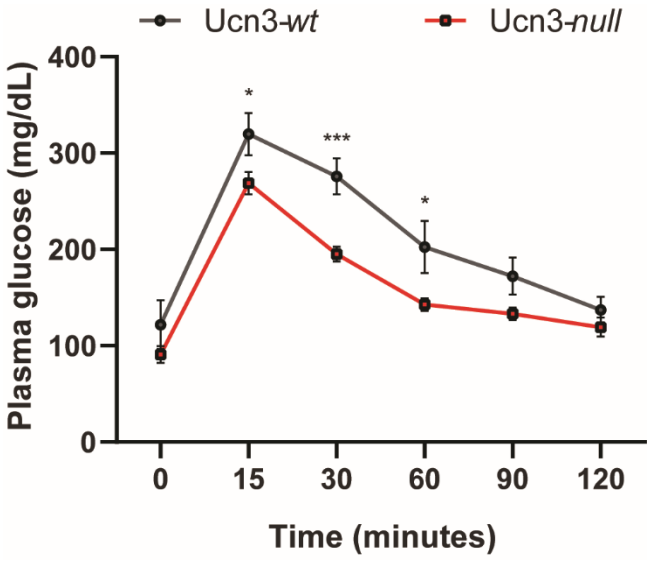

Figure 2.9: S4, related to Figure 2.5. Glucose tolerance test of 5-month old *Ucn3-null* mice and littermate wild-type controls. *Ucn3-null* mice are significantly more glucose tolerant relative to wild-type controls.

2.9 References

Artner I, Hang Y, Mazur M, Yamamoto T, Guo M, Lindner J, Magnuson MA & Stein R 2010 MafA and MafB regulate genes critical to β-cells in a unique temporal manner. *Diabetes* **59** 2530–2539. (doi:10.2337/db10-0190)

Beamish CA, Strutt BJ, Arany EJ & Hill DJ 2016 Insulin-positive, Glut2-low cells present within mouse pancreas exhibit lineage plasticity and are enriched within extra-islet endocrine cell clusters. *Islets* **8** 65–82. (doi:10.1080/19382014.2016.1162367)

Bergsten P, Grapengiesser E, Gylfe E, Tengholm A & Hellman B 1994 Synchronous oscillations of cytoplasmic Ca2+ and insulin release in glucose-stimulated pancreatic islets. *Journal of Biological Chemistry* **269** 8749–8753.

Blum B, Hrvatin S, Schuetz C, Bonal C, Rezania A & Melton DA 2012 Functional beta-cell maturation is marked by an increased glucose threshold and by expression of urocortin 3. *Nature Biotechnology* **30** 261–264. (doi:10.1038/nbt.2141)

Blum B, Roose AN, Barrandon O, Maehr R, Arvanites AC, Davidow LS, Davis JC, Peterson QP, Rubin LL & Melton DA 2014 Reversal of β cell de-differentiation by a small molecule inhibitor of the TGFβ pathway. *ELife* **3** e02809. (doi:10.7554/eLife.02809)

Carboneau BA, Le TDV, Dunn JC & Gannon M 2016 Unexpected effects of the MIP-CreER transgene and tamoxifen on β-cell growth in C57Bl6/J male mice. *Physiological Reports* **4**. (doi:10.14814/phy2.12863)

Coleman DL 1978 Obese and diabetes: Two mutant genes causing diabetes-obesity syndromes in mice. *Diabetologia* **14** 141–148. (doi:10.1007/BF00429772)

DiGruccio MR, Mawla AM, Donaldson CJ, Noguchi GM, Vaughan J, Cowing-Zitron C, van der Meulen T & Huising MO 2016 Comprehensive alpha, beta and delta cell transcriptomes reveal that ghrelin selectively activates delta cells and promotes somatostatin release from pancreatic

islets. *Molecular Metabolism* **5** 449–458. (doi:10.1016/j.molmet.2016.04.007)

Huising MO, van der Meulen T, Huang JL, Pourhosseinzadeh MS & Noguchi GM 2018 The Difference δ-Cells Make in Glucose Control. *Physiology* **33** 403–411. (doi:10.1152/physiol.00029.2018)

Hunter CS & Stein RW 2017 Evidence for loss in identity, de-differentiation, and trans-differentiation of islet β-cells in type 2 diabetes. *Frontiers in Genetics* **8**. (doi:10.3389/fgene.2017.00035)

Jermendy A, Toschi E, Aye T, Koh A, Aguayo-Mazzucato C, Sharma A, Weir GC, Sgroi D & Bonner-Weir S 2011 Rat neonatal beta cells lack the specialised metabolic phenotype of mature beta cells. *Diabetologia* **54** 594–604. (doi:10.1007/s00125-010-2036-x)

Kim-Muller JY, Fan J, Kim YJR, Lee SA, Ishida E, Blaner WS & Accili D 2016 Aldehyde dehydrogenase 1a3 defines a subset of failing pancreatic β cells in diabetic mice. *Nature Communications* **7** 1–11. (doi:10.1038/ncomms12631)

Lewis K, Li C, Perrin MH, Blount A, Kunitake K, Donaldson C, Vaughan J, Reyes TM, Gulyas J, Fischer W *et al.* 2001 Identification of urocortin III, an additional member of the corticotropin-releasing factor (CRF) family with high affinity for the CRF2 receptor. *Proceedings of the National Academy of Sciences of the United States of America* **98** 7570–7575. (doi:10.1073/pnas.121165198)

Li C, Chen P, Vaughan J, Blount A, Chen A, Jamieson PM, Rivier J, Smith MS & Vale W 2003 Urocortin III is expressed in pancreatic β-cells and stimulates insulin and glucagon secretion. *Endocrinology* **144** 3216–3224. (doi:10.1210/en.2002-0087)

Li C, Chen P, Vaughan J, Lee K-F & Vale W 2007 Urocortin 3 regulates glucose-stimulated insulin secretion and energy homeostasis. *Proc Natl Acad Sci* **10** 4206–4211. (doi:10.1073pnas.0611641104)

Liu JSE & Hebrok M 2017 All mixed up: Defining roles for β-cell subtypes in mature islets. *Genes*

and Development **31** 228–240. (doi:10.1101/gad.294389.116)

Madisen L, Garner AR, Shimaoka D, Chuong AS, Klapoetke NC, Li L, van der Bourg A, Niino Y, Egolf L, Monetti C *et al.* 2015 Transgenic mice for intersectional targeting of neural sensors and effectors with high specificity and performance. *Neuron* **85** 942–958. (doi:10.1016/j.neuron.2015.02.022)

van der Meulen T & Huising MO 2014 Maturation of stem cell-derived beta-cells guided by the expression of urocortin 3. *Review of Diabetic Studies* **11** 115–132. (doi:10.1900/RDS.2014.11.115)

van der Meulen T, Xie R, Kelly OG, Vale WW, Sander M & Huising MO 2012 Urocortin 3 Marks Mature Human Primary and Embryonic Stem Cell-Derived Pancreatic Alpha and Beta Cells. *PLoS ONE* **7** 1–12. (doi:10.1371/journal.pone.0052181)

van der Meulen T, Donaldson CJ, Cáceres E, Hunter AE, Cowing-Zitron C, Pound LD, Adams MW, Zembrzycki A, Grove KL & Huising MO 2015 Urocortin3 mediates somatostatin-dependent negative feedback control of insulin secretion. *Nature Medicine* **21** 769–776. (doi:10.1038/nm.3872)

van der Meulen T, Mawla AM, DiGruccio MR, Adams MW, Nies V, Dolleman S, Liu S, Ackermann AM, C??ceres E, Hunter AE *et al.* 2017 Virgin Beta Cells Persist throughout Life at a Neogenic Niche within Pancreatic Islets. *Cell Metabolism* **25** 911-926.e6. (doi:10.1016/j.cmet.2017.03.017)

Nair GG, Liu JS, Russ HA, Tran S, Saxton MS, Chen R, Juang C, Li M lan, Nguyen VQ, Giacometti S *et al.* 2019 Recapitulating endocrine cell clustering in culture promotes maturation of human stem-cell-derived β cells. *Nature Cell Biology* **21** 263–274. (doi:10.1038/s41556-018-0271-4)

Pagliuca FW, Millman JR, Gürtler M, Segel M, Van Dervort A, Ryu JH, Peterson QP, Greiner D & Melton DA 2014 Generation of functional human pancreatic β cells in vitro. *Cell* **159** 428–439. (doi:10.1016/j.cell.2014.09.040)

Ravier M, Sehlin J & Henquin J 2002 Disorganization of cytoplasmic Ca2+ oscillations and pulsatile

insulin secretion in islets from ob/ob mice. *Diabetologia* **45** 1154–1163. (doi:10.1007/s00125-002-0883-9)

Rezania A, Bruin JE, Arora P, Rubin A, Batushansky I, Asadi A, O'Dwyer S, Quiskamp N, Mojibian M, Albrecht T *et al.* 2014 Reversal of diabetes with insulin-producing cells derived in vitro from human pluripotent stem cells. *Nature Biotechnology* **32** 1121–1133. (doi:10.1038/nbt.3033)

Rorsman P & Renström E 2003 Insulin granule dynamics in pancreatic beta cells. *Diabetologia* **46** 1029–1045. (doi:10.1007/s00125-003-1153-1)

Rozzo A, Meneghel-Rozzo T, Delakorda SL, Yang SB & Rupnik M 2009 Exocytosis of insulin: In vivo maturation of mouse endocrine pancreas. In *Annals of the New York Academy of Sciences*, pp 53–62. Blackwell Publishing Inc. (doi:10.1111/j.1749-6632.2008.04003.x)

Russ HA, Parent A V., Ringler JJ, Hennings TG, Nair GG, Shveygert M, Guo T, Puri S, Haataja L, Cirulli V *et al.* 2015 Controlled induction of human pancreatic progenitors produces functional beta-like cells in vitro. *The EMBO Journal* **34** 1759–1772. (doi:10.15252/embj.201591058)

Thompson PJ, Shah A, Ntranos V, Gool F Van, Atkinson M, Bhushan A, Thompson PJ, Shah A, Ntranos V, Gool F Van *et al.* 2019 Targeted Elimination of Senescent Beta Cells Prevents Type 1 Diabetes Article Targeted Elimination of Senescent Beta Cells Prevents Type 1 Diabetes. *Cell Metabolism* 1–16. (doi:10.1016/j.cmet.2019.01.021)

Velazco-Cruz L, Song J, Maxwell KG, Goedegebuure MM, Augsornworawat P, Hogrebe NJ & Millman JR 2019 Acquisition of Dynamic Function in Human Stem Cell-Derived β Cells. *Stem Cell Reports* **12** 351–365. (doi:10.1016/j.stemcr.2018.12.012)

Veres A, Faust AL, Bushnell HL, Engquist EN, Kenty JHR, Harb G, Poh YC, Sintov E, Gürtler M, Pagliuca FW *et al.* 2019 Charting cellular identity during human in vitro β-cell differentiation. *Nature* **569** 368–373. (doi:10.1038/s41586-019-1168-5)

Wicksteed B, Brissova M, Yan W, Opland DM, Plank JL, Reinert RB, Dickson LM, Tamarina NA,

Philipson LH, Shostak A *et al.* 2010 Conditional gene targeting in mouse pancreatic β-cells: Analysis of ectopic cre transgene expression in the brain. *Diabetes* **59** 3090–3098. (doi:10.2337/db10-0624)

Xie R, Everett LJ, Lim HW, Patel NA, Schug J, Kroon E, Kelly OG, Wang A, D'Amour KA, Robins AJ *et al.* 2013 Dynamic chromatin remodeling mediated by polycomb proteins orchestrates pancreatic differentiation of human embryonic stem cells. *Cell Stem Cell* **12** 224–237. (doi:10.1016/j.stem.2012.11.023)

Chapter 3

Effect of somatostatin on beta and alpha cell gene expression

3.1 Preface

This chapter contains unpublished work. I performed the experiments and analyzed the RNA-seq data with the help of Dr. Alex Mawla. Observations made from these data will be expanded upon by another PhD student in the lab, Ryan Hart. A version of the figures and text may be used for a future manuscript. I will be a co-author on any publications that come from this work and will participate in the editing process.

3.2 Abstract

Over 30 million people in the US have diabetes, a disease characterized by chronic hyperglycemia that occurs due to insulin insufficiency. As beta cells are the sole producers of insulin, there is strong interest in identifying ways to preserve or create functional beta cell mass for the treatment of diabetes. Alpha cells act in opposition to beta cells by secreting glucagon to increase blood glucose levels. While this generally occurs only under hypoglycemic conditions in non-diabetic individuals, alpha cells have been demonstrated to secrete excess glucagon even under hyperglycemic conditions in diabetic patients, aggravating the disease. Clustered with beta and alpha cells within the islets of Langerhans are delta cells, which secrete somatostatin (SST). SST acts as a paracrine inhibitor for both beta and

alpha cells, and is therefore a key regulator within the pancreatic islet. While the inhibitory action of SST is known, the potential contribution of SST signaling to beta cell and alpha cell gene expression as a mechanism for shaping function has not been studied. Here we investigate the effect of exogenous SST treatment on the beta and alpha cell transcriptome, as well as the effect of blocking endogenous SST signaling through selective SST receptor antagonists. We also provide data on changes in whole islet gene expression in the absence of SST and in the absence of delta cells. We conclude that SST signaling contributes to changes in gene expression that reflect function, and propose a potential role of SST in regulating actin remodeling within the islet.

3.3 Introduction

Diabetes affects over 30 million people in the US, and the number is projected to rise substantially throughout the next decade. (Menke *et al.* 2015) This disease is characterized by the failure to produce or respond properly to the hormone insulin, leading to chronic hyperglycemia. As beta cells are the only cell type in our body capable of producing insulin, there is considerable interest in learning how to maintain them in a state of functional maturity. The neighboring alpha cells, which secrete glucagon to increase blood glucose levels, have also been shown to contribute to diabetes through excess glucagon secretion during hyperglycemia, further exacerbating the high blood glucose levels in diabetic patients (Müller *et al.* 1970; Unger & Cherrington 2012). There is also evidence that they demonstrate impaired counterregulatory response to hypoglycemia in diabetic patients (Segel *et al.* 2002). Thus, there is increasing interest in developing ways to regulate alpha cells and inhibit them under hyperglycemic conditions while preserving their ability to secrete glucagon under hypoglycemic conditions.

Beta cells and alpha cells cluster with several other hormone-secreting cells to form the islets of Langerhans, which are found scattered throughout the pancreas. The third most common cell type

within the islet is the somatostatin (SST)-secreting delta cells. In contrast to beta cells and alpha cells, which release their respective hormones into the bloodstream to signal to other tissues, delta cells release SST as a paracrine signal to beta cells and alpha cells, repressing secretion of insulin and glucagon respectively (Hauge-Evans *et al.* 2009). There was five different subtypes of the SST receptors (SSTR), with SSTR3 predominantly expressed on beta cells in primary cilia (Iwanaga *et al.* 2011; DiGruccio *et al.* 2016) and SSTR2 predominantly expressed on alpha cells (Kailey *et al.* 2012) in mice. Due to the role of delta cells in regulating both beta cells and alpha cells, there is an opportunity to target and modulate their activity for the treatment of diabetes.

SST secretion in delta cells is stimulated by Urocortin3 (UCN3), a hormone that beta cells co-secrete with insulin in mice (van der Meulen *et al.* 2015). Under hyperglycemic conditions, this triggers a negative feedback loop in which UCN3-mediated SST secretion timely attenuates insulin secretion. UCN3 is an established marker of mature beta cells, and the rise of UCN3 expression in beta cells correlates with beta cells developing functional maturity (Blum *et al.* 2012; van der Meulen *et al.* 2012). During chronic hyperglycemia, beta cells lose expression of UCN3, marking the beginning of dedifferentiation (Blum *et al.* 2014; van der Meulen *et al.* 2015). This decreases in local SST tone within the beta cell environment, despite reports that pancreatic delta cell numbers are stable (Braun 2014) or increase (Strowski & Blake 2008) in diabetic patients. The subsequent disinhibition of insulin then allows for increased insulin secretion to combat rising hyperglycemia. While this may be an adaptive response to rising insulin demand, sustained demand for insulin leads to beta cell exhaustion and dysfunction (Weir & Bonner-Weir 2004). This exacerbates hyperglycemia and frank diabetes. Decreased SST signaling may therefore contribute to beta cell dysfunction by enabling beta cell exhaustion. Indeed, a clinical study showed that overnight infusion of SST restored more normal insulin secretion in Type 2 Diabetes patients, but the direct effect on beta cells was not investigated (Laedtke *et al.* 2000). Likewise, the loss of SST signaling within the pancreatic islet has been suggested

to contribute to the dysregulation of alpha cells in diabetes, as absence of somatostatin leads to glucagon hypersecretion (Hauge-Evans *et al.* 2009) and the disinhibition of alpha cells may allow for excess glucagon secretion that aggravates hyperglycemia (Noguchi & Huising 2019).

In addition to the direct effects of SST on beta and alpha cell secretion, there is a distinct but completely unexplored possibility that SST mediates changes in gene expression. After beta cells lose UCN3 and local SST tone decreases, other genes associated with beta cell identity and beta cell function are gradually lost as diabetes progresses (Talchai *et al.* 2012; Dor & Glaser 2013; Guo *et al.* 2013). Therefore, there is an association between SST signaling and beta cell functional maturity. While UCN3 is not required for beta cell maturity and its absence *per se* does not drive dedifferentiation (Huang *et al.* 2020), there is a possibility of a direct effect of SST on mature beta cell gene expression as well as alpha cell expression.

Here we examine the effect of SST on beta and alpha cell gene expression, as well as the effect of blocking SST signaling using antagonists against SST receptors (SSTR). We observe changes in genes involved in beta cell function, and in particular note the significant upregulation of genes involved in actin remodeling in SST-treated beta cells, which may also be the case for SST-treated alpha cells. There is strong overlap between genes upregulated upon SST treatment and downregulated upon SSTR antagonist treatment and vice versa, suggesting the changes we observe upon intervention in SST signaling are specific. We also examine the effects of chronic loss of SST and loss of delta cells on the whole islet transcriptome. We conclude that changes in gene expression that reflect function in beta and alpha cells occur due to acute response to SST signaling.

3.4 Results

3.4.1 FACS-purification of beta and alpha cells

To obtain transcriptomic data in beta and alpha cells from the same islets, we crossed *mIns1*-H2B-mCherry mice to *Gcg*-CreERT mice with a Rosa-LSL-YFP reporter to label beta cells with nuclear mCherry and alpha cells with YFP (Figure 3.1). This enabled us to purify beta and alpha cells using FACS from each of the treated samples. To assess the effect of SST on gene expression, we incubated islets with 100 nM SST for 6 hours. We chose the 6-hour time point to ensure that we would be able to observe any potential changes that would occur. Since alpha cells express both SSTR2 and SSTR3 and beta cells selectively express SSTR3 (Kailey *et al.* 2012; DiGruccio *et al.* 2016), we also incubated islets with 100 nM of the SSTR2-selective antagonist #406–028–15 (Cescato *et al.* 2008) and SSTR3-selective antagonist #315–260–15 (Reubi *et al.* 2000) to investigate the effects of blocking SST signaling. We also performed a combination treatment of SST with both SSTR antagonists.

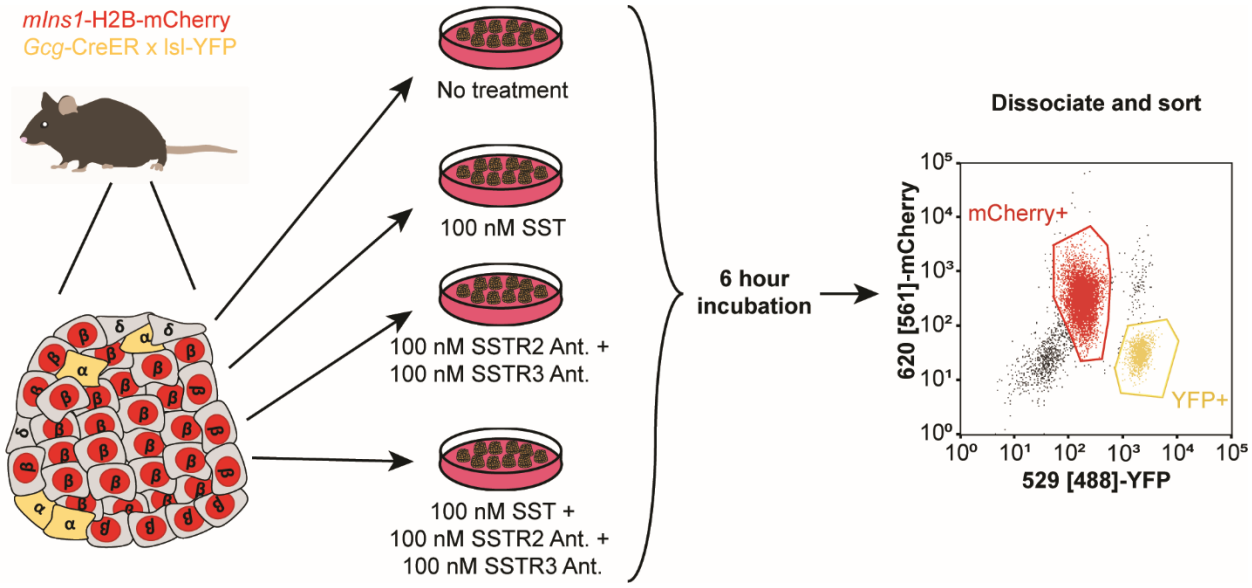

Figure 3.1: Schematic of islet incubation and cell sorting strategy. Islets were isolated from multiple mIns1-H2B-mCherry x Gcg-CreER x lsl-YFP mice, pooled together, and then split into four different treatment groups. After a 6-hour incubation, islets from each group were dissociated to obtain both beta and alpha cells from each sample. A representative FACS plot showing dissociated beta and alpha cells from a single sample is shown.

3.4.2 Effect of SST and SSTR antagonists on beta cell gene expression

Transcriptomic comparison of beta cells treated with 100 nM SST for 6 hours relative to the non-treated control revealed 43 significantly upregulated genes in SST-treated samples and 12 downregulated, as defined by an absolute $\log_2$ fold change of greater than 0.5 and a FDR value of less than 0.05 (Figure 3.2A, Table 3.1). We observed a significant increase in *Slc2a2*, a known beta cell maturity marker that encodes for the primary glucose transporter in beta cells, as well as *Cox6a2*, which encodes Complex IV in the mitochondria and contributes to the generation of ATP needed for insulin secretion. However, we also observed a significant decrease in *Mafa* expression, which encodes a transcription factor that is essential for driving beta cell maturation. Unexpectedly, we discovered that several of the top differentially regulated genes encoded for proteins involved in actin regulation. These include *Rflna*, *Fhod3*, *Tmod1*, and *Mical3*. As actin remodeling is required for insulin secretion, it is possible that these genes are involved in this process. Thus, exogenous SST does not affect beta cell maturity but may regulate several genes that contribute to insulin secretion.

Similarly, transcriptomic comparison with beta cells treated with SSTR antagonists revealed 44 significantly upregulated genes and 37 downregulated genes (Figure 3.2B, Table 3.2). Among the downregulated genes, many overlapped with the upregulated genes in SST-treated beta cells, including *Rflna* and *Fhod3* (Table 3.3). There was also overlap between the upregulated genes in the SSTR antagonist-treated samples and the downregulated genes in the SST-treated samples. There was no significant change in the expression of many of these genes in samples simultaneously treated with SST and the SSTR antagonists, and those that were differentially regulated exhibited smaller changes in expression (Figure 3.2C, Table 3.4). This provides confidence that the changes in these genes are specific to SST signaling or blockage thereof.

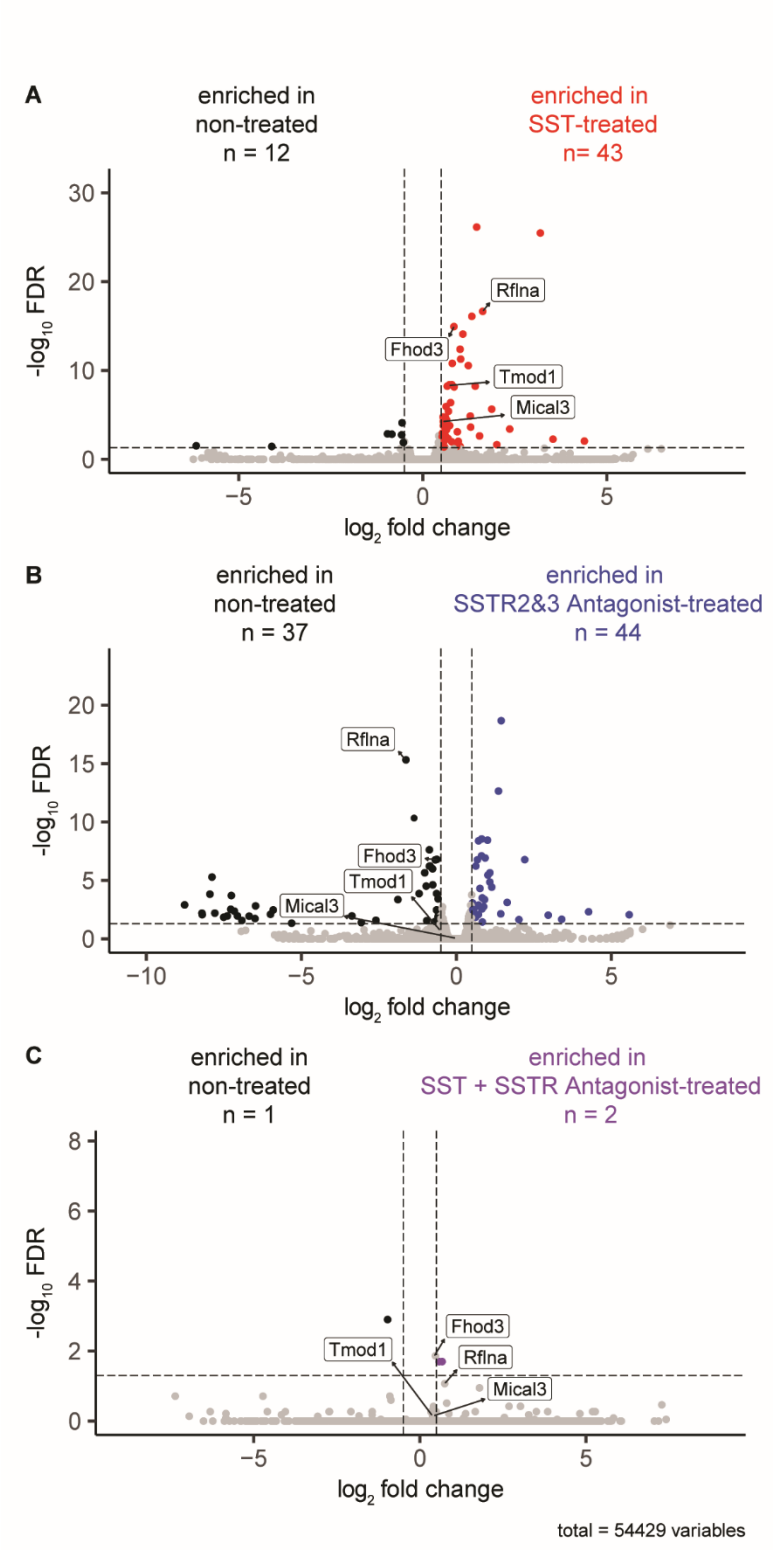

Figure 3.2: Changes in beta cell gene expression in response to SST and SSTR antagonists. Volcano plots showing differentially expressed genes in beta cells in response to A) SST, B) SST antagonists, and C) SST with SST antagonists, with actin-related genes highlighted.

3.4.3 Effect of SST and SSTR antagonists on alpha cell gene expression

We reported the same analyses for SST- and SSTR antagonist-treated alpha cells. Due to insufficient separation of beta cells from alpha cells in one of the samples, only one SST-treated replicate was available for analyses. We found 1 gene downregulated by and 16 upregulated by SST treatment (Figure 3.3A, Table 3.5). Interestingly, in the SSTR antagonist-treated samples, *Rflna* and *Spon2* both displayed the same decrease in expression observed in SSTR antagonist-treated beta cells (Figure 3.3B, Table 3.6). Although we were unable to conduct statistics, our results indicate upregulation in SST-treated alpha cells as well (Table 3.5). As in beta cells, a combination of SST and SSTR antagonist treatment led to few differentially expressed genes (Figure 3.3C, Table 3.7).

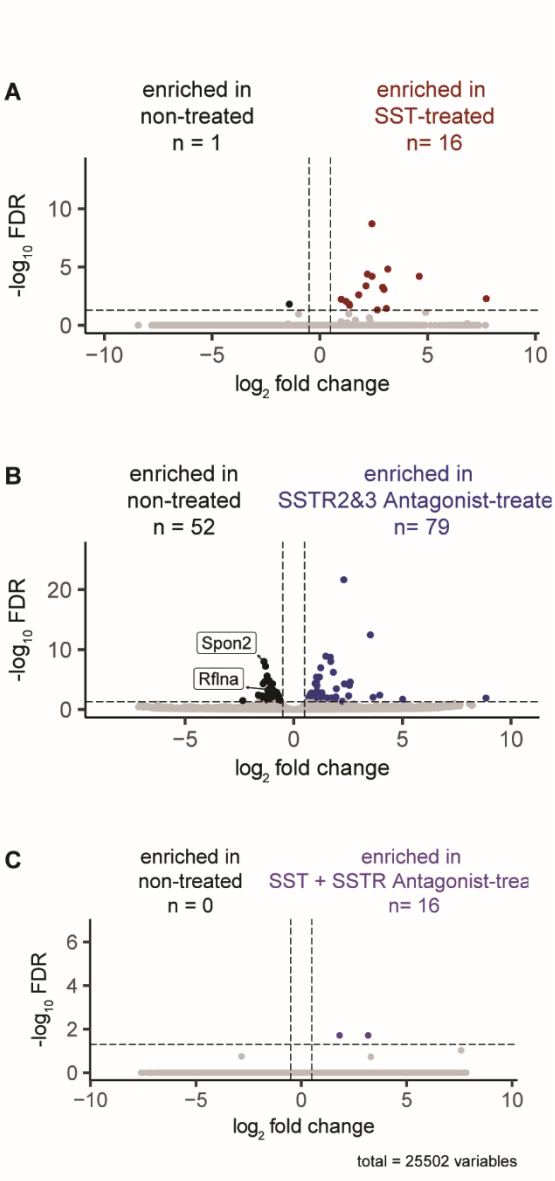

Figure 3.3: Changes in alpha cell gene expression in response to SST and SSTR antagonists. Volcano plots showing differentially expressed genes in alpha cells in response to A) SST, B) SST antagonists, and C) SST with SST antagonists.

3.5 Discussion

Within the pancreatic islet, paracrine SST signaling from delta cells plays an important regulatory role for both beta and alpha cells. SST signals through SSTRs, which are all $G_{\alpha i/o}$-coupled receptors that inhibit cell activity through the inhibition of adenylyl cyclase. This is thought to be the primary mechanism by which SST inhibits secretory activity, although SST has also been reported to block exocytosis directly and through activation of G-coupled inwardly-rectifying potassium channels, which help repolarize the cell (Kailey *et al.* 2012). While the effects of exogenous SST on beta and alpha cell secretory activity is well-established, there have been no studies investigating effects on gene expression. Our data provide insight into transcriptional changes that occur due to stimulation of or blocking of the SSTRs found on beta and alpha cells, and suggest an entirely novel mechanism for regulation of exocytosis by SST in beta and alpha cells in addition to known mechanisms of decreased cAMP and calcium signaling.

The development of cell-specific fluorescent reporter mouse lines allows for highly pure isolation of different cell types from the same samples. Using mCherry fluorescent in beta cells and YFP fluorescent in alpha cells, we obtained both beta and alpha cells from islets that underwent the same treatment of SST, SSTR antagonists, or both in combination. One of the signals that stimulates SST release within the pancreatic islet is UCN3 from beta cells. (van der Meulen *et al.* 2015) UCN3 is a known markers of beta cell maturity, and furthermore its expression coincides with the acquisition of beta cell maturity (Blum *et al.* 2012). Thus, increased UCN3 expression and a subsequent increase in SST signaling within the islet are associated with beta cell maturation. We hypothesized that there may be a more direct role of SST signaling on beta cell maturation. Analysis of differential gene expression in beta cells treated with SST revealed that while there was an increase in expression of beta cell maturity marker *Slc2a2*, there was in contrast a decrease in *Mafa*. Conversely, *Mafa* expression increased with blocking of endogenous SST signaling using SSTR antagonists. No difference was

observed in the expression of other beta cell maturity markers. While it is possible that SST may play a more important role during beta cell development, these data suggest that it is unlikely that SST contributes to the retention of beta cell maturity in islets from adult mice.

Unexpectedly, we observed an enrichment in a cluster of genes involved in actin regulation in both beta and alpha cells obtained from islets treated with SST. The opposite effect was observed in cells from islets treated with the SSTR antagonists. Actin dynamics are known to play an important role to hormone and neurotransmitter release. It has also been demonstrated that failure to remodel the actin cytoskeleton inhibits insulin secretion from beta cells (Naumann *et al.* 2018). While SST has been proposed to regulate actin dynamics to modulate cell migration in other tissues (Buchan *et al.* 2002; Peverelli *et al.* 2018), this is a novel mechanism for the inhibition of hormone secretion in beta and alpha cells.

Overall, SST may regulate actin dynamics within beta and alpha cells through similar downstream mechanisms. The transcriptomic changes observed may reflect the cell replenishing the proteins needed to continue remodeling the actin cytoskeleton. The role of these proteins in regulating actin dynamics within beta and alpha cells and the specific mechanism by they are regulated by SST signaling will be further investigated.

3.6 Funding & Acknowledgements

This work was supported by the National Institute of Diabetes and Digestive and Kidney Disease (NID DK-110276), the Juvenile Diabetes Research Foundation (CDA-2-2013-54 and 2-SRA-2019-700-S-B), and the American Diabetes Association (#1-19-IBS-078). JLH was supported by a National Institute of General Medical Sciences-funded Pharmacology Training Program (T32 GM-099608).

3.7 Materials and Methods

3.7.1 Animals

Mice were maintained in group housing on a 12-hour light/12-hour dark cycle with free access to water and standard rodent chow. Mice were used between 16-22 weeks of age. The *mIns1*-H2B-mCherry x *Gcg*-CreER x Rosa-LSL-YFP mice were generated by breeding *mIns1*-H2B-mCherry (Benner *et al.* 2014), *Gcg*-creER (Ackermann *et al.* 2016), and Rosa-LSL-YFP (Srinivas *et al.* 2001) mice with complementary transgenes. These mice selectively and efficiently expressed YFP in alpha cells upon oral administration of tamoxifen (Sigma-Aldritch, T5648) dissolved in sunflower seed oil (Trader Joe's) at 20 mg/mL for 5 consecutive days. Euthanization and islet isolation were carried out after a 3-day washout period for mice treated with tamoxifen. All mouse experiments were approved by the UC Davis Institutional Animals Care and Use Committee and were performed in compliance with the Animal Welfare Act and the Institute for Laboratory Animal Research (ILAR) Guide to the Care and Use of Laboratory Animals.

3.7.2 Islet isolation and FACS sorting

Islets were isolated by injecting collagenaseP (0.8 mg/mL, Invitrogen) dissolved in HBSS (Roche Diagnostics) into the pancreas via the common bile duct while the ampulla of Vater was clamped. The pancreas was collected and incubated at 37°C, then dissociated through gentle manual shaking. After passing the dissociated pancreas through a nylon mesh (pore size 425 um, Small Parts), islets were isolated by density gradient centrifugation on a Histopaque gradient (1.077 g/mL, Sigma) for 20 min at 1400 x g without brake. Islets were collected from the interface then hand-picked several times under a dissecting microscope before culturing in RPMI (Roche Diagnostics) containing 5.5 mM glucose, 10% FBS, and pen/strep. Islets were pooled and allowed to recover overnight. The next

morning, the islets were split into groups and incubated for 6 hours with their respective treatments, followed by dissociation. Islets from *Sst*-Cre$^{+/TG}$, *Sst*-Cre$^{TG/TG}$, *Sst*-Cre x lsl-DTR mice were not pooled and were dissociated immediately following the islet isolation. Dissociation was achieved using 0.25% trypsin-EDTA (Gibco) followed by manual pipetting. The dispersed cells were resuspended in RPMI and kept on ice until sorting. Cell sorting was performed using a Beckman Coulter Astrios EQ cell sorter. The 405 nm excitation line was used to exclude dead cells identified by Dapi. The 488 nm and 561 nm excitation lines were used to for mCherry and eYFP, respectively. Each sample was sorted directly into Trizol to ensure immediate cell lysis and to preserve RNA integrity.

3.7.4 RNA isolation and library prep

RNA isolation, library preparation, sequencing, and alignment were performed as previously described (van der Meulen *et al.* 2015). Briefly, RNA was isolated from Trizol by a chloroform extraction, then precipitated by isopropanol and cleaned up over an RNEasy microcolumn (Qiagen, Valencia, CA) per the manufacturer's instructions. RNA quality was determined by BioAnalyzer (Agilent, Santa Clara, CA). Libraries were generated using the TruSeq Stranded mRNA Library Prep Kit (Illumina Inc., San Diego, CA) and sequenced at 50 cycles, single read on an Illumina HiSeq 2000 platform.

3.7.5 Next generation sequencing and bioinformatics

Reads were aligned to mouse genome version mm9 using STAR (Dobin *et al.* 2013). FeatureCounts was used to create counts tables (Liao *et al.* 2014). Differential gene expression analysis was performed using edgeR (Robinson *et al.* 2009). GO term and KEGG pathway analysis were performed using clusterProfiler (Yu *et al.* 2012).

3.7.6 Statistical analysis

Data were analyzed by Student's t-test, corrected for multiple comparisons using the Holm-Sidak method where appropriate, and represented as mean ± SEM, with n representing number of animals in each group. Differences were considered significant when $p < 0.05$. Statistics were computed using Prism (GraphPad Software, La Jolla, CA).

3.8 Supplemental Information

To be continued on the next page

Table 3.1: Top 40 differentially expressed genes in SST-treated beta cells

Gene name	Expression in NT	Expression in SST-treated	Fold change	Enriched in	FDR
Zdhhc22	5.22	14.45	1.46	SST	7.18E-27
Gm572	13.01	26.61	1.03	SST	5.28E-12
3425401B19Rik	0.56	1.37	1.30	SST	2.43E-04
Gm49477	0.49	2.52	2.36	SST	3.98E-04
Gm34759	23.61	38.04	0.69	SST	4.69E-03
Npas4	0.46	4.22	3.19	SST	3.34E-26
Gm44698	0.72	2.98	2.01	SST	2.28E-02
Rflna	10.15	31.33	1.63	SST	2.22E-17
Kcnn3	3.43	8.66	1.33	SST	8.13E-17
Fhod3	15.11	27.24	0.85	SST	1.15E-15
Gpr161	2.74	5.85	1.09	SST	8.04E-15
Tmtc1	3.99	8.08	1.01	SST	4.11E-13
Pip4k2a	8.30	14.48	0.80	SST	1.59E-11
Spon2	4.05	9.57	1.24	SST	2.81E-11
Tmod1	7.40	12.81	0.79	SST	3.98E-09
Glb1l2	8.91	14.75	0.72	SST	4.03E-09
Hdac9	0.39	1.06	1.43	SST	5.97E-09
Anks4b	11.60	18.40	0.66	SST	5.97E-09
Hdac5	14.43	26.11	0.85	SST	7.16E-09
Defb1	127.77	216.33	0.76	SST	4.22E-07
Pitpnm3	6.55	10.17	0.63	SST	1.16E-06
Mical3	2.76	4.49	0.70	SST	3.97E-06
Arhgef37	1.23	3.02	1.29	SST	1.35E-05
Dgke	5.02	7.37	0.55	SST	1.75E-05
Cntn1	6.62	10.12	0.61	SST	1.79E-05
Slc2a2	28.95	45.44	0.65	SST	3.68E-05
Lgi2	5.41	7.98	0.56	SST	5.50E-05
Star	9.34	6.32	0.56	NT	7.90E-05
Osbpl3	1.69	2.80	0.73	SST	1.63E-04
Arhgap44	7.35	10.86	0.56	SST	1.65E-04
Il6st	11.58	18.15	0.65	SST	4.69E-04
Tmem117	2.15	4.12	0.94	SST	8.19E-04
Cited2	12.48	18.84	0.59	SST	9.68E-04
Tom1l1	3.18	4.64	0.54	SST	1.08E-03
Lgalsl	7.69	11.16	0.54	SST	1.12E-03
Fam167a	2.19	1.13	0.96	NT	1.38E-03
Mafa	58.57	32.87	0.84	NT	1.53E-03
Rhou	7.19	4.84	0.57	NT	1.79E-03
Kcnip2	0.44	1.29	1.54	SST	2.38E-03
Prkacb	52.19	79.33	0.60	SST	2.38E-03

Table 3.2: Top 40 differentially expressed genes in SSTR Antagonist-treated beta cells

Gene name	Expression in NT	Expression in ANT-treated	Fold change	Enriched in	FDR
Igf1r	16.08	41.83	1.45	ANT	2.11E-19
Rflna	10.15	3.14	1.63	NT	4.76E-16
Etv5	2.37	5.81	1.36	ANT	2.24E-13
Spon2	4.05	1.50	1.36	NT	4.62E-11
Plk3	35.55	59.79	0.82	ANT	2.79E-09
Dusp4	6.19	11.90	1.01	ANT	3.58E-09
Star	9.34	14.63	0.71	ANT	4.08E-09
Rasd1	19.47	10.20	0.87	NT	2.40E-08
Lrrc10b	44.21	74.17	0.81	ANT	7.90E-08
Shisal1	4.36	7.91	0.93	ANT	1.19E-07
Fhod3	15.11	9.33	0.63	NT	1.58E-07
Nptx2	0.47	2.06	2.21	ANT	1.66E-07
Per2	11.57	17.67	0.68	ANT	1.71E-07
Glb1l2	8.91	5.31	0.68	NT	1.72E-07
Zdhhc22	5.22	2.78	0.85	NT	5.90E-07
Ext1	5.33	7.87	0.63	ANT	5.90E-07
Bmf	4.03	2.11	0.87	NT	6.02E-07
Hdac5	14.43	8.12	0.77	NT	1.02E-06
Fos	12.30	5.79	1.02	NT	2.21E-06
Mafa	58.57	118.82	1.08	ANT	2.21E-06
Pde10a	2.32	4.47	1.02	ANT	3.51E-06
Cpb1	2.22	0.01	7.88	NT	5.14E-06
Areg	7.09	14.36	1.08	ANT	1.40E-05
Rgs4	39.24	22.17	0.76	NT	2.38E-05
Egr1	11.68	5.67	0.97	NT	3.06E-05
Ubr4	27.68	58.02	1.14	ANT	3.76E-05
Tnfrsf21	10.29	16.63	0.76	ANT	4.87E-05
Defb1	127.77	78.56	0.64	NT	1.33E-04
Hdac9	0.39	0.16	1.20	NT	1.33E-04
Reg1	4.70	0.01	7.95	NT	1.49E-04
Gpt2	14.48	19.46	0.49	ANT	1.74E-04
Ctrb1	57.77	0.36	7.26	NT	1.97E-04
Pdyn	4.87	8.29	0.84	ANT	3.13E-04
Slc40a1	7.26	4.60	0.59	NT	3.74E-04
Npas4	0.46	0.12	1.89	NT	4.36E-04
Spred2	2.92	5.27	0.91	ANT	4.37E-04
Hcar2	0.74	2.19	1.64	ANT	7.72E-04
Inpp5f	12.77	17.48	0.52	ANT	8.45E-04
Pnliprp2	0.96	0.00	8.76	NT	1.25E-03
Gabbr2	11.02	17.25	0.72	ANT	1.30E-03

Table 3.3: Overlap of genes between SST-treated and SSTR Antagonist treated beta cells

Gene Name	SST	ANT
Zdhhc22	Up	Down
Npas4	Up	Down
Rflna	Up	Down
Kcnn3	Up	Down
Fhod3	Up	Down
Gpr161	Up	Down
Spon2	Up	Down
Glb1l2	Up	Down
Hdac9	Up	Down
Hdac5	Up	Down
Defb1	Up	Down
Rgs4	Up	Down
Fam189a2	Up	Down
Bmf	Up	Down
Star	Down	Up
Fam167a	Down	Up
Mafa	Down	Up
Lrrc10b	Down	Up

Table 3.4: Differentially expressed genes in SST + SSTR Antagonist-treated beta cells

Gene name	Expression in NT	Expression in SST + ANT-treated	Fold change	Enriched in	FDR
Kcnn3	3.43	5.33	0.67	SST + ANT	1.47E-06
Tmtc1	3.99	5.82	0.58	SST + ANT	1.33E-06
Fos	12.30	6.18	-0.97	NT	2.32E-08

Table 3.5: Differentially expressed genes in SST-treated alpha cells

Gene name	Expression in NT	Expression in SST-treated	Fold change	Enriched in	FDR
Sytl4	0.35	1.81	2.42	SST	1.96E-09
Flt1	0.03	0.21	3.15	SST	1.51E-05
Gad1	0.22	0.96	2.21	SST	4.08E-05
Gpr158	0.22	1.17	2.42	SST	6.34E-05
Msln	0.07	1.92	4.61	SST	6.34E-05
Prlr	0.05	0.24	2.14	SST	4.19E-04
Fam151a	0.19	1.35	2.92	SST	5.47E-04
Kdr	0.02	0.17	2.98	SST	8.40E-04
Tmem215	0.23	0.77	1.80	SST	2.46E-03
Cd93	0.00	0.17	7.72	SST	5.26E-03
Calb1	10.86	21.29	0.99	SST	5.91E-03
Slc2a2	0.73	1.63	1.22	SST	9.02E-03
Ucn3	1.91	4.73	1.37	SST	1.54E-02
Sik1	4.14	1.53	1.42	NT	1.54E-02
Npas4	1.86	4.81	1.38	SST	1.97E-02
Olfm4	0.04	0.40	3.09	SST	3.63E-02
Eng	0.09	0.68	2.67	SST	4.80E-02
Spon2	17.15	24.86	0.56	SST	1
Rflna	32.61	49.35	0.62	SST	1

Table 3.6: Top 40 differentially expressed genes in SSTR Antagonist-treated alpha cells

Gene Name	Expression in NT	Expression in ANT-treated	Fold change	Enriched in	FDR
Pde10a	2.23	10.87	2.30	ANT	2.21E-22
Tac1	0.60	6.81	3.53	ANT	3.60E-13
Peg10	7.66	20.90	1.47	ANT	1.29E-09
Pde1c	2.07	6.50	1.68	ANT	1.85E-09
Nr4a2	3.01	9.64	1.70	ANT	9.88E-09
Spon2	17.15	6.61	1.37	NT	9.88E-09
Junb	75.44	30.39	1.30	NT	6.24E-08
Lrrc10b	16.30	38.23	1.24	ANT	1.10E-07
Ppargc1a	1.49	5.24	1.82	ANT	6.30E-07
Hdac5	18.37	7.80	1.23	NT	2.61E-06
Oxtr	18.10	36.76	1.05	ANT	3.89E-06
Igf1r	4.15	9.28	1.18	ANT	3.89E-06
Insrr	8.47	3.86	1.13	NT	1.46E-05
Dbp	9.17	3.50	1.34	NT	2.38E-05
Syt5	20.87	42.46	1.04	ANT	2.64E-05
Gm26799	1.71	10.31	2.60	ANT	2.69E-05
Ier2	59.43	27.44	1.09	NT	3.25E-05
Stk32a	23.18	45.25	0.99	ANT	4.66E-05
Bbc3	18.22	6.84	1.41	NT	5.03E-05
Gucy2c	0.55	2.71	2.33	ANT	5.31E-05
Mapk15	37.97	19.25	0.97	NT	5.31E-05
Diras2	0.57	3.30	2.56	ANT	9.75E-05
Larp1b	2.97	6.13	1.06	ANT	1.03E-04
Jun	108.10	50.20	1.09	NT	2.53E-04
Prlr	0.05	0.16	1.96	ANT	3.51E-04
Fos	78.82	33.86	1.20	NT	6.01E-04
Rflna	32.61	17.01	0.94	NT	6.18E-04
Fbp1	19.35	39.75	1.07	ANT	8.94E-04
Pfkl	15.94	9.24	0.78	NT	1.48E-03
Mettl27	14.80	7.55	0.94	NT	1.63E-03
C1galt1	9.01	21.42	1.29	ANT	1.63E-03
Esr1	11.33	19.58	0.81	ANT	1.74E-03
Notch1	5.14	2.85	0.84	NT	1.94E-03
Rasd1	19.97	10.04	0.99	NT	2.47E-03
Sik1	4.14	8.98	1.12	ANT	2.79E-03
Ifih1	10.17	17.03	0.76	ANT	2.93E-03
Gm45774	3.95	1.30	1.63	NT	4.03E-03
5330413D20Rik	0.36	5.86	3.96	ANT	4.08E-03
Arl5a	6.57	13.97	1.15	ANT	4.30E-03
Thra	23.18	14.03	0.71	NT	4.84E-03

Table 3.7: Differentially expressed genes in SST + SSTR Antagonist-treated alpha cells

Gene name	Expression in NT	Expression in SST + ANT-treated	Fold change	Enriched in	FDR
H2-Ab1	0.10	1.09	3.17	SST + ANT	1.93E-02
CD31	1.89	7.00	1.81	SST + ANT	1.93E-02

3.9 References

Ackermann AM, Zhang J, Heller A, Briker A & Kaestner KH 2016 High-fidelity Glucagon-CreER mouse line generated by CRISPR-Cas9 assisted gene targeting. *Molecular Metabolism* **6** 236–244. (doi:10.1016/j.molmet.2017.01.003)

Benner C, van der Meulen T, Cacéres E, Tigyi K, Donaldson CJ & Huising MO 2014 The transcriptional landscape of mouse beta cells compared to human beta cells reveals notable species differences in long non-coding RNA and protein-coding gene expression. *BMC Genomics* **15** 620. (doi:10.1186/1471-2164-15-620)

Blum B, Hrvatin S, Schuetz C, Bonal C, Rezania A & Melton DA 2012 Functional beta-cell maturation is marked by an increased glucose threshold and by expression of urocortin 3. *Nature Biotechnology* **30** 261–264. (doi:10.1038/nbt.2141)

Blum B, Roose AN, Barrandon O, Maehr R, Arvanites AC, Davidow LS, Davis JC, Peterson QP, Rubin LL & Melton DA 2014 Reversal of β cell de-differentiation by a small molecule inhibitor of the TGFβ pathway. *ELife* **3** e02809. (doi:10.7554/eLife.02809)

Braun M 2014 *The Somatostatin Receptor in Human Pancreatic β-Cells*. Elsevier Inc. (doi:10.1016/B978-0-12-800174-5.00007-7)

Buchan AMJ, Lin CY, Choi J & Barber DL 2002 Somatostatin, acting at receptor subtype 1, inhibits Rho activity, the assembly of actin stress fibers, and cell migration. *Journal of Biological Chemistry* **277** 28431–28438. (doi:10.1074/jbc.M201261200)

Cescato R, Erchegyi J, Waser B, Piccand V, Mäcke HR, Rivier JE & Reubi JC 2008 Design and in vitro Characterization of Highly Sst2 -selective Somatostatin Antagonists Suitable for Radio-Targeting. *J Med Chem* **51** 4030–4037. (doi:10.1021/jm701618q)

DiGruccio MR, Mawla AM, Donaldson CJ, Noguchi GM, Vaughan J, Cowing-Zitron C, van der Meulen T & Huising MO 2016 Comprehensive alpha, beta and delta cell transcriptomes reveal

that ghrelin selectively activates delta cells and promotes somatostatin release from pancreatic islets. *Molecular Metabolism* **5** 449–458. (doi:10.1016/j.molmet.2016.04.007)

Dobin A, Davis CA, Schlesinger F, Drenkow J, Zaleski C, Jha S, Batut P, Chaisson M & Gingeras TR 2013 STAR: Ultrafast universal RNA-seq aligner. *Bioinformatics* **29** 15–21. (doi:10.1093/bioinformatics/bts635)

Dor YP & Glaser BMD 2013 Beta-Cell Dedifferentiation and Type 2 Diabetes. *The New England Journal of Medicine* **368** 572–573. (doi:10.1056/NEJMcibr1214034)

Guo S, Dai C, Guo M & Taylor B 2013 Inactivation of specific β cell transcription factors in type 2 diabetes. *The Journal of Clinical Investigation* **123** 3305–3316. (doi:10.1172/JCI65390.Experiments)

Hauge-Evans AC, King AJ, Carmignac D, Richardson CC, Robinson ICAF, Low MJ, Christie MR, Persaud SJ & Jones PM 2009 Somatostatin secreted by islet δ-cells fulfills multiple roles as a paracrine regulator of islet function. *Diabetes* **58** 403–411. (doi:10.2337/db08-0792)

Huang JL, Lee S, Hoek P, van der Meulen T, Van R & Huising MO 2020 Genetic deletion of urocortin 3 does not prevent functional maturation of beta cells. *Journal of Endocrinology* **246** 69–78. (doi:10.1530/JOE-19-0535)

Iwanaga T, Miki T & Takahashi-Iwanaga H 2011 Restricted expression of somatostatin receptor 3 to primary cilia in the pancreatic islets and adenohypophysis of mice. *Biomedical Research* **32** 73–81. (doi:10.2220/biomedres.32.73)

Kailey B, van de Bunt M, Cheley S, Johnson PR, MacDonald PE, Gloyn AL, Rorsman P & Braun M 2012 SSTR2 is the functionally dominant somatostatin receptor in human pancreatic β- and α-cells. *AJP: Endocrinology and Metabolism* **303** E1107–E1116. (doi:10.1152/ajpendo.00207.2012)

Laedtke T, Kjems L, Porksen N, Schmitz O, Veldhuis J, Kao PC & Butler PC 2000 Overnight inhibition of insulin secretion restores pulsatility and proinsulin/insulin ratio in type 2 diabetes. *American Journal of Physiology. Endocrinology and Metabolism* **279** E520-8.

Liao Y, Smyth GK & Shi W 2014 FeatureCounts: An efficient general purpose program for assigning sequence reads to genomic features. *Bioinformatics* **30** 923–930. (doi:10.1093/bioinformatics/btt656)

Menke A, Casagranden S, Geissa L & Cowie CC 2015 Prevalence of and Trends in Diabetes Among Adults in the United States, 1988-2012. *JAMA* **314** 1021–1029. (doi:10.1001/jama.2015.10029)

van der Meulen T, Xie R, Kelly OG, Vale WW, Sander M & Huising MO 2012 Urocortin 3 Marks Mature Human Primary and Embryonic Stem Cell-Derived Pancreatic Alpha and Beta Cells. *PLoS ONE* **7** 1–12. (doi:10.1371/journal.pone.0052181)

van der Meulen T, Donaldson CJ, Cáceres E, Hunter AE, Cowing-Zitron C, Pound LD, Adams MW, Zembrzycki A, Grove KL & Huising MO 2015 Urocortin3 mediates somatostatin-dependent negative feedback control of insulin secretion. *Nature Medicine* **21** 769–776. (doi:10.1038/nm.3872)

Müller WA, Faloona GR, Aguilar-Parada E & Unger RH 1970 Abnormal Alpha-Cell Function In Diabetes- Response to Carohydrate and Protein Ingestion. *New England Journal of Medicine* **283** 109–115. (doi:10.1056/NEJM197007162830301)

Naumann H, Rathjen T, Poy MN & Spagnoli FM 2018 The RhoGAP Stard13 controls insulin secretion through F-actin remodeling. *Molecular Metabolism* **8** 96–105. (doi:10.1016/j.molmet.2017.12.013)

Noguchi GM & Huising MO 2019 Integrating the inputs that shape pancreatic islet hormone release. *Nature Metabolism* **1** 1189–1201. (doi:10.1038/s42255-019-0148-2)

Peverelli E, Giardino E, Treppiedi D, Catalano R, Mangili F, Locatelli M, Lania AG, Arosio M, Spada A & Mantovani G 2018 A novel pathway activated by somatostatin receptor type 2 (SST2): Inhibition of pituitary tumor cell migration and invasion through cytoskeleton protein recruitment. *International Journal of Cancer* **142** 1842–1852. (doi:10.1002/ijc.31205)

Reubi JC, Schaer JC, Wenger S, Hoeger C, Erchegyi J, Waser B & Rivier J 2000 SST3-selective potent peptidic somatostatin receptor antagonists. *Proceedings of the National Academy of Sciences of the United States of America* **97** 13973–13978. (doi:10.1073/pnas.250483897)

Robinson MD, Mccarthy DJ & Smyth GK 2009 edgeR : a Bioconductor package for differential expression analysis of digital gene expression data. *Bioinformatics* **26** 139–140. (doi:10.1093/bioinformatics/btp616)

Segel SA, Paramore DS & Cryer PE 2002 Hypoglycemia-associated autonomic failure in advanced type 2 diabetes. *Diabetes* **51** 724–733. (doi:10.2337/diabetes.51.3.724)

Srinivas S, Watanabe T, Lin CS, William CM, Tanabe Y, Jessell TM & Costantini F 2001 Cre reporter strains produced by targeted insertion of EYFP and ECFP into the ROSA26 locus. *BMC Developmental Biology* **1** 1–8. (doi:10.1186/1471-213X-1-4)

Strowski MZ & Blake AD 2008 Function and expression of somatostatin receptors of the endocrine pancreas. *Molecular and Cellular Endocrinology* **286** 169–179. (doi:10.1016/j.mce.2008.02.007)

Talchai C, Xuan S, Lin H V., Sussel L & Accili D 2012 Pancreatic β cell dedifferentiation as a mechanism of diabetic β cell failure. *Cell* **150** 1223–1234. (doi:10.1016/j.cell.2012.07.029)

Unger RH & Cherrington AD 2012 Glucagonocentric restructuring of diabetes: A pathophysiologic and therapeutic makeover. *Journal of Clinical Investigation* **122** 4–12. (doi:10.1172/JCI60016)

Weir GC & Bonner-Weir S 2004 Five stages of evolving beta-cell dysfunction during progression to diabetes. *Diabetes* **53**. (doi:10.2337/diabetes.53.suppl_3.S16)

Yu G, Wang LG, Han Y & He QY 2012 ClusterProfiler: An R package for comparing biological themes among gene clusters. *OMICS A Journal of Integrative Biology* **16** 284–287. (doi:10.1089/omi.2011.0118)

Chapter 4

Paracrine signaling by pancreatic delta cells determines the glycemic set point

4.1 Preface

This chapter is being prepared for submission to *Cell Metabolism*.

4.1.1 Authorship

Jessica L Huang, Sharon Lee, Mohammad S. Pourhosseinzadeh, Niels Kraemer, Jaresley V. Guillen, Naomi Cinque, Paola Aniceto, Mark O. Huising

I designed and performed the majority of the experiments. Sharon Lee collected the data for Figure 4.4 and provided experimental assistance. Mohammad Pourhosseinzadeh wrote the script to measure the first response of each cell and provided experimental assistance. Niels Kraemer collected Figure 4.7F. Naomi carried out the experiment for Figure 4.9A. The article has been modified to satisfy the formatting requirements of this dissertation.

4.2 Abstract

Pancreatic islets are composed of several types of endocrine cells that coordinate to maintain blood glucose homeostasis. While beta cells and alpha cells are thought to be the main drivers of glucose homeostasis through their secretion of insulin and glucagon respectively, the contribution of delta

cells and somatostatin (SST) secretion to establishing the glycemic set point has not been studied. We have previously demonstrated that co-secretion of Urocortin 3 (UCN3) with insulin from beta cells triggers SST secretion from neighboring delta cells to provide feedback inhibition. We have further demonstrated that premature induction of UCN3 in beta cells causes an increase in basal glucose levels, likely by triggering SST secretion from delta cells to create a negative feedback loop that attenuates insulin secretion. Here we use remove local SST signaling from delta cells within the pancreatic islet to investigate their contribution to the glycemic set point. Our data demonstrate that ablation of delta cells leads to a sustained decrease in the glycemic set point that coincides with a decrease in the glucose threshold for insulin response from beta cells, leading to increased insulin secretion. Conversely, alpha cell ablation had no effect on glycemia. Collectively, these data establish a role of delta cells in determining the glycemic set point through their interaction with beta cells.

4.3 Introduction

Blood glucose levels are maintained within a narrow range around the glycemic set point, defined as a fixed level of blood glucose that the body aims to achieve (Matschinsky & Davis 1998) Glucose homeostasis changes during postnatal development in rodents, but is generally stable within an adult individual throughout the lifespan unless disrupted by disease. In humans, this set point is around 90 mg/dL (approximately 5 mM) (Gerich 1993), while in mice it is around 120-140 mg/dL (approximately 7-8 mM) (Ewing & Tauber 1964; Blum *et al.* 2012; Rodriguez-Diaz *et al.* 2018). Tight regulation of blood glucose homeostasis is crucial, as chronic hyperglycemia causes a plethora of complications and hypoglycemia is acutely life-threatening.

The glycemic set point is often attributed to the crossover point between alpha and beta cell glucose response (Pagliara *et al.* 1974; Rodriguez-Diaz *et al.* 2018). However, the question where and how the glycemic set point is determined continues to elicit debate. The central nervous system (CNS)

is a key regulator of blood glucose homeostasis that has been proposed to be responsible for the glycemic set point (Alonge *et al.* 2021). Indeed, glucose-sensing neurons are present at various regions of the brain, including the ventromedial nucleus, paraventricular nucleus, and lateral hypothalamus (Thorens 2012). Moreover, defects in glucose sensing at these sites contributes to type 2 diabetes. It has also been demonstrated that the CNS is capable of lowering glycemia in an insulin-independent manner (German *et al.* 2011; Morton *et al.* 2013; Ryan *et al.* 2013).

While these observations clearly indicate that the CNS can control glucose levels, there is limited evidence to indicate that CNS sites determine the glycemic set point. In contrast, there is compelling evidence that the pancreatic islet is the major glucostat of the body. Grafting islets from different donor species into diabetic nude mice causes recipients to re-establish a set point matching that of the donors, demonstrating that islets are both sufficient to restore normoglycemia and responsible for determining the homeostatic set point of glucose (Carroll *et al.* 1992). More recently, an experiment in which human islets were grafted into the anterior chamber of the eye in diabetic nude mice demonstrated that the lower glycemic set point established by the donor human islets is dependent on paracrine interactions within the islet (Rodriguez-Diaz *et al.* 2018). These experiments provide evidence that paracrine signals within the pancreatic islet are key players in establishing the glycemic set point.

The hormones released by pancreatic islets are known to play a critical role in blood glucose homeostasis. Under prandial conditions when glycemia is high, beta cells within the islet secrete insulin to signal for the uptake and storage of glucose. Conversely, under post-prandial conditions when glycemia is low, alpha cells secrete glucagon to stimulate hepatic glucose production. There is increasing evidence that paracrine glucagon signaling also amplifies glucose-stimulated insulin secretion (GSIS) by direct stimulation of beta cells (Chambers *et al.* 2017; Svendsen *et al.* 2018; Capozzi *et al.* 2019a, b; Zhu *et al.* 2019; Tellez *et al.* 2020; Liu *et al.* 2021). This suggests that glucagon acts locally

to stimulate GSIS as a paracrine factor during the prandial state, while systemic glucagon action in the absence of insulin release is responsible for its counterregulatory function during the post-prandial state (Huising 2020).

The third major cell type of the islet is the delta cell, which releases somatostatin (SST). At the glycemic set point, beta cells are not yet activated, and alpha cell activity is at a nadir. In contrast, delta cells are active over a range of glucose levels and are known to inhibit beta and alpha cells in a paracrine manner (Hauge-Evans *et al.* 2009; van der Meulen *et al.* 2015; Lai *et al.* 2018; Xu *et al.* 2020; Singh *et al.* 2021). While knockout of SST has been shown to augment glucose-stimulated insulin secretion and arginine-stimulated glucagon secretion, the physiological contribution of delta cell-secreted SST to the glycemic set point remains poorly understood.

There are clear indications that indirectly point to a role of delta cell-derived SST in determining the glycemic set point through their communication with beta cells. Our lab has established that beta cells co-secrete the hormone Urocortin 3 (UCN3) with insulin, and that UCN3 acts in a paracrine manner to stimulate SST secretion from delta cells (van der Meulen *et al.* 2015). Onset of UCN3 expression is associated with an increase in the glycemic set point in mice at around 2 weeks of age (Blum *et al.* 2012). Premature induction in neonatal mice caused a comparable increase in glycemia, while induction after endogenous UCN3 is expressed had no effect, demonstrating that the increase in the set point observed in young mice is caused by the onset of UCN3 expression. On the other hand, UCN3 expression is known to be downregulated in Type 2 Diabetes (T2D), which reduces SST secretion and is thought to allow for a compensatory increase in insulin in the face of insulin resistance (Blum *et al.* 2014; van der Meulen *et al.* 2015; Kavalakatt *et al.* 2019). Indeed, restoring UCN3 expression and inducing SST feedback to suppress insulin secretion in diabetic *ob/ob* mice aggravates hyperglycemia. From these observations, we predicted that SST feedback initiated by

UCN3 stimulation determines the glycemic set point (Huising *et al.* 2018), although this prediction has not been rigorously tested until now.

Here, we demonstrate using three complementary mouse models that removing SST-mediated inhibition of beta cells in adult mice leads to an immediate and sustained decrease of 20-30 mg/dL in glycemia. We demonstrate that the effect on the glycemic set point is specific to the loss of pancreatic delta cell-derived SST, ruling out contributions of non-pancreatic sources of SST to this phenotype. We then demonstrate that this acute drop in the plasma glucose set point is due to an increase in insulin secretion by measuring plasma insulin *in vivo* and secreted insulin *ex vivo*. Similar ablation experiments of pancreatic alpha cells do not shift the glycemic set point. Furthermore, we observe from imaging the calcium response of intact islets over time that there is a decrease in the glucose threshold for beta cell response that matches the observed reduction in the glycemic set point observed *in vivo*. We conclude that in mice, alpha cells do not contribute to the glycemic set point, while delta cells shift the glycemic set point through modulating the glucose threshold for insulin secretion from neighboring beta cells.

4.4 Results

4.4.1 Absence of somatostatin lowers the glycemic set point

To investigate the contribution of SST to the glycemic set point, we first used mice with the *Sst*-IRES-Cre transgene, which is known to disrupt the expression of SST (Viollet *et al.* 2017). Using homozygous *Sst*-IRES-Cre mice (*Sst*-Cre$^{TG/TG}$) crossed to a floxed YFP reporter (lsl-YFP) allowed for identification of delta cells with YFP and confirmed that SST is absent but delta cells remain in *Sst*-Cre$^{TG/TG}$ mice. In contrast, SST remains present in delta cells of heterozygous littermates (*Sst*-Cre$^{+/TG}$ x lsl-YFP) (Figure 4.1A and 4.1B). The absence of *Sst* mRNA in *Sst*-Cre$^{TG/TG}$ mice was also confirmed by qPCR (Figure 4.1C). While *Sst*-Cre$^{+/TG}$ mice had slightly reduced *Sst* expression compared to wild

type control islets, as has been previously reported (Viollet *et al.* 2017), the difference was not statistically significant. We took advantage of how these *Sst*-Cre$^{TG/TG}$ mice are in effect *Sst*-null mice to test the hypothesis that the absence of SST would decrease the glycemic set point.

To determine whether the absence of SST affects glycemia, we conducted weekly glucose measurements on the mice. Both male and female *Sst*-Cre$^{TG/TG}$ mice exhibited lower non-fasting glucose levels compared to control *Sst*-Cre$^{+/TG}$ mice of the same sex (Figures 4.1D and 4.1E). We then investigated whether there were also changes to fasting and challenged glycemia using an intraperitoneal (IP) glucose tolerance test. Neither sex exhibited significant changes in glucose tolerance (Figures 4.1F and 4.1G). While plasma insulin levels were significantly higher in male *Sst*-Cre$^{TG/TG}$ mice relative to male *Sst*-Cre$^{+/TG}$ mice, there was no significant difference in the fold change in insulin levels when we compared plasma insulin levels before and after glucose administration (Figure 4.1H). There was no significant difference in plasma insulin levels or fold change in insulin between female *Sst*-Cre$^{+/TG}$ and *Stoc*ket$^{t/TG}$ mice (Figure 4.1I). However, islets from female *Sst*-Cre$^{TG/TG}$ mice secreted significantly more insulin under 11 mM glucose (Figure 4.1J and 4.1K), matching the phenotype reported for *Sst*$^{-/-}$ mice (Hauge-Evans *et al.* 2009).

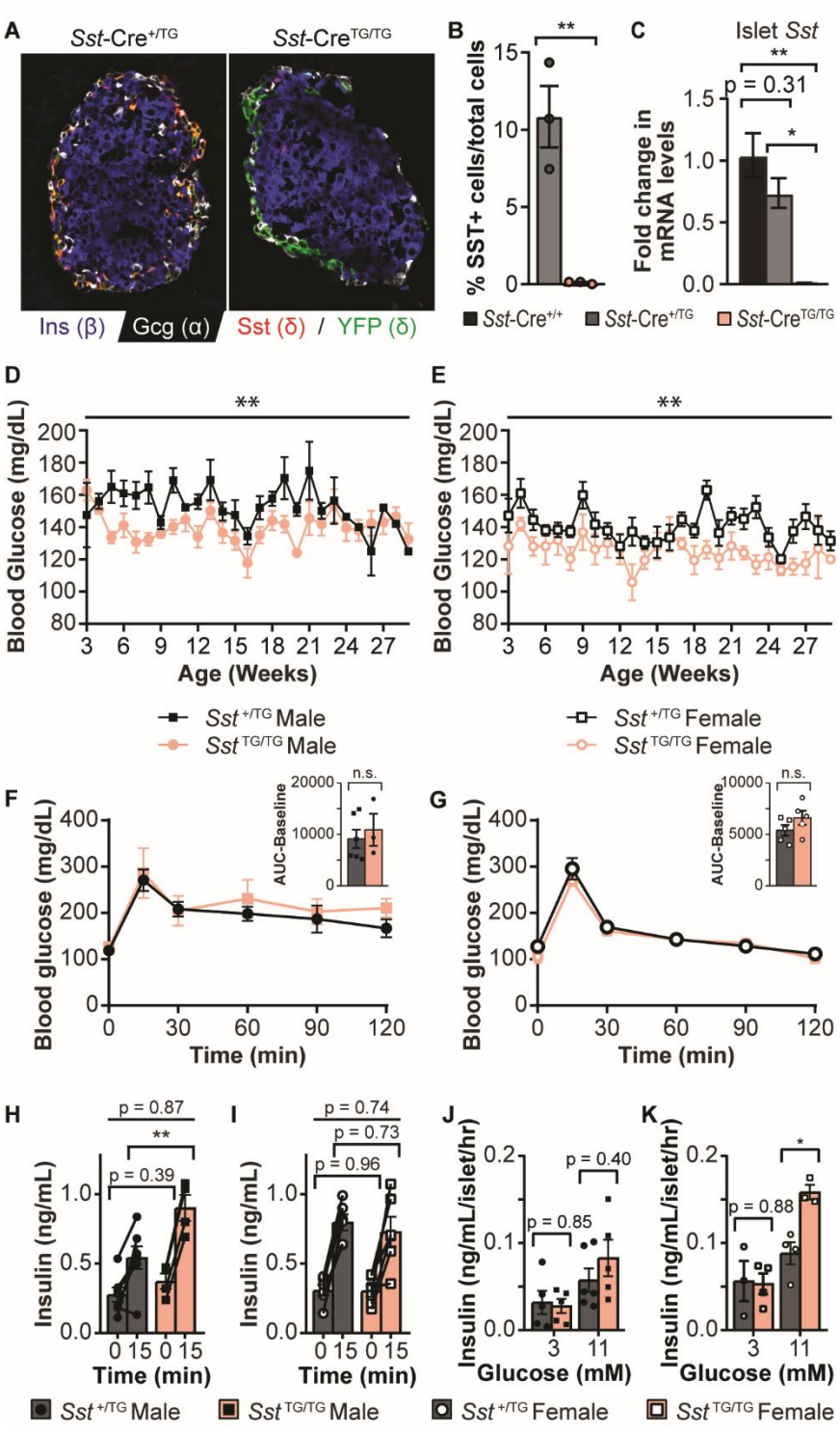

Figure 4.1: Homozygous *Sst*-Cre mice exhibit loss of *Sst* and a decreased glycemic set point.

Figure 4.1: (continued) A) Immunofluorescent stain of pancreas section from a *Sst*-Cre$^{+/TG}$ x lsl-YFP (left) and *Sst*-Cre$^{TG/TG}$ x lsl-YFP mouse (right). Insulin is stained in blue, glucagon in white, somatostatin in red, and YFP in green. B) Quantification of the number of SST+ cells in *Sst*-Cre$^{+/TG}$ and *Sst*-Cre$^{TG/TG}$ mice. Data from n = 3 mice per group, and at least 10 islets and 500 cells per mouse. C) *Sst* mRNA levels in *Sst*-Cre$^{+/+}$, *Sst*-Cre$^{+/TG}$, and *Sst*-Cre$^{TG/TG}$ islets. D and E) Weekly blood glucose measurements of D) male *Sst*-Cre$^{+/TG}$ (n = 6) and *Sst*-Cre$^{TG/TG}$ (n = 9) mice and E) female *Sst*-Cre$^{+/TG}$ (n = 7) and *Sst*-Cre$^{TG/TG}$ (n = 7) mice, grouped by age. F and G) Glucose tolerance and quantification of the area under the curve after subtracting baseline of male (F) and female (G) mice. H and I) Plasma insulin levels before and 15 min after IP glucose administration in male (H) and female (I) mice. Fold change, calculated as insulin levels at 15 minutes divided by insulin levels at 0 minutes, was also compared between *Sst*-Cre$^{+/TG}$ and *Sst*-Cre$^{TG/TG}$ mice. J and K) Static insulin secretion assay using islets from male (J) and female (K) mice incubated at 3 mM glucose and 11 mM glucose. Error bars represent SEM, *$p < 0.05$, **$p < 0.01$.

4.4.2 Delta cell ablation lowers the glycemic set point

Although *Sst*-Cre$^{TG/TG}$ mice have lower non-fasting glycemia and can secrete more insulin in response to the same glucose challenge, the absence of a difference in glucose tolerance suggests that there may be some compensation for the constitutive absence of SST from birth. We therefore turned to a model that would allow us to ablate delta cells and therefore SST signaling within the islet at a time of our choosing using diphtheria toxin (DT). We generated *Sst*-Cre x lsl-DTR mice expressing the diphtheria toxin receptor (DTR) in SST-expressing cells that would be ablated upon administration of DT. Only *Sst*-Cre$^{+/TG}$ mice were used for these experiments, as *Sst*-Cre$^{TG/TG}$ mice already have lower glycemia (Figure 4.1). We confirmed complete ablation of delta cells in DT-treated *Sst*-Cre x lsl-DTR mice, while beta and alpha cell numbers did not significantly change relative to saline (SAL)-treated *Sst*-Cre x lsl-DTR littermate controls (Figures 4.2A and 4.2B). Similarly, *Sst* mRNA levels were reduced by approximately 40-fold after ablation, while *Ins2* and *Gcg* levels were unaffected (Figure 4.2C).

SST is also expressed in other tissues throughout the body, primarily the stomach, duodenum, and throughout the hypothalamus. Thus, we collected these tissues to assess the extent of ablation in these areas. Staining for SST revealed that gastric D cells were lost upon acute ablation, but began

recovering within two weeks and recovered completely within three months (Figure 4.7A and 4.7B). Similarly, duodenal D cells could be found in both mice that experienced ablation and mice that did not, which was reflected by partial ablation immediately following DT administration based on *Sst* transcript level and complete recovery by 2 weeks (Figures 4.7C and 4.7D). In the hypothalamus, there was a slight decrease in *Sst* transcript, while immunofluorescent stains showed that SST+ neurons remained intact (Figure 4.7E and 4.7F). In contrast, pancreatic delta cells do not recover from ablation after 3 months (Figure 4.7G), consistent with reports that they are long-lived cells without a high turnover rate (Arrojo e Drigo *et al.* 2019).

To determine the effect of delta cell ablation on glycemia, we conducted weekly glucose measurements on the mice, with daily measurements throughout the period of injection. In both sexes, glucose levels between groups were comparable prior to delta cell ablation (Figure 4.2D and 4.2E). Following IP injection of DT, both male and female *Sst*-Cre x DTR mice immediately exhibited a significant and lasting decrease in glucose levels compared to *Sst*-Cre x DTR littermates that received SAL. The difference in basal glycemia between the control and delta cell-ablated mice remained even after 3 months. To obtain higher temporal resolution of changes in the glycemic set point, we put continuous glucose monitors on the mice to obtain glucose profiles with 5-minute resolution (van der Meulen *et al.* 2015). Within 12 hours of a single dose of DT, the blood glucose levels of *Sst*-Cre x DTR mice began to drop and remained steady for the duration of the experiment (Figure.4.2F). This confirmed that the changes seen through the weekly glucose measurements indeed reflected an acute and lasting change in the glycemic set point of the mice.

We also observed that *Sst*-Cre x lsl-DTR mice treated with DT had a lower body weight relative to controls, although the difference was not significant in female mice (Figure 4.8A and 4.8B). This brought up the possibility that lower food intake was contributing to the decreased glycemia. It had also been previously demonstrated that ablation of SST-expressing neurons specifically in the

tuberal nucleus of the hypothalamus decreases food intake (Luo *et al.* 2018). To determine whether the mice were indeed feeding less, we measured food intake in DT-treated *Sst*-Cre x lsl-DTR mice and *Sst*-Cre littermates without the lsl-DTR transgene. We observed no significant changes in food intake (Figure 4.8C), suggesting that there is not sufficient ablation within the hypothalamus to affect feeding patterns and that the decrease in glycemia is not due to decreased food intake. Given that the glycemic set point remains lower even after 3 months and only the pancreatic delta cells are completely absent at that time point, this suggests that the change in the glycemic set point in these mice can be specifically attributed to the ablation of pancreatic delta cells.

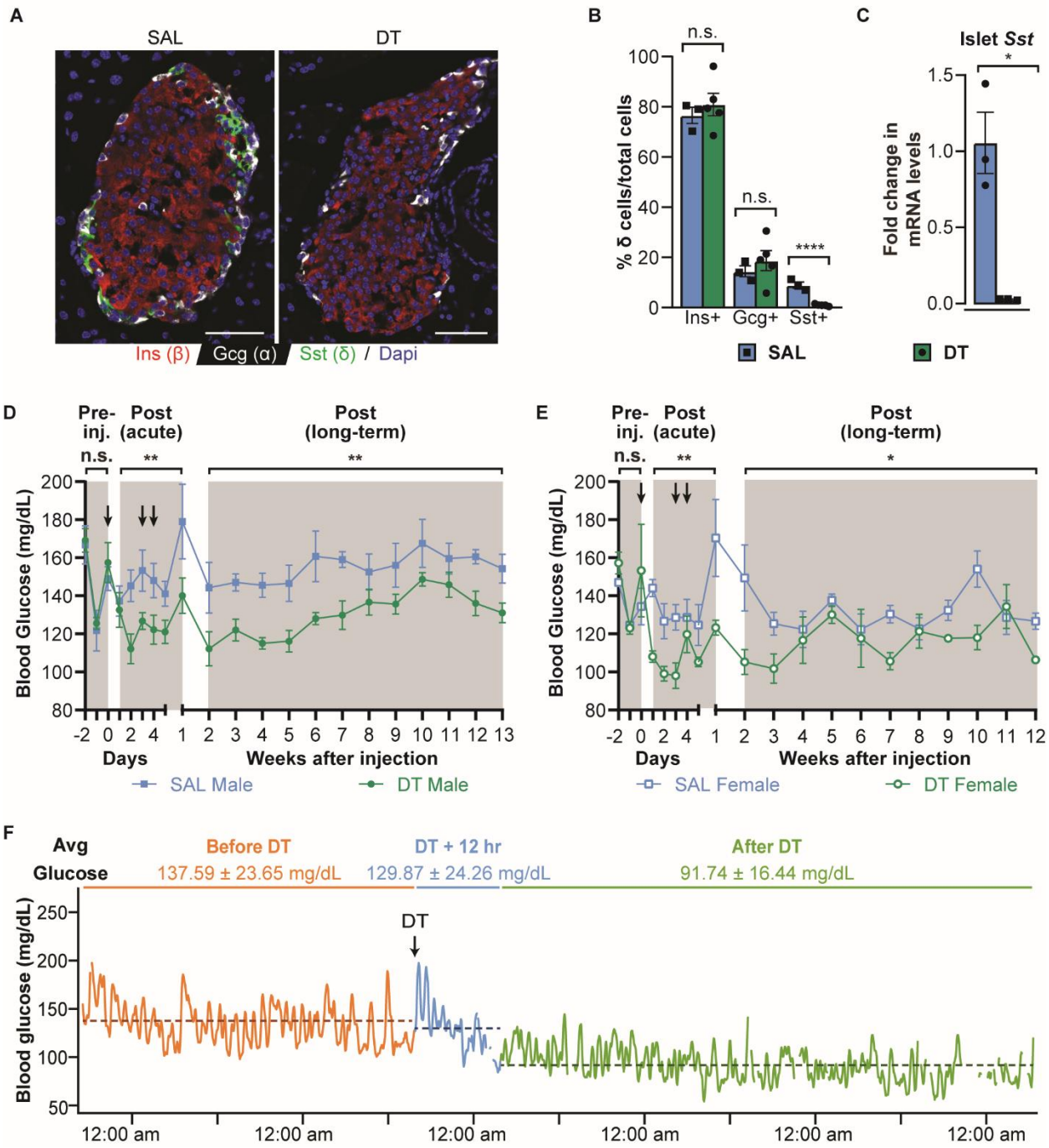

Figure 4.2: Delta cell ablation leads to a lasting decrease in the glycemic set point.

Figure 4.2: (continued) A) Immunofluorescent stain of pancreas section from a SAL-treated (left) and DT-treated (right) *Sst*-Cre x lsl-DTR mouse. Insulin is stained in red, glucagon in white, and somatostatin in green. Scale represent 50 μm. B) Quantification of the number of insulin, glucagon, and SST+ cells. Data from n = 3 SAL and n = 5 DT mice. C) *Sst* mRNA levels in islets from SAL- and DT-treated mice. D and E) Blood glucose measurements of (D) male SAL-treated (n = 4) and DT-treated (n = 6) mice, and E) female SAL-treated (n = 3) and DT-treated (n = 3) mice. Black arrows represent IP administration of SAL or DT. F) Representative continuous glucose monitoring data from a mouse. Orange represents glucose levels measured prior to single IP injection of DT. Blue represents the point at which DT was administered and the 12 hours following. Green represents glucose levels measured 12 hours after DT administration until the end of the experiment. Dashed lines represent average glucose level throughout each time period. Error bars represent SEM, *$p < 0.05$, **$p < 0.01$, ****$p < 0.0001$.

4.4.3 Delta cell ablation increases glucose tolerance and glucose-stimulated insulin secretion

To determine the effect of delta cell ablation during glucose stimulation, we conducted IP glucose tolerance tests on the mice before and after administration of SAL or DT. As expected, there was no significant difference between the glucose tolerance of the different groups of mice prior to delta cell ablation (Figures 4.3A). Glucose tolerance tests performed 36 hours after the last administration of DT revealed that DT-treated male *Sst*-cre x DTR mice had significantly improved glucose tolerance (Figure 4.3B). As with males, female *Sst*-cre x DTR mice did not exhibit a significant difference in glucose tolerance prior to injection of SAL or DT (Figure 4.3C). After injection, DT-treated female mice demonstrated significantly lower fasting blood glucose levels but no statistically significant difference in overall glucose tolerance, in contrast to our observations in male mice (Figure 4.3D).

Given that the ablation of delta cells would lead to a decrease in SST tone and remove its local inhibition of beta cells, we hypothesized that the decrease in the glucose set point and increase in glucose tolerance would both be the result of an increase in glucose-stimulated insulin secretion (GSIS). To test this hypothesis, we measured plasma insulin in fasted SAL- or DT-treated *Sst*-Cre x DTR mice before and 15 minutes after IP injection of glucose. Fasting and glucose-stimulated plasma insulin

levels were comparable between groups in both sexes prior to ablation (Figure 4.3E). After delta cell ablation, there was a slight but non-statistically significant increase in glucose-stimulated plasma insulin levels in male (Figure 4.3F). However, there was a significant increase in the fold-change of plasma insulin after ablation, as determined by dividing plasma insulin levels 15 minutes after glucose injection by baseline plasma insulin levels in each mouse. No differences in plasma insulin levels were observed in females (Figure 4.3G and 4.3H).

To confirm our *in vivo* findings *in vitro*, we compared static GSIS in the presence and absence of delta cells in isolated intact islets. This revealed a consistent increase in GSIS at glucose levels mildly or moderately above the beta cell glucose threshold, which reached significance at 16.8 mM glucose in islets from both sexes (Figure 4.3I and 4.3J). Thus, GSIS increases in the absence of pancreatic delta cells, and the effect is islet autonomous since the increase is observed in isolated islets *in vitro*.

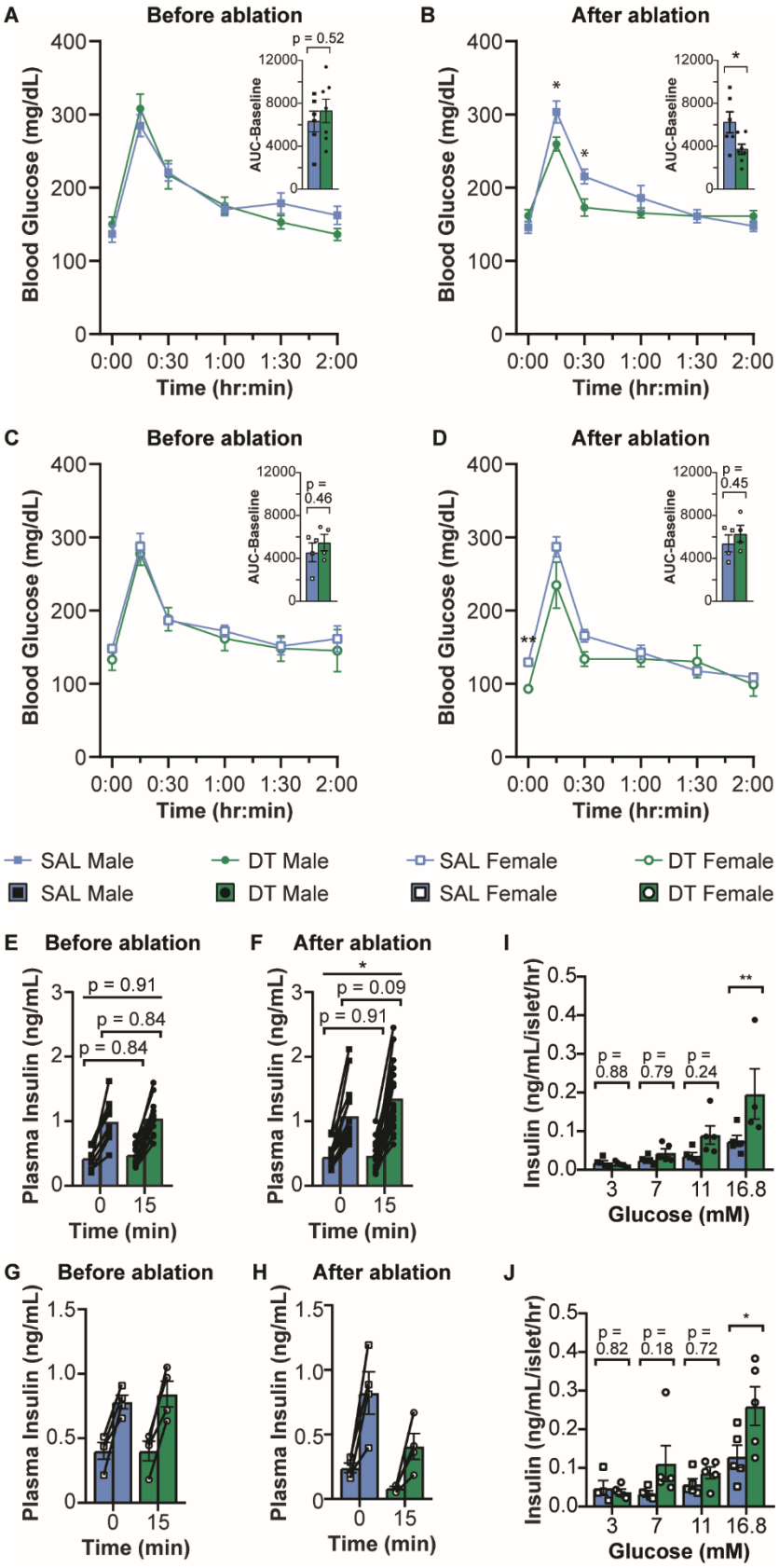

Figure 4.3: Delta cell ablation increases glucose tolerance and insulin secretion.

Figure 4.3: (continued) A-D) Glucose tolerance test of A) male mice before delta cell ablation, B) male mice after delta cell ablation, C) female mice before delta cell ablation, and D) female mice after delta cell ablation. Bar graphs in the upper right hand corner of each line graph represent area under the curve with the baseline subtracted. E-H) Plasma insulin measurements E) male mice before ablation, F) male mice after ablation, G) female mice before ablation, and H) female mice after ablation. Blood for insulin measurement was collected at 0 minutes (before glucose administration) and 15 minutes after glucose administration. The 0 minute time point, 15 minute time point, and fold change in plasma insulin levels are compared. I and J) Static insulin secretion assay performed on islets isolated from ablated I) male and J) female mice. Error bars represent SEM. *$p < 0.05$, **$p < 0.01$.

4.4.4 Alpha cell ablation does not affect basal glycemia

Since SST inhibits glucagon secretion, it is possible that the drop in glucose set point and increased insulin secretion we observe upon delta cell ablation are indirectly mediated by increased glucagon release. The role of the alpha cell in amplifying insulin secretion induced by nutrient stimulation in the prandial state is increasingly appreciated. Removing glucagon signaling to the beta cell by knocking out glucagon or its receptor, or inhibiting alpha cell activity using Gi-DREADD all lead to decreased GSIS (Svendsen *et al.* 2018; Capozzi *et al.* 2019a, b; Zhu *et al.* 2019). This demonstrates that although glucagon is generally thought of as a hormone that acts to raise glucose levels, it also contributes to GSIS to bring glucose levels down in the prandial state. Furthermore, a comprehensive paper establishing that the glycemic set point is set by the islet concluded that the underlying mechanism was paracrine crosstalk between beta and alpha cells (Rodriguez-Diaz *et al.* 2018). However, mouse models of alpha cell ablation generally demonstrated no change in glycemia nor insulin secretion (Thorel *et al.* 2011; Pedersen *et al.* 2013; Shiota *et al.* 2013), although a more recent study observed decreased GSIS from a pancreas perfusion (Svendsen *et al.* 2018). Thus, we aimed to first resolve the effect that alpha cell ablation has on glycemia and insulin secretion while also comparing it to the effects of delta cell ablation.

We set up *Gcg*-CreER x lsl-DTR mice to enable DT-mediated ablation of alpha cells, with the *Gcg*-CreER line chosen for its superior and more specific labeling of alpha cells (Ackermann *et al.* 2016). Successful ablation of alpha cells was confirmed by immunofluorescence analysis and qPCR (Figure 4.4A-C), as with the ablation of delta cells. Alpha cell ablation did not have a significant effect on the glycemic set point in mice of both sexes (Fig 4.4D and 4.4E). There was also no significant difference in glucose tolerance and plasma insulin levels between groups of mice both before and after administration of DT (Figure 4.4F-M). These findings are in close agreement with previous studies that investigated changes in glycemia after alpha cell ablation. Therefore, our findings confirm that ablating alpha cells in mice does not alter non-fasting blood glucose levels, in sharp contrast to our experiments in which we ablated delta cells.

To determine whether absence of delta cells leads to increased alpha cell activity, we stimulated alpha cells with 100 nM epinephrine under low glucose. Epinephrine-induced glucagon secretion significantly increased in islets without delta cells, suggesting that loss of paracrine SST from delta cell ablation does indeed disinhibit alpha cells (Figure 4.9A). To determine whether glucagon signaling may contribute to the increase in insulin secretion observed at different glucose concentrations, we also measured glucagon concentration from the same samples. A general pattern of higher glucagon secretion in the absence of delta cells was observed, with significantly higher glucagon secretion from islets from male mice that were incubated in 16.8 mM glucose (Figure 4.8B and 4.9C). This suggests that the absence of local SST signaling leads to reduced inhibition of alpha cell activity under high glucose, and this may contribute to the increase GSIS observed at higher glucose levels well above the glucose threshold for insulin secretion.

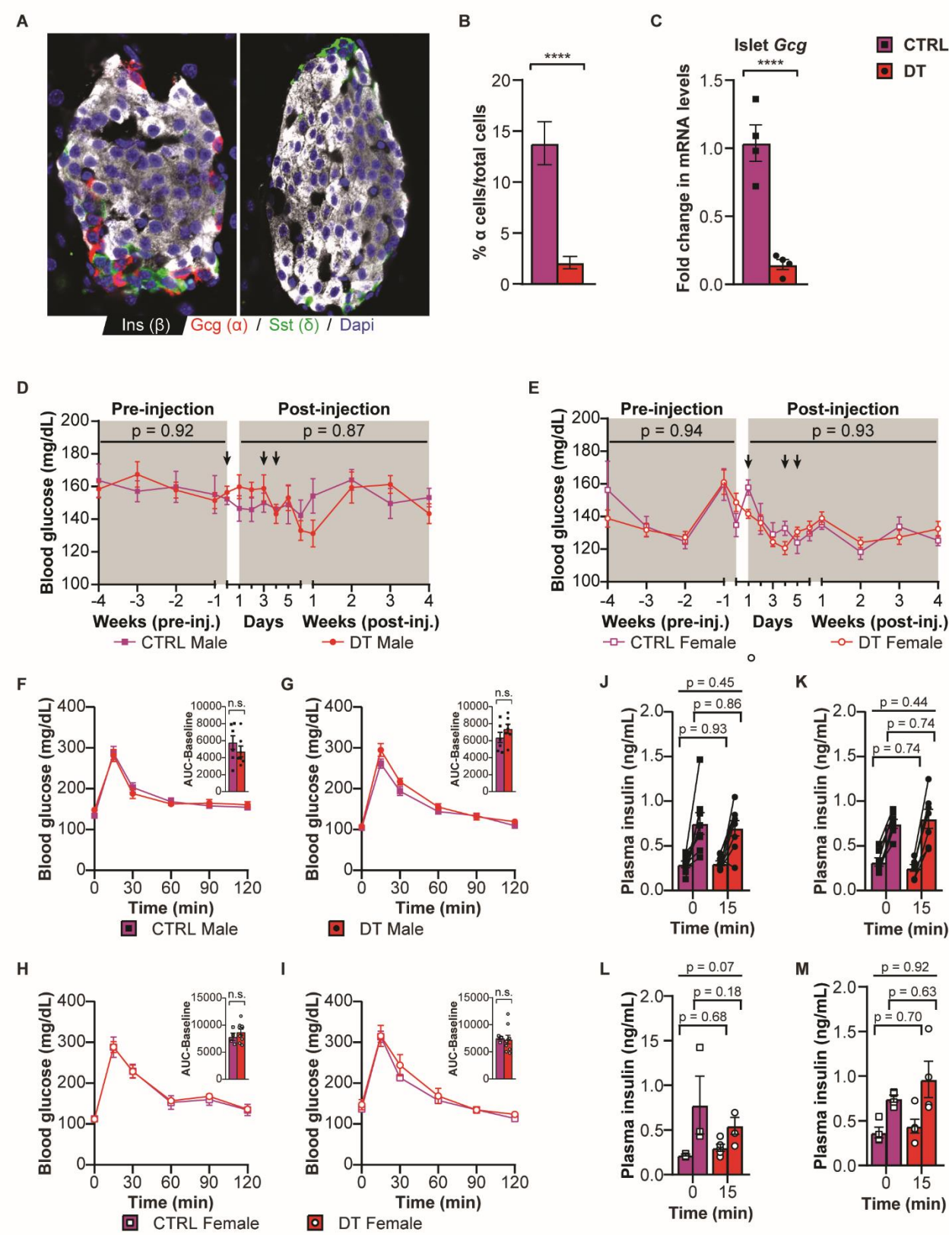

Figure 4.4: Alpha cell ablation does not affect basal glycemia.

Figure 4.4: (continued) A) Immunofluorescent stain of pancreas section from a non-ablated (left) and alpha cell-ablated mouse (right). Insulin is stained in white, glucagon in red, and SST in green. B) Quantification of number of alpha cells. C) *Gcg* mRNA levels in control and ablated mice. D and E) Glucose measurements of D) male and E) female mice. Arrows represent IP administration of DT. F-I) Glucose tolerance tests in F) male mice before alpha cell ablation, G) male mice after alpha cell ablation, H) female mice before alpha cell ablation, and I) female mice after alpha cell ablation. Bar graphs in the upper right corner of each line graph represent area under the curve with baseline subtracted. J-M) Plasma insulin levels in J) male mice before ablation, K) male mice after ablation, L) female mice before ablation, and M) female mice after ablation.

4.4.5 Delta cell ablation decreases the glucose threshold for beta cell response

To more precisely assess how the absence of delta cells changes the glucose response of individual islets, we turned to calcium imaging. As calcium is necessary for insulin secretion, changes in intracellular calcium levels are an excellent proxy for insulin secretion. Importantly, calcium imaging using genetically-encoded sensors such as GCaMP6s allows for single-cell resolution and subsequent fixation and *post hoc* immunofluorescent staining to validate the identity of the recorded cells. To this end, we generated quadruple transgenic mice expressing *MIP*-Cre/ERT x *Sst*-Cre x lsl-DTR x lslGCaMP6. In this line, mice constitutively express both DTR and GCaMP6 in SST-expressing cells. After delta cell ablation with DT, tamoxifen administration to the mice allows for the translocation of Cre/ERT to the nucleus, activating GCaMP6 expression in insulin-expressing beta cells. The simultaneous induction of DTR in beta cells does not lead to beta cell ablation as DT is no longer administered. This strategy allows us to ablate delta cells, then observe beta cell calcium response. Due to the complexity of the cross, we used a mix of SAL-treated *MIP*-Cre/ERT x *Sst*-cre x DTR x GCaMP6 mice and also DT-treated mice expressing *MIP*-Cre/ERT x GCaMP6 with or without DTR or *Sst*-cre as controls. We hypothesized that the loss of delta cells would shift the beta cell glucose threshold to the left. To test this hypothesis, we performed glucose step experiments starting below the beta cell glucose threshold at 4 mM glucose and increasing in 1 mM increments every 20 minutes.

Islets from non-ablated mice and islets from ablated mice were imaged simultaneously to ensure that any differences observed were not due to trace-to-trace variations. After each trace, islets were fixed to confirm the absence of delta cells in ablated islets and ensure that each GCaMP6 expressing cell was insulin-positive via *post hoc* whole mount immunofluorescence.

For analysis of beta cell calcium response, we defined the activity threshold as the half-max of the signal for each individual beta cell. We then determined the glucose level at which each cell first reaches that threshold of activity. In control islets with intact delta cells, individual beta cells generally began responding shortly after exposure to 6 or 7 mM glucose, with a synchronized response between the majority of beta cells by 8 or 9 mM glucose (Figure 4.5A and 4.5B, Supplementary Video 1). In islets with ablated delta cells, individual beta cells generally began to respond shortly after exposure to 5 or 6 mM glucose, with a synchronized response by 7 or 8 mM glucose (Figure 4.5C and 4.5D, Supplementary Video 1). Quantified across over 2000 beta cells from at least 10 islets per mouse in 3 pairs of mice, the beta cell glucose threshold in islets without delta cells was on average 1 mM glucose (approximately 18 mg/dL) lower and statistically significantly different from islets with intact delta cell feedback (Figure 5E and 5F).

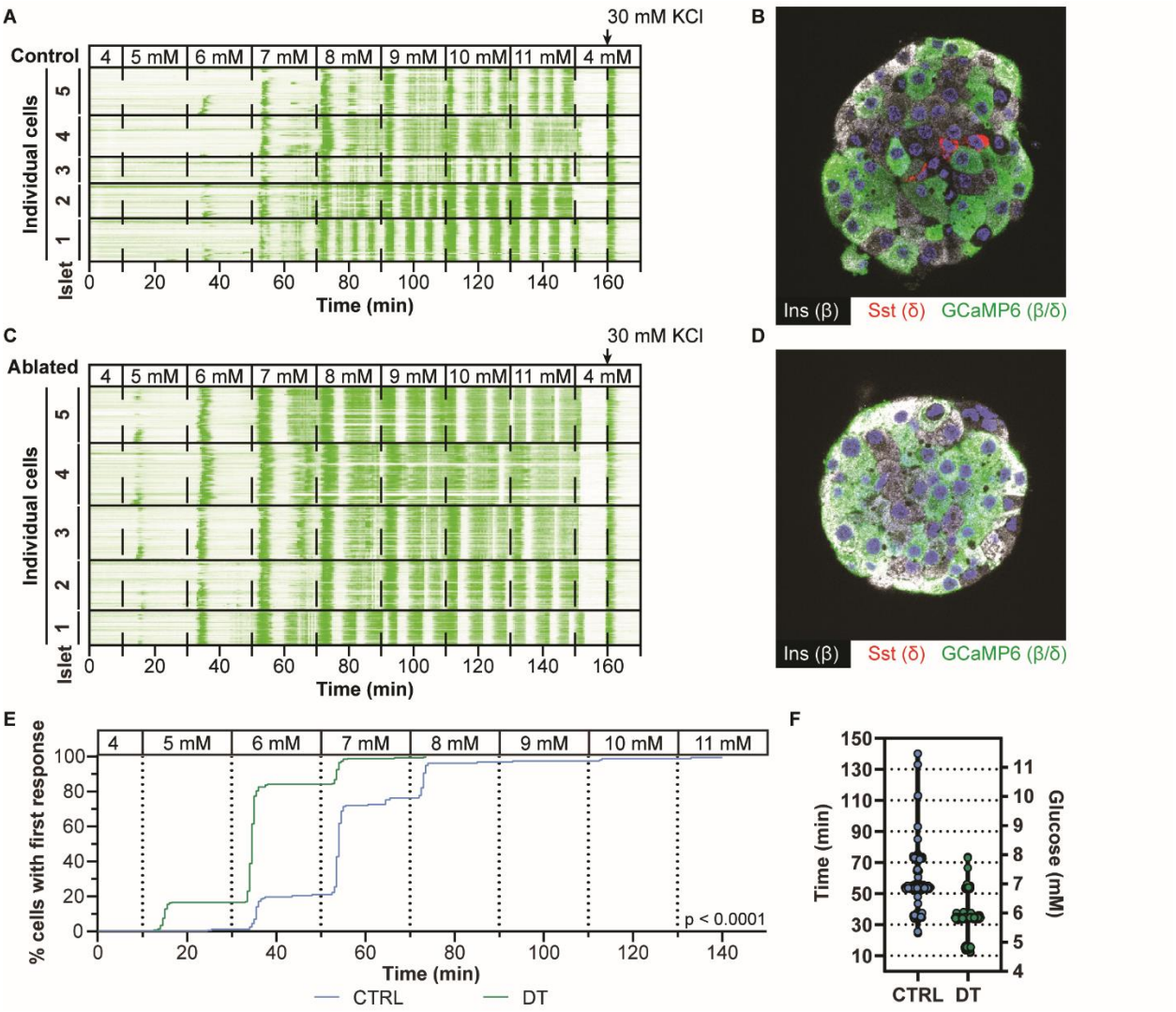

Figure 4.5: Beta cells exhibit calcium response at a lower glucose threshold in the absence of delta cells. A) Representative trace of beta cells from a mouse with intact pancreatic delta cells. Each line represents the calcium activity of a single beta cell, with green corresponding to an increase in intracellular calcium. Each box represents an islet. Dashed lines represent the point at which the glucose levels were changed. 30 mM KCl was added at the end of each trace to confirm viability of the cells. B) *Post hoc* whole mount stain of an islet with intact delta cells. C) Representative trace of beta cells from a mouse with ablated delta cells. D) *Post hoc* whole mount stain of an islet confirming absence of delta cells. E) Curve representing the % of cells that have their first response at each glucose level, with the first response defined as the point at which a cell first reaches half-max of its signal intensity. F) Violin plot in which each dot represents a cell and the point at which it first responded.

To determine whether the shift in calcium response also represents a shift in insulin secretion, we simultaneously imaged beta cell calcium activity while collecting the outflow for measurement of insulin secretion. This demonstrated that beta cells secrete insulin at a higher amplitude in islets without delta cells (Figure 4.6). From these experiments, we concluded that the ablation of delta cells decreases the glucose threshold at which beta cells become active and observe that the 1 mM, or 18 mg/dL decrease in the glucose threshold is similar to the approximately 20 mg/dL decrease in the glycemic set point observed in mice *in vivo*.

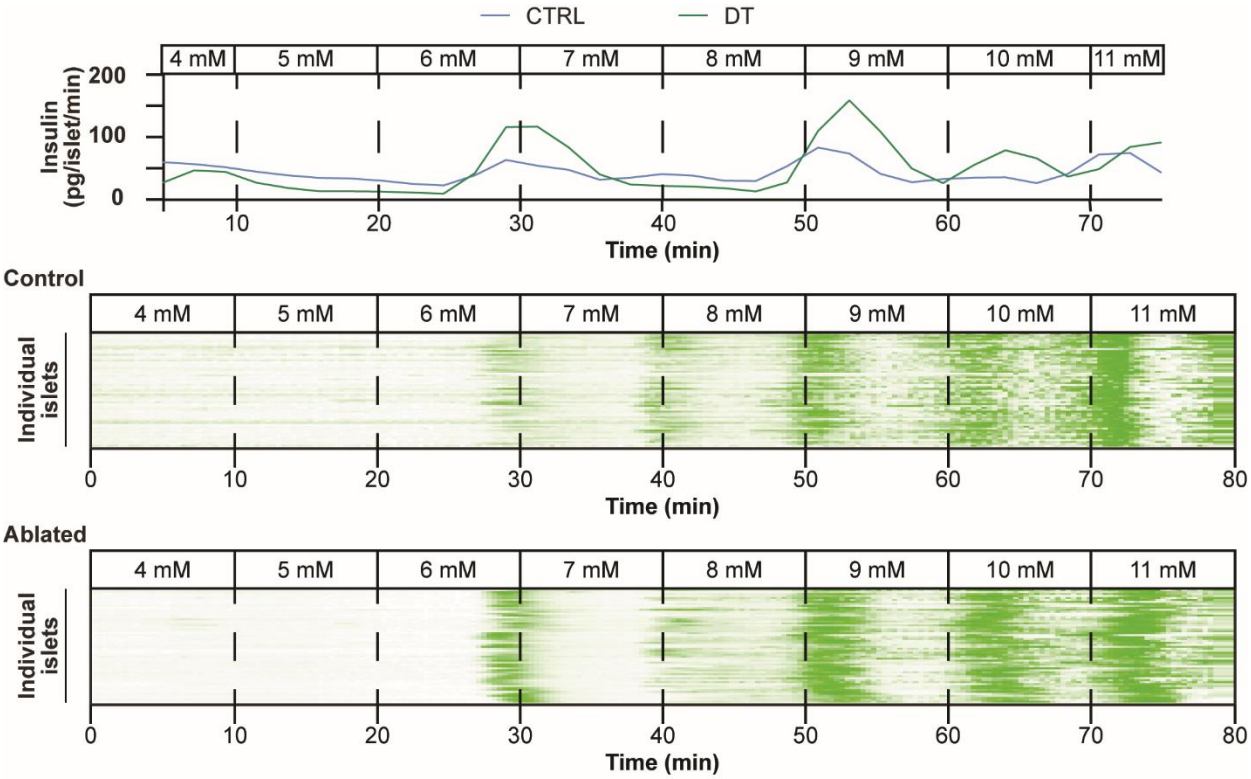

Figure 4.6: Simultaneous collection of calcium dynamics in islets and insulin secretion. Secretion dynamics are on the top. Below are calcium traces of whole islets from control or delta cell-ablated mice.

4.5 Discussion

SST has long been known to inhibit both beta and alpha cells. Secretion of SST from delta cells has been proposed to prevent excess insulin secretion (van der Meulen *et al.* 2015; Huising *et al.* 2018) and has also been demonstrated to play an important role in inhibiting glucagon secretion in the prandial phase (Lai *et al.* 2018; Xu *et al.* 2020). However, the full physiological contribution of local delta cell-mediated feedback on the glycemic set point has not been addressed. Here we demonstrate that delta cells help determine the glycemic set point in mice by modulating the glucose threshold for beta cell response. Both male and female mice exhibit a decrease in basal blood glucose levels upon ablation of delta cells. Male mice also exhibit an increase in glucose tolerance that occurs due to an increase in

the fold-change of plasma insulin secreted in response to glucose. Static secretion assays of isolated islets confirmed an increase in GSIS from islets in both sexes. This suggests that there may be other physiological factors in female mice that prevent the increase in plasma insulin levels seen in male mice, and may also explain why they do not exhibit changes in glucose tolerance. Calcium imaging with single-cell resolution revealed that in the absence of delta cells, beta cells respond to lower levels of glucose, demonstrating increased glucose sensitivity. The consistency with which beta cells respond at a 1 mM lower glucose level in islets without delta cells is in line with the approximately 1 mM decrease in blood glucose levels.

One *Sst*-null mouse model has been previously observed to have increased non-fasting blood glucose levels at 3 weeks of age (Richardson *et al.* 2015), in contrast to the lower glycemia we observe after 3 weeks of age. Another *Sst*-null mouse model has also been noted to have lower blood glucose levels but no differences in non-fasting insulin levels (Luque & Kineman 2007). These mice also display no differences in glucose tolerance relative to wild-type mice but a slight elevation in fasting insulin (Gahete *et al.* 2011; Luque *et al.* 2016), matching our observations with *Sst*-Cre$^{TG/TG}$ mice. Thus, it is indeed likely that there are compensatory effects when SST is absent from birth.

On the other hand, delta cell ablation using *Sst*-Cre x lsl-DTR leads to decreased glucose levels, increased glucose tolerance, and increased insulin secretion. However, due to SST having many effects throughout the body, including but not limited to the brain, the stomach, and the intestines, it is important to determine their potential contributions. The duodenum is unlikely to contribute since there is little ablation and any ablation that does occur recovers within 2 weeks. SST in the gut has also been implicated to promote satiety (Lieverse *et al.* 1995). The stomach is also unlikely to contribute since it recovers within 3 months, at which point the mice still exhibit a decreased glycemic set point. Furthermore, D cells in the stomach are known to inhibit gastrin release (Bloom *et al.* 1974; Holst *et al.* 1992), which leads to inhibition of gastric secretion. It is also thought to decrease gastric motility

(Johansson *et al.* 1981) and gastric emptying (Holst *et al.* 2016), both of which lead to a decrease in rate of nutrient absorption.. Overall, SST-expressing enteroendocrine cells appear to contribute to lower glucose absorption, which would decrease postprandial glycemia. Ablating D cells would then potentially be expected to promote an increase in glycemia instead.

Since the hypothalamus plays an important role in energy metabolism, it is possible that ablation of SST-expressing cells there would contribute to the decrease in glycemia. SST neurons have already been implicated in food and water intake (Karasawa *et al.* 2014; Stengel & Taché 2019). Furthermore, specific ablation of SST-expressing neurons in the tuberal nucleus have been shown to decrease food intake (Luo *et al.* 2018). However, we did not observe any changes in food intake between mice with and without beta cells. This suggests that any ablation that may have occurred in the hypothalamus was not sufficient to modulate feeding behavior and does not have an effect on glucose levels. Another recent paper has reported that specifically ablating SST-neurons in the hypothalamus by stereotaxic injection of DTA, the catalytic unit of diphtheria toxin, had no effect on blood glucose, or non-fasting insulin levels (Huang *et al.* 2021). These suggest that the change in the glycemic set point we observe is also not due to ablation of SST-expressing neurons.

A recent paper reported that ablation of pancreatic delta cells leads to neonatal death, and the authors attributed it to hypoglycemia (Li *et al.* 2018). In contrast, the mice used in this study remained healthy months after ablation. It is likely that this difference is due to their use of the lsl-DTA mouse, which expresses the catalytic subunit of diphtheria toxin upon expression of Cre. This would cause all SST-expressing cells, including those in the central nervous system and enteroendocrine system, to be destroyed upon expression of Cre. The ablation of cells during development and the continued loss of SST-expressing neurons, which would presumably lead to brain defects, as well as lack of SST-expressing gastric D cells, which would affect their ability to take in nutrients, likely contributed to the lethal phenotype they observed. Given that *Hhex*-KO mice, which are unable to develop pancreatic

delta cells due to the lack of the essential transcription factor HHEX (Zhang *et al.* 2014), as well as *Sst*-null mice are shown to be viable, it is unlikely that the ablation of pancreatic delta cells contributed solely to the lethality of these mice. While our data agree that ablation of pancreatic delta cells leads to increased insulin secretion and decreased glucose levels, the viability of our mice allowed us to demonstrate that the hypoglycemia is not transient but a stable change in the glycemic set point of these mice. This also illustrates the utility of using the DTR mouse line rather than the DTA mouse line, since it allows us to choose the timing of ablation as well as the dose, which allowed us to ablate pancreatic delta cells without also ablating all SST-expressing neurons.

Our data agrees with previous studies that ablation of alpha cells does not have an effect on glycemia in mice as demonstrated by two previous studies (Thorel *et al.* 2011; Pedersen *et al.* 2013). Thus, while alpha cells undoubtedly play an important role in both the counterregulatory response through systemic action and the stimulation of insulin secretion through paracrine action in the prandial phase, their contribution appears to be dispensable around the non-fasting glycemic set point in mice. However, in human islets the paracrine interactions and islet interactions are substantially different (Noguchi & Huising 2019). Alpha cells in human islets may therefore contribute more directly to the glycemic set point, as has been shown in xenoplants of human islets into mice (Rodriguez-Diaz *et al.* 2018). We also provide evidence that increased glucagon secretion in the absence of delta cells may contribute to the enhanced insulin secretion we observe. Thus, it would be interesting to investigate whether blocking glucagon signaling would partially block the effects of delta cell ablation.

Since these experiments were all performed in the context of healthy mice, it would be useful to observe the effect that the absence of delta cells can have in models of diabetes, and whether they would ameliorate the progression due to the subsequent increase in glucose sensitivity of beta cells, or

exacerbate it due to beta cells reaching a state of exhaustion more quickly. Whether delta cells play a similar role in humans, who have a lower glucose set point, remains to be seen as well.

4.6 Funding and Acknowledgements

This work was supported by the National Institute of Diabetes and Digestive and Kidney Disease (NID DK-110276). JLH was supported by a National Institute of General Medical Sciences-funded Pharmacology Training Program (T32 GM-099608). SL was supported by the NSF Graduate Research Fellowship (1650042), the UC Davis Training Program in Molecular and Cellular Biology (T32 GM-007377), and the UC Davis NSF Bridge to Doctorate Program (1612490).

4.7 Materials and Methods

4.7.1 Animals

Mice were maintained in group housing (4 mice per cage) on a 12 hr light:12 hr darkness cycle with water and standard rodent chow provided *ad libitum*. Heterozygous *Sst*-IRES-Cre mice (*Sst*$^{tm2.1(cre)Zjh}$/J, Jax #013044) (Taniguchi *et al.* 2011) were crossed together to generate homozygous *Sst*-IRES-Cre mice (*Sst*-Cre$^{TG/TG}$). *Sst*-Cre$^{+/TG}$ x lsl-YFP (B6.129X1-*Gt(ROSA)26Sor*$^{tm1(EYFP)Cos}$/J, Jax # 006148) (Srinivas *et al.* 2001) mice were crossed to *Sst*-Cre$^{+/TG}$ to generate heterozygous and homozygous *Sst*-Cre x lsl-YFP mice. *Sst*-Cre x lsl-DTR mice were initially generated by crossing *Sst*-Cre$^{+/TG}$ mice to homozygous *R26-iDTR* mice (C57BL/6-*Gt(ROSA)26Sor*$^{tm1(HBEGF)Awai}$/J, Jax # 007900) (Buch *et al.* 2005), then maintained by crossing bi-transgenic offspring to C57BL/6N mice or by crossing mice with complementary transgenes. For tdTomato lineage-labeling, some of the mice were also crossed to *Ai14(RCL-tdT)-D* mice (B6.Cg-Gt(ROSA)26Sor$^{tm14(CAG-tdTomato)Hze/J}$, Jax # 007914) (Madisen *et al.*

2010). To ablate alpha cells, mice expressing *Gcg*-CreERT2 (B6;129S4-*Gcg*$^{em1(cre/ERT2)Khk}$/Mmjax, Jax #030346) (Ackermann *et al.* 2016) were also crossed to lsl-DTR mice. For beta cell calcium imaging, *Sst*-Cre x lsl-DTR mice were crossed to mice expressing *MIP*-CreERT (B6.Cg-Tg(Ins1-cre/ERT)1Lphi/J, Jax # 024709) (Wicksteed *et al.* 2010) and *Ai96(RCL-GCaMP6s)* (B6;129S6-*Gt(ROSA)26 Sor*$^{tm96(CAG-GCaMP6s)Hze}$/J, Jax # 24106) (Madisen *et al.* 2015), then maintained by crossing mice expressing complementary transgenes, with one parent expressing lsl-DTR and the other expressing lsl-GCaMP6. *Sst*-Cre x lsl-Gi-DREADD mice were generated by crossing *Sst*-Cre$^{+/TG}$ mice to homozygous *R26-LSL-Gi-DREADD* mice (B6.129-Gt(ROSA)26 Sor$^{tm1(CAG-CHRM4*,-mCitrine)Ute}$/J, Jax # 026219) (Zhu *et al.* 2016), then maintained by crossing bi-transgenic offspring to C57BL/6N mice or to complementary littermates. *Sst*-Cre$^{TG/TG}$ mice were not used for breeding. Mice were used between 2 and 4 months of age unless otherwise indicated. All mouse experiments were approved by the UC Davis Institutional Animals Care and Use Committee and were performed in compliance with the Animal Welfare Act and the Institute for Laboratory Animal Research Guide to the Care and Use of Laboratory Animals.

4.7.2 DT, tamoxifen, and STZ treatments

For delta cell ablation, 126 ng diphtheria toxin (List Biological Laboratories, Product # 150) in 200 μL 0.9% saline was injected into mice via IP injection on days 0, 3, and 4. The same timeline for DT administration was followed for alpha cell ablation, except 300 ng was given. Control mice were given an intraperitoneal injection on the same days with an equivalent volume of 0.9% saline. Tamoxifen (Sigma-Aldrich, Catalog # T5648) was dissolved in sunflower oil (Trader Joe's, Monrovia, CA, USA) at 20 mg/mL, then administered to mice via oral gavage with a volume of 250 μL for 5 consecutive days. STZ (Calbiochem, now EMD Millipore, Catalog # 572201) was dissolved in 100 mM sodium citrate pH 4.5 and administered to mice at 50 mg/kg via IP injection for 5 consecutive days.

4.7.3 Glucose tolerance test and plasma insulin collection

Mice were fasted overnight for 16 hours. The next morning, they were weighed and put into individual cages. Tails were clipped with a surgical scissor and baseline glucose measured before administration of 2 mg/kg glucose via IP injection (Dextrose, Sigma-Aldritch, Catalog # D9559). All blood glucose measurements over the 2 hr time period were done using a OneTouch Ultra glucometer. To collect plasma insulin, tail blood from mice was collected using the Microvette CB300 EDTA (Sarstedt, Product # 16.444.100) and kept on ice. After all the 15 min time points were collected, the samples were spun down at 4°C at 5000 rpm for 10 minutes and the plasma collected into a non-stick tube (Ambion Catalog # AM12300). Samples were stored at -20°C until assayed.

4.7.4 Islet isolation

Islets were isolated by injecting 2 mL collagenaseP (0.8 mg/mL in HBSS, Roche Diagnostics, Catalog # 11249002001) into the bile duct with the ampulla of Vater clamped. The pancreas was removed into a conical tube to which an additional 2 mL of collagenaseP was added, then incubated at 37°C for 11 min. This was followed by gentle manual shaking to dissociate the pancreata, then three washes with cold HBSS + 5% NCS (Newborn Calf Serum). After the digested suspension was passed through a nylon mesh (pore size 425 μm, Small Parts), the islets were isolated by density gradient centrifugation using Histopaque (Sigma-Aldrich, Catalog # 10771) for 20 min at 1400 x g without brake. Islets were then collected from the interface, washed with cold HBSS + 5% NCS, and hand-picked several times under a dissecting microscope, followed by culture in RPMI + 5.5 mM Glucose + 10% FBS + pen/strep.

4.7.5 Static insulin secretion assays

Islets were picked twice into Krebs Ringer Buffer (20 mM Hepes pH 7.4, 1.2 mM KH_2PO_4, 25 mM $NaHCO_3$, 130 mM NaCl, 5 mM KCl, 1.2 mM $MgCl_2$, 1.2 mM $CaCl_2$) containing 0.1% BSA and 3 mM glucose, then incubated at 37°C for 1 hour. For each group, islets were pooled and split into different treatments with at least 5 replicates each. Static insulin secretion was carried out using 10 islets per well, with different treatments added after the islets had been placed into the wells.

4.7.6 Calcium imaging and dynamic insulin secretion assays

Microfluidics chambers were bonded to 35 mm dishes with a glass bottom. Islets were set down into these chambers and allowed to adhere to the glass by overnight culture. Continuous perfusion of Krebs Ringer Buffer at a rate of 200 μL per minute was maintained using the Elveflow microfluidics system, with different treatments adjusted using the Mux distributor. The calcium response of islets over time was imaged using a Nikon Microscope using a 60x lens with oil. Simultaneous collection of dynamic insulin perfusate was done by collecting the outflow into non-stick tubes.

4.7.7 Hormone measurements

Plasma insulin was measured using the Ultra-Sensitive Mouse Insulin ELISA Kit wide range assay (Crystal Chem Catalog # 90080). Secreted insulin was measured using the Insulin LUMIT kit (Promega CS3037A01) in 384-well plates (Corning #3572) at 10 μL (static secretion) or 25 μL (dynamic secretion) sample volumes.

4.7.8 Immunofluorescence and cell counting

Pancreata were isolated with the spleen and fixed in 4% PFA for 5 hours, then protected with 30% sucrose overnight prior to embedding with OCT (Fisher Healthcare Catalog # 4585). Cryosections were collected using a Leica cryostat. The same procedure was conducted with the stomach, which was isolated, halved lengthwise, and washed twice in PBS prior to fixation in PFA, and the duodenum, which was collected as an approximately 1 cm piece adjacent to the stomach and opened up prior to fixation. For immunofluorescence, slides were first washed for 5 minutes three times in KBS, then incubated with antibodies diluted in donkey block (KPBS supplemented with 2% donkey serum and 0.4% Triton X-100) overnight at 4°C. For whole mount staining of islets after calcium imaging, islets were fixed in 4% PFA in the chamber for 15 minutes at room temperature, then washed in PBS twice before a 15 minute incubation at 4°C. Islets were incubated in donkey block overnight at 4°C, followed by overnight incubation with primary antibodies diluted in donkey block, overnight wash in PBS + 0.15% Tween 20, and overnight incubation with secondary antibodies diluted in donkey block. Finally, islets were incubated in 4% PFA either overnight at 4°C or for 1 hour at room temperature, followed by several washes in PBS + 0.15% Tween 20 every 30 minutes. After the washes, the islets were put in Rapiclear (SunJin Lab Catalog # RC152001) and imaged on a Nikon Microscope. Cells were counted manually using ImageJ.

4.7.9 RNA Extraction and qPCR

Prior to the start of the RNA extraction, hypothalamus, stomach, and duodenal tissue collected into Trizol were sonicated. Islets were directly broken down in Trizol. RNA was isolated by chloroform extraction and precipitated by isoproponal. Once pellets were resuspended, cDNA was made using a reverse transcription kit. qPCR was performed using the PowerUp Sybr or iTaq on a BioRad CFX 384.

4.7.10 Continuous Glucose Monitoring

Mice were anesthetized, shaved, and sterilized. A Dexcom G6 sensor was introduced subcutaneously into mice and bonded using veterinary glue. Receivers were left adjacent to cages and monitored. Continuous Glucose Monitoring Profiles were collected for approximately a week.

4.7.11 Statistical Analysis

Data were analyzed by Student's t-test, corrected for multiple comparisons using the Holm-Sidak method where appropriate, and represented as mean ± SEM, with n representing number of animals in each group. Differences were considered significant when $p < 0.05$. Statistics were computed using Prism (GraphPad Software, La Jolla, CA).

4.8 Supplemental Information

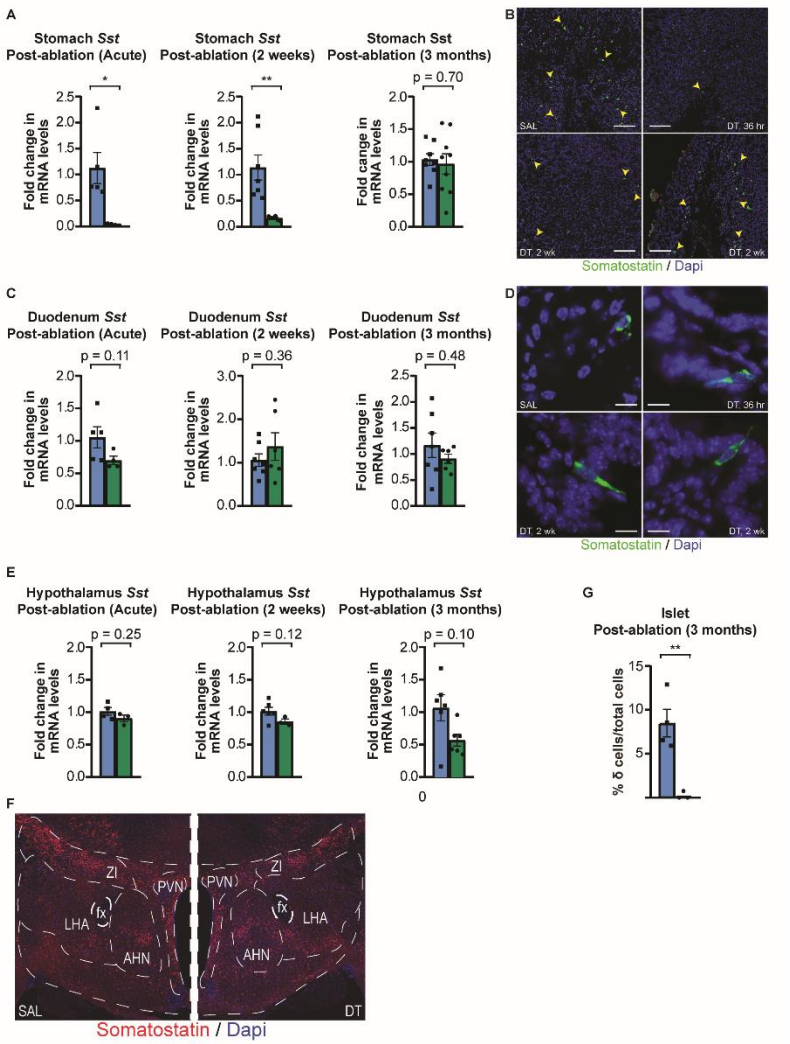

Figure 4.7: S1, related to Figure 4.2. Effect of DT-mediated ablation on other SST-expressing tissue. A) Transcript levels of *Sst* mRNA in the stomach 36 hours (acute), 2 weeks, or 3 months after the last injection of DT. B) Immunofluorescent stains showing the presence or absence of gastric D cells, which are labeled as green using the SST antibody. Yellow arrows denote some of the D cells observed in the samples. C) Transcript levels of *Sst* mRNA in the duodenum 36 hours (acute), 2 weeks, or 3 months after the last injection of DT. E) Immunofluorescent stain showing the presence of intestinal D cells. E) Transcript levels of *Sst* mRNA in the hypothalamus 36 hours, 2 weeks, or 3 months after the last injection of DT. F) Immunofluorescent stain of the hypothalamus showing that SST+ neurons remain. G) Transcript levels of *Sst* mRNA in the islet 3 months after the last injection of DT.

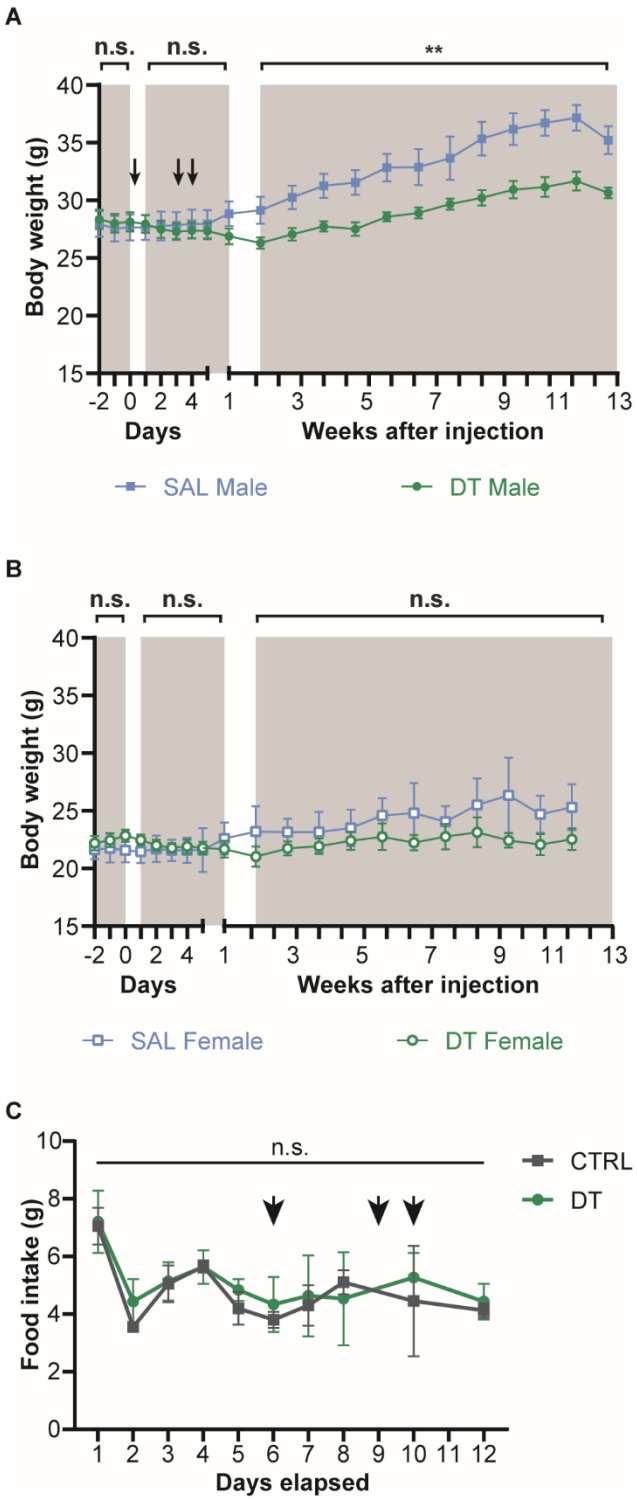

Figure 4.8: S2, related to Figure 4.2. Effect of delta cell ablation on body weight and food intake. Arrows represent days DT was administered. A and B) Body weight of A) male and B) female mice over time. C) Measurement of food intake of a separate cohort of mice. *Sst*-Cre mice without lsl-DTR that were injected with DT were used as controls. Error bars represent SEM. **p < 0.01

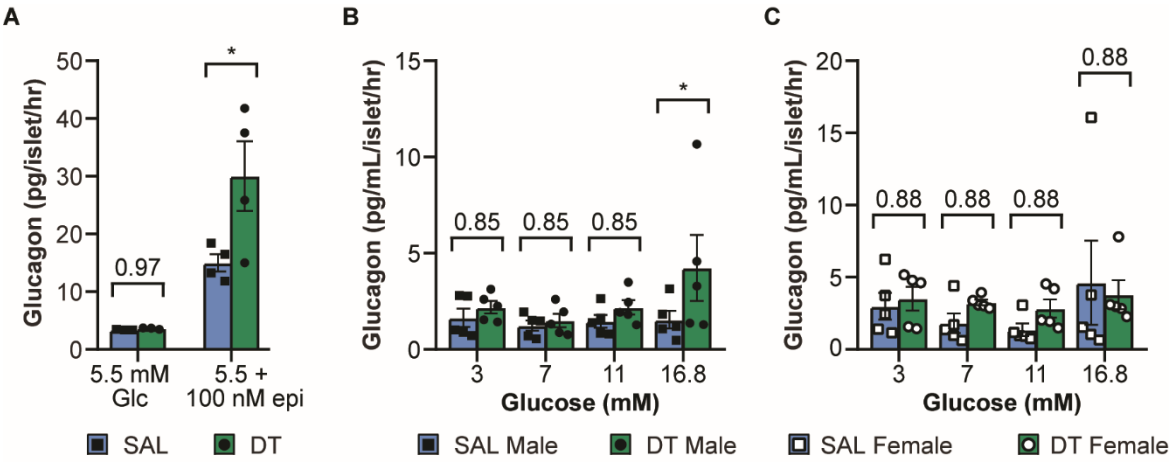

Figure 4.9: S3, related to Figure 4.4. Glucagon secretion increases in the absence of delta cells. A) Static glucagon secretion performed on SAL-treated or DT-treated *Sst*-Cre x lsl-DTR mice, in the absence or presence of epinephrine. B and C) Measurement of glucagon from islets incubated under 3 mM, 7 mM, 11 mM, and 16.8 mM glucose. Islets were isolated from B) male or C) female mice.

4.9 References

Ackermann AM, Zhang J, Heller A, Briker A & Kaestner KH 2016 High-fidelity Glucagon-CreER mouse line generated by CRISPR-Cas9 assisted gene targeting. *Molecular Metabolism* **6** 236–244. (doi:10.1016/j.molmet.2017.01.003)

Alonge KM, D'Alessio DA & Schwartz MW 2021 Brain control of blood glucose levels: implications for the pathogenesis of type 2 diabetes. *Diabetologia* **64** 5–14. (doi:10.1007/s00125-020-05293-3)

Arrojo e Drigo R, Jacob S, García-Prieto CF, Zheng X, Fukuda M, Nhu HTT, Stelmashenko O, Peçanha FLM, Rodriguez-Diaz R, Bushong E *et al.* 2019 Structural basis for delta cell paracrine regulation in pancreatic islets. *Nature Communications* **10** 3700. (doi:10.1038/s41467-019-11517-x)

Bloom SR, Mortimer CH, Thorner MO, Besser GM, Hall R, Gomez-Pan A, Roy VM, Russell RCG, Coy DH, Kastin AT *et al.* 1974 Inhibition of Gastrin and Gastric-Acid Secretion By Growth-Hormone Release-Inhibiting Hormone. *The Lancet* **304** 1106–1109. (doi:10.1016/S0140-6736(74)90869-1)

Blum B, Hrvatin S, Schuetz C, Bonal C, Rezania A & Melton DA 2012 Functional beta-cell maturation is marked by an increased glucose threshold and by expression of urocortin 3. *Nature Biotechnology* **30** 261–264. (doi:10.1038/nbt.2141)

Blum B, Roose AN, Barrandon O, Maehr R, Arvanites AC, Davidow LS, Davis JC, Peterson QP, Rubin LL & Melton DA 2014 Reversal of β cell de-differentiation by a small molecule inhibitor of the TGFβ pathway. *ELife* **3** e02809. (doi:10.7554/eLife.02809)

Buch T, Heppner FL, Tertilt C, Heinen TJAJ, Kremer M, Wunderlich FT, Jung S & Waisman A 2005 A Cre-inducible diphtheria toxin receptor mediates cell lineage ablation after toxin administration. *Nature Methods* **2** 419–426. (doi:10.1038/nmeth762)

Capozzi ME, Wait JB, Koech J, Gordon AN, Coch RW, Svendsen B, Finan B, D'Alessio DA & Campbell JE 2019a Glucagon lowers glycemia when β cells are active. *JCI Insight* **4**. (doi:10.1172/jci.insight.129954)

Capozzi ME, Svendsen B, Encisco SE, Lewandowski SL, Martin MD, Lin H, Jaffe JL, Coch RW, Haldeman JM, MacDonald PE *et al.* 2019b β Cell tone is defined by proglucagon peptides through cAMP signaling. *JCI Insight* **4**. (doi:10.1172/jci.insight.126742)

Carroll PB, Zeng Y, Alejandro R, Starzl TE & Ricordi C 1992 Glucose homeostasis is regulated by donor islets in xenografts. *Transplantation Proceedings* **24** 2980–2981.

Chambers AP, Sorrell JE, Haller A, Roelofs K, Hutch CR, Kim KS, Gutierrez-Aguilar R, Li B, Drucker DJ, D'Alessio DA *et al.* 2017 The Role of Pancreatic Preproglucagon in Glucose Homeostasis in Mice. *Cell Metabolism* **25** 927-934.e3. (doi:10.1016/j.cmet.2017.02.008)

Ewing KL & Tauber OE 1964 Blood chemistry changes in mice fed high levels of polyoxyethylene sorbitan derivatives. *Toxicology and Applied Pharmacology* **6** 442–446. (doi:10.1016/S0041-008X(64)80010-7)

Gahete MD, Pozo-salas AI, Martínez-fuentes AJ, Lecea L De, Gracia-navarro F, Kineman RD, Castan JP & Luque RM 2011 Cortistatin Is Not a Somatostatin Analogue but Stimulates Prolactin Release and Inhibits GH and ACTH in a Gender-Dependent Fashion : Potential Role of Ghrelin. **152** 4800–4812. (doi:10.1210/en.2011-1542)

Gerich JE 1993 *Control of Glycaemia*. (doi:10.1016/S0950-351X(05)80207-1)

German JP, Thaler JP, Wisse BE, Oh-I S, Sarruf DA, Matsen ME, Fischer JD, Taborsky GJ, Schwartz MW & Morton GJ 2011 Leptin activates a novel CNS mechanism for insulin-independent normalization of severe diabetic hyperglycemia. *Endocrinology* **152** 394–404. (doi:10.1210/en.2010-0890)

Hauge-Evans AC, King AJ, Carmignac D, Richardson CC, Robinson ICAF, Low MJ, Christie MR,

Persaud SJ & Jones PM 2009 Somatostatin secreted by islet δ-cells fulfills multiple roles as a paracrine regulator of islet function. *Diabetes* **58** 403–411. (doi:10.2337/db08-0792)

Holst JJ, Orskov C & Seier-Poulsen S 1992 Somatostatin is an essential paracrine link in acid inhibition of gastrin secretion. *Digestion* **51** 95–102. (doi:10.1159/000200882)

Holst JJ, Gribble F, Horowitz M & Rayner CK 2016 Roles of the gut in glucose homeostasis. *Diabetes Care* **39** 884–892. (doi:10.2337/dc16-0351)

Huang C, Rosencrans RF, Bugescu R, Vieira CP, Hu P, Adu-Agyeiwaah Y, Gamble KL, Longhini ALF, Fuller PM, Leinninger GM *et al.* 2021 Depleting hypothalamic somatostatinergic neurons recapitulates diabetic phenotypes in mouse brain, bone marrow, adipose and retina. *Diabetologia* **64** 2575–2588. (doi:10.1007/s00125-021-05549-6)

Huising MO 2020 Paracrine regulation of insulin secretion. *Diabetologia* **63** 2057–2063. (doi:10.1007/s00125-020-05213-5)

Huising MO, van der Meulen T, Huang JL, Pourhosseinzadeh MS & Noguchi GM 2018 The Difference δ-Cells Make in Glucose Control. *Physiology* **33** 403–411. (doi:10.1152/physiol.00029.2018)

Johansson C, Wisen O, Efendic S & Uvnäs-Wallensten K 1981 Effects of Somatostatin on Gastrointestinal Propagation and Absorption of Oral Glucose in Man. *Digestion* **22** 126–137. (doi:https://doi.org/10.1159/000198619)

Karasawa H, Yakabi S, Wang L, Stengel A, Rivier J & Taché Y 2014 Brain somatostatin receptor 2 mediates the dipsogenic effect of central somatostatin and cortistatin in rats: Role in drinking behavior. *American Journal of Physiology - Regulatory Integrative and Comparative Physiology* **307** R793–R801. (doi:10.1152/ajpregu.00248.2014)

Kavalakatt S, Khadir A, Madhu D, Hammad M, Devarajan S, Abubaker J, Al-Mulla F, Tuomilehto J & Tiss A 2019 Urocortin 3 Levels Are Impaired in Overweight Humans With and Without

Type 2 Diabetes and Modulated by Exercise. *Frontiers in Endocrinology* **10** 1–11. (doi:10.3389/fendo.2019.00762)

Lai BK, Chae H, Gómez-Ruiz A, Cheng P, Gallo P, Antoine N, Beauloye C, Jonas JC, Seghers V, Seino S *et al.* 2018 Somatostatin is only partly required for the glucagonostatic effect of glucose but is necessary for the glucagonostatic effect of KATP channel blockers. In *Diabetes*, pp 2239–2253. (doi:10.2337/db17-0880)

Li N, Yang Z, Li Q, Yu Z, Chen X, Li JC, Li B, Ning SL, Cui M, Sun JP *et al.* 2018 Ablation of somatostatin cells leads to impaired pancreatic islet function and neonatal death in rodents article. *Cell Death and Disease* **9**. (doi:10.1038/s41419-018-0741-4)

Lieverse RJ, Jansen JBMJ, Masclee AAM & Lamers CBHW 1995 Effects of somatostatin on human satiety. *Neuroendocrinology* **61** 112–116. (doi:10.1159/000126831)

Liu L, Dattaroy D, Simpson KF, Barella LF, Cui Y, Xiong Y, Jin J, König GM, Kostenis E, Roman JC *et al.* 2021 Gq signaling in α cells is critical for maintaining euglycemia. *JCI Insight* **6** 1–17. (doi:10.1172/jci.insight.152852)

Luo SX, Huang J, Li Q, Mohammad H, Lee CY, Krishna K, Kok AMY, Tan YL, Lim JY, Li H *et al.* 2018 Regulation of feeding by somatostatin neurons in the tuberal nucleus. *Science* **361** 76–81. (doi:10.1126/science.aar4983)

Luque RM & Kineman RD 2007 Gender-Dependent Role of Endogenous Somatostatin in Regulating Growth Hormone-Axis Function in Mice. **148** 5998–6006. (doi:10.1210/en.2007-0946)

Luque RM, Cordoba-chacon J & Pozo-salas AI 2016 Obesity- and gender-dependent role of endogenous somatostatin and cortistatin in the regulation of endocrine and metabolic homeostasis in mice. *Nature Publishing Group* 1–12. (doi:10.1038/srep37992)

Madisen L, Zwingman TA, Sunkin SM, Oh SW, Zariwala HA, Gu H, Ng LL, Palmiter RD,

Hawrylycz MJ, Jones AR *et al.* 2010 A robust and high-throughput Cre reporting and characterization system for the whole mouse brain. *Nature Neuroscience* **13** 133–140. (doi:10.1038/nn.2467)

Madisen L, Garner AR, Shimaoka D, Chuong AS, Klapoetke NC, Li L, van der Bourg A, Niino Y, Egolf L, Monetti C *et al.* 2015 Transgenic mice for intersectional targeting of neural sensors and effectors with high specificity and performance. *Neuron* **85** 942–958. (doi:10.1016/j.neuron.2015.02.022)

Matschinsky FM & Davis EA 1998 The Distinction between 'Glucose Setpoint', 'Glucose Threshold' and 'Glucose Sensor' is Critical for Understanding the Role of the Pancreatic β-Cell in Glucose Homeostasis. *Molecular and Cell Biology of Type 2 Diabetes and Its Complications* **14** 14–29. (doi:10.1159/000060872)

van der Meulen T, Donaldson CJ, Cáceres E, Hunter AE, Cowing-Zitron C, Pound LD, Adams MW, Zembrzycki A, Grove KL & Huising MO 2015 Urocortin3 mediates somatostatin-dependent negative feedback control of insulin secretion. *Nature Medicine* **21** 769–776. (doi:10.1038/nm.3872)

Morton GJ, Matsen ME, Bracy DP, Meek TH, Nguyen HT, Stefanovski D, Bergman RN, Wasserman DH & Schwartz MW 2013 FGF19 action in the brain induces insulin-independent glucose lowering. *Journal of Clinical Investigation* **123** 4799–4808. (doi:10.1172/JCI70710)

Noguchi GM & Huising MO 2019 Integrating the inputs that shape pancreatic islet hormone release. *Nature Metabolism* **1** 1189–1201. (doi:10.1038/s42255-019-0148-2)

Pagliara AS, Stillings SN, Hover B, Martin DM & Matschinsky FM 1974 Glucose modulation of amino acid induced glucagon and insulin release in the isolated perfused rat pancreas. *Journal of Clinical Investigation* **54** 819–832. (doi:10.1172/JCI107822)

Pedersen J, Ugleholdt RK, Jørgensen SM, Windeløv JA, Grunddal K V, Schwartz TW, Füchtbauer

EM, Poulsen SS, Holst PJ & Holst JJ 2013 Glucose metabolism is altered after loss of L cells and α-cells but not influenced by loss of K cells. *American Journal of Physiology - Endocrinology and Metabolism* **304** 60–73. (doi:10.1152/ajpendo.00547.2011)

Richardson CC, To K, Foot VL, Hauge-Evans AC, Carmignac D & Christie MR 2015 Increased perinatal remodelling of the pancreas in somatostatin-deficient mice: Potential role of transforming growth factor-beta signalling in regulating beta cell growth in early life. *Hormone and Metabolic Research* **47** 56–63. (doi:10.1055/s-0034-1390427)

Rodriguez-Diaz R, Molano RD, Weitz JR, Abdulreda MH, Berman DM, Leibiger B, Leibiger IB, Kenyon NS, Ricordi C, Pileggi A *et al.* 2018 Paracrine Interactions within the Pancreatic Islet Determine the Glycemic Set Point. *Cell Metabolism* **27** 549-558.e4. (doi:10.1016/j.cmet.2018.01.015)

Ryan KK, Kohli R, Gutierrez-Aguilar R, Gaitonde SG, Woods SC & Seeley RJ 2013 Fibroblast growth factor-19 action in the brain reduces food intake and body weight and improves glucose tolerance in male rats. *Endocrinology* **154** 9–15. (doi:10.1210/en.2012-1891)

Shiota C, Prasadan K, Guo P, El-Gohary Y, Wiersch J, Xiao X, Esni F & Gittes GK 2013 α-cells are dispensable in postnatal morphogenesis and maturation of mouse pancreatic islets. *American Journal of Physiology - Endocrinology and Metabolism* **305** 1030–1040. (doi:10.1152/ajpendo.00022.2013)

Singh B, Khattab F, Chae H, Desmet L, Herrera PL & Gilon P 2021 KATP channel blockers control glucagon secretion by distinct mechanisms: A direct stimulation of α-cells involving a [Ca2+]c rise and an indirect inhibition mediated by somatostatin. *Molecular Metabolism* **53** 101268. (doi:10.1016/j.molmet.2021.101268)

Srinivas S, Watanabe T, Lin CS, William CM, Tanabe Y, Jessell TM & Costantini F 2001 Cre reporter strains produced by targeted insertion of EYFP and ECFP into the ROSA26 locus.

BMC Developmental Biology **1** 1–8. (doi:10.1186/1471-213X-1-4)

Stengel A & Taché Y 2019 Central somatostatin signaling and regulation of food intake. *Annals of the New York Academy of Sciences* **1455** 98–104. (doi:10.1111/nyas.14178)

Svendsen B, Larsen O, Gabe MBN, Christiansen CB, Rosenkilde MM, Drucker DJ & Holst JJ 2018 Insulin Secretion Depends on Intra-islet Glucagon Signaling. *Cell Reports* **25** 1127-1134.e2. (doi:10.1016/j.celrep.2018.10.018)

Szot GL, Koudria P & Bluestone JA 2007 Transplantation of pancreatic islets into the kidney capsule of diabetic mice. *Journal of Visualized Experiments* 9–10. (doi:10.3791/404)

Taniguchi H, He M, Wu P, Kim S, Paik R, Sugino K, Kvitsani D, Fu Y, Lu J, Lin Y *et al.* 2011 A Resource of Cre Driver Lines for Genetic Targeting of GABAergic Neurons in Cerebral Cortex. *Neuron* **71** 995–1013. (doi:10.1016/j.neuron.2011.07.026)

Tellez K, Hang Y, Gu X, Chang CA, Stein RW & Kim SK 2020 In vivo studies of glucagon secretion by human islets transplanted in mice. *Nature Metabolism* **2** 547–557. (doi:10.1038/s42255-020-0213-x)

Thorel F, Damond N, Chera S, Wiederkehr A, Thorens B, Meda P, Wollheim CB & Herrera PL 2011 Normal glucagon signaling and β-cell function after near-total α-cell ablation in adult mice. *Diabetes* **60** 2872–2882. (doi:10.2337/db11-0876)

Thorens B 2012 Sensing of glucose in the brain. *Handbook of Experimental Pharmacology* **209** 277–294. (doi:10.1007/978-3-642-24716-3_12)

Viollet C, Simon A, Tolle V, Labarthe A, Grouselle D, Loe-Mie Y, Simonneau M, Martel G & Epelbaum J 2017 Somatostatin-IRES-cre mice: Between knockout and wild-type? *Frontiers in Endocrinology* **8** 1–8. (doi:10.3389/fendo.2017.00131)

Wicksteed B, Brissova M, Yan W, Opland DM, Plank JL, Reinert RB, Dickson LM, Tamarina NA, Philipson LH, Shostak A *et al.* 2010 Conditional gene targeting in mouse pancreatic β-cells:

Analysis of ectopic cre transgene expression in the brain. *Diabetes* **59** 3090–3098. (doi:10.2337/db10-0624)

Xu SFS, Andersen DB, Izarzugaza JMG, Kuhre RE & Holst JJ 2020 In the rat pancreas, somatostatin tonically inhibits glucagon secretion and is required for glucose-induced inhibition of glucagon secretion. *Acta Physiologica*. (doi:10.1111/apha.13464)

Zhang J, Mckenna LB, Bogue CW & Kaestner KH 2014 The diabetes gene Hhex maintains δ -cell differentiation and islet function. *Genes and Development* 829–834. (doi:10.1101/gad.235499.113)

Zhu H, Aryal DK, Olsen RHJ, Urban DJ, Swearingen A, Forbes S, Roth BL & Hochgeschwender U 2016 Cre-dependent DREADD (Designer Receptors Exclusively Activated by Designer Drugs) mice. *Genesis* **54** 439–446. (doi:10.1002/dvg.22949)

Zhu L, Dattaroy D, Pham J, Wang L, Barella LF, Cui Y, Wilkins KJ, Roth BL, Hochgeschwender U, Matschinsky FM *et al.* 2019 Intraislet glucagon signaling is critical for maintaining glucose homeostasis. *JCI Insight* **4**. (doi:10.1172/jci.insight.127994)

Chapter 5

The Difference Delta Cells Make in Glucose Control

5.1 Preface

This chapter was originally published in *Physiology*:

Huising MO, van der Meulen T, Huang JL, Pourhosseinzadeh MS, Noguchi GM. (2018) The Difference δ-Cells Make in Glucose Control. Physiology (Bethesda). 33(6):403-411.

I contributed to analysis of experiments and editing of this manuscript. This article has been modified to satisfy the requirements of this dissertation.

5.2 Abstract

The role of beta and alpha cells to glucose control are established, but the physiological role of delta cells is poorly understood. Delta cells are ideally positioned within pancreatic islets to modulate insulin and glucagon secretion at their source. We review the evidence for a negative feedback loop between delta and beta cells that determines the blood glucose set point and suggest that local delta cell-mediated feedback stabilizes glycemic control.

5.3 Introduction

Over half of US adults are now estimated to have diabetes or pre-diabetes (44). Type 1 diabetes (T1D) is caused by the autoimmune destruction of beta cells, while Type 2 diabetes (T2D) results from

peripheral insulin resistance precipitated by factors associated with lifestyle and genetic predisposition. Both diseases are characterized by absolute (T1D) or relative (T2D) insulin deficiency. Consequently, pancreatic beta cells have been studied intently for decades. Less appreciated is that excess glucagon secretion from pancreatic alpha cells is responsible for as much as half of the hyperglycemia in diabetes (77), which is the immediate cause for most diabetes-related complications. Successful diabetes management therefore requires effective strategies to not only restore insulin or improve insulin action, but to prevent glucagon-induced hepatic glucose production from aggravating hyperglycemia. Here we make the case that pancreatic delta cells provide crucial feedback control of alpha and beta cells to coordinate insulin and glucagon secretion in healthy islets that breaks down in diabetes.

5.4 The pancreatic islet is home to more than beta cells

The principal endocrine output of the pancreatic islets are insulin and glucagon. During and shortly after feeding nutrients absorbed across the intestinal epithelia stimulate insulin secretion. Conversely, under catabolic conditions that occur between meals or during a fast, beta cells are silent as alpha cell activity increases to safeguard against hypoglycemia. Healthy islets are capable of balancing insulin and glucagon output with tremendous precision. This is illustrated by continuous glucose monitoring (CGM) experiments in mice (78) that reveal the narrow range within blood glucose is maintained over multiple diurnal cycles despite *ad libitum* food access. Similarly, a healthy human pancreas maintains euglycemia over 87,000 meals consumed in a lifetime[1]. While alpha and beta cells each possess the ability to sense glucose in a cell-autonomous fashion, it is no coincidence that they are organized in close proximity within the islets of Langerhans. This arrangement enables careful coordination between insulin and glucagon at their source by a potent combination of paracrine, neural, and

[1] *Assuming three meals a day, average US life expectancy of 79.56 years (source: cia.gov/library/publications/the-world-factbook/fields/2102.html).*

endocrine inputs (Figure 5.1A). Among the most prominent of these signals is somatostatin released by pancreatic delta cells (62), which make up approximately 5-10% of the endocrine cells within the islet.

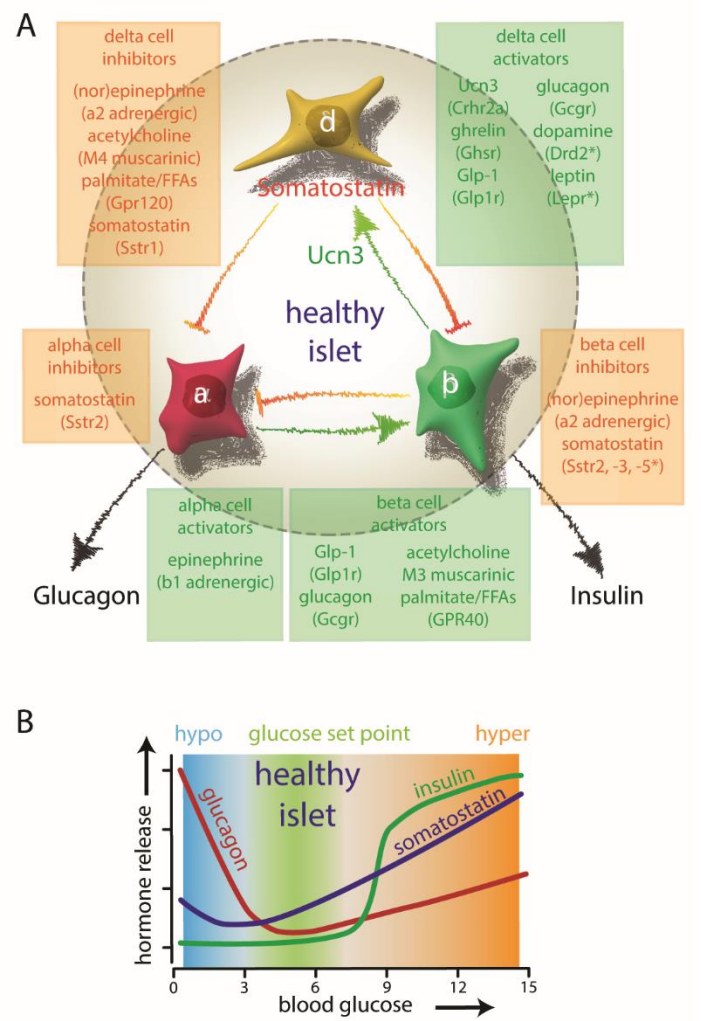

Figure 5.1: (A) Pancreatic delta cells receive input from numerous paracrine, endocrine and neural inputs and translate this into appropriate inhibition of glucagon and insulin release by alpha and beta cells. Select stimulatory and inhibitory inputs are given for each of the islet cell types. (B) Schematic representation of the profiles of insulin, glucagon and somatostatin secretion as a function of blood glucose.

5.5 Discovery of delta cells

Pancreatic delta cells were first recognized as a distinct cell type from alpha and beta cells based on alcohol- and aqueous-based histological staining methods, and were originally referred to as A1 cells, C cells, gamma cells, or D cells (3). These cells had no known function and were considered to

represent a distinct functional stage of alpha or beta cells. This changed with the discovery that somatostatin, a novel hypothalamic peptide named for its ability to suppress somatic growth by inhibiting growth hormone (11), is found in all pancreatic delta cells (21, 32). Synthetic somatostatin peptide was subsequently confirmed to potently inhibit insulin and glucagon secretion from isolated islets (13). However, the pancreatic delta cell has long been understudied, in part because it has been challenging to quantify the impact of local delta cell-dependent feedback on alpha and beta cells. The physiological importance of delta cell-mediated feedback on insulin and glucagon release is only now coming into focus.

5.6 Paracrine crosstalk within pancreatic islets

While beta and alpha cell activity is inextricably tied to glucose levels, many signals from inside and outside the islet ultimately contribute to shape the final insulin and glucagon output. Insulin release from beta cells is triggered when glucose exceeds a threshold of approximately 7 mM glucose (16, 80) (Figure 5.1B). Glucose-stimulated insulin secretion (GSIS) can be further amplified via the actions of incretin hormones such as glucagon-like peptide-1 (GLP-1). GLP-1 activates its cognate GLP-1 receptor (GLP1R), a Gαs-coupled class B GPCR abundantly expressed on beta cells. This amplifying pathway is largely ineffective below the glucose threshold of beta cells, preventing incretins from stimulating insulin release under low glucose. This greatly reduces the risk of insulin-induced hypoglycemia, which underlies the success and safety of incretin-based therapies in treating T2D.

Control of glucagon release is complex and follows a biphasic response to glucose (Figure 5.1B). Maximal glucagon secretion occurs under low glucose and decreases towards a nadir around 5 mM glucose (24, 43, 80). Alpha cells are directly suppressed by glucose via an alpha cell-intrinsic mechanism that involves K_{ATP} channel inhibition (80). On top of the direct stimulatory effects of low glucose, alpha cells respond robustly to adrenergic stimulation as part of the counterregulatory

response to hypoglycemia (75). A rise in glucose beyond 5 mM activates an ER Ca^{2+} store-operated mechanism that – paradoxically – facilitates glucagon release under hyperglycemic conditions (41, 80). It has long been known that glucagon *stimulates* insulin secretion (66, 67), even though the systemic actions of glucagon functionally oppose those of insulin. This effect is mediated by the glucagon receptor (GCGR), a class B GPCR related to the incretin receptors that like GLP1R is Gαs-coupled and expressed by beta cells (Figure 5.1). Glucagon essentially acts in an incretin-like fashion to amplify GSIS within the islet. In fact, the most recent evidence suggests that glucagon from alpha cells may be required for full GSIS in response to hyperglycemia (59). Glucagon secretion is suppressed by beta cell-dependent inhibitory control (28, 29), which is often attributed to the direct inhibitory actions of beta cell-derived factors such as insulin, GABA and Zn^{2+} on alpha cells (22, 43, 53, 60, 80, 83). However, none of these beta cell-derived factors has consistently emerged as the predominant inhibitor of alpha cell activity. Therefore, the possibility of beta cell-dependent activation of delta cells that inhibits alpha cells via somatostatin during hyperglycemia is likely. Collectively, this illustrates how hormone release from the islets is controlled by a complex – at times paradoxical - web of paracrine interactions.

5.7 The delta cell provides paracrine feedback within the islet

Delta cells are organized together with alpha cells around the mouse islet periphery, where they envelop a core of beta cells. In humans, they are intermingled with the other endocrine cell types. Delta cells release a 14 amino acid form of somatostatin (Sst-14) that is proteolytically cleaved from a larger precursor (50). Somatostatin is also released from other peripheral sites, notably from enteroendocrine D cells in the gastrointestinal (GI) tract, which primarily secrete a larger, 28 amino acid form (Sst-28). Circulating somatostatin concentrations are largely unaffected by pancreatectomy and therefore do not reflect pancreatic delta cell activity (25, 74). Instead, the GI tract is the major

source of circulating somatostatin, which may influence islet beta and alpha cells (14, 42). Nevertheless, circulating somatostatin (~5-25 pM) is an order of magnitude below the IC50 and EC50 values of somatostatin receptors (55, 56), suggesting that delta cells are the predominant source of somatostatin within the islet. Therefore, the main function of the pancreatic delta cell is to provide feedback control of neighboring beta and alpha cells via local circulation and the interstitial compartment (13, 65). The inhibitory actions of somatostatin are mediated via five somatostatin receptors, SSTR1 – SSTR5. These are class A GPCRs that generally inhibit their target cells by activating the inhibitory G□i protein or G protein-coupled inwardly rectifying K^+ (GIRK) channels (50). Islets or beta cells have been suggested to express each of the somatostatin receptors, mostly by antibody-dependent methods that critically depend on the quality and careful validation of the reagents (reviewed by 9, 38, 50, 51). However, comprehensive alpha, beta and delta cell transcriptomes do not support much of this prior work. While it is true that somatostatin receptors are expressed by each of the islet cell types (Figure 5.1A), abundant expression of Sstr2 by alpha cells is the only aspect that unequivocally holds up from these earlier reports (reviewed by 1, 20). Mouse beta cells abundantly (but not exclusively) express Sstr3, which is rarely mentioned in reviews of islet somatostatin receptors. Somatostatin secretion is stimulated dose-dependently by glucose in a linear fashion (Figure 5.1B) (65, 82). But even below the glucose threshold for beta cells, alpha cells are activated upon the addition of somatostatin antagonists, suggesting that significant basal somatostatin tone restrains alpha cell activity across the glucose spectrum. In addition to glucose, sulfonylureas, amino acids and cAMP are all capable of stimulating somatostatin secretion (2, 10, 23, 34, 69). However, until recently, the physiological cues that govern delta cell activity during normal glucose metabolism were not understood.

5.8 Urocortin3 is required for normal glucose-stimulated somatostatin secretion

We discovered that normal glucose-stimulated somatostatin secretion (GSSS) requires the peptide hormone Urocortin 3 (UCN3), which is related to corticotropin-releasing hormone (CRH) and activates the type 2 CRH receptor (CRHR2). UCN3 is the 3rd most abundant beta cell hormone after insulin and amylin and is co-released with insulin from beta cells (40, 78). UCN3 selectively activates delta cells, which express the □ isoform of CRHR2 (20, 33), to release somatostatin. This finding closed a novel intra-islet negative feedback loop that is initiated by beta cell release of UCN3 to promote delta cell somatostatin secretion, which inhibits beta cells. Indeed, *Ucn3* null mice show impaired somatostatin secretion, which can be fully rescued by addition of synthetic UCN3 peptide (78). Predictably, the impaired somatostatin secretion enables exaggerated first- and second phase GSIS, which is also immediately normalized upon perfusion with synthetic UCN3. This *Ucn3* null phenotype closely resembles the phenotype of somatostatin null mice, which also demonstrate an exaggerated first- and second-phase GSIS that is acutely normalized by the supplementation of synthetic somatostatin peptide (26). The similar phenotype of the null mice offers strong support for the participation of UCN3 and somatostatin in the same feedback loop. Blocking endogenous UCN3 with the selective CRHR2 peptide antagonist Astressin2b (Ast2b) (56) prevents GSSS from mouse and human islets (78). This demonstrates that during hyperglycemia, endogenous Ucn3 released from beta cells is necessary and sufficient for somatostatin secretion, which proceeds to inhibit beta cells. Taken together, these observations have established that UCN3 activates a beta cell-dependent, delta cell-mediated negative feedback loop to attenuate insulin secretion.

5.9 Bidirectional exchange of paracrine signals within the islet

The paracrine role of delta cell and the viability of the UCN3-mediated negative feedback loop rests on the ability of delta cells to efficiently receive and relay signals within the islet. Crosstalk is often considered to occur via intra-islet capillary circulation, but there is no consensus whether circulation

in the rodent islets favors mantle-to-core communication (46, 49) or vice versa (8, 48, 68). Several factors favor the model of a feedback loop mediated by UCN3 and somatostatin that relies on a bidirectional exchange of signals between in the mantle and beta cells in the core. First, there is emerging evidence that islet blood flow is dynamically regulated (19). Second, somatostatin and/or UCN3 may reach their target cells by diffusion through the interstitial space. Third, beta cells within an islet are electrically coupled via Connexin-36 gap junctions (5, 27), implying that not every individual beta cell needs to be directly suppressed by somatostatin to ensure effective inhibition of all beta cells within an islet. Fourth, mouse delta cells have axon-like projections that enable the release and receipt of signals at some distance from the cell body and make them readily distinguishable from beta and alpha cells (Figure 5.2A). Finally, adult human islets feature a more random intermingling of alpha, beta, and delta cells (Figure 5.2B) that would only be more conducive to the bidirectional feedback between beta and delta cells first identified in mouse islet. Interestingly, human delta cells lack the characteristic axon-like projections of mouse delta cells and are significantly more compact than mouse delta cells (Figure 5.2C), which may represent a morphological correlate of the distribution of delta cells throughout the human islet.

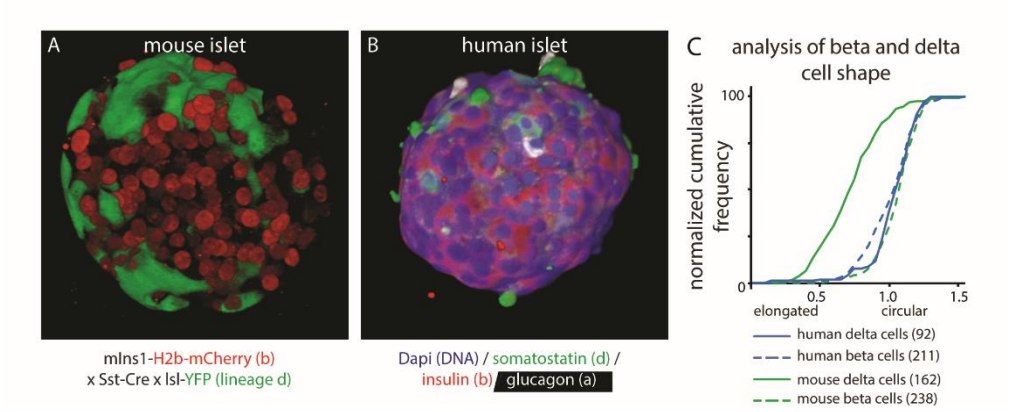

Figure 5.2: (A) Projection of a 3D reconstruction of a pancreatic islet from a transgenic reporter strain, captured by confocal microscope. Beta cells are visualized by the nuclear expression of an mCherry under control of the *Ins1* promoter. Delta cells are visualized by the expression of Cre recombinase under control of the somatostatin (*Sst*) promotor, which leads to their irreversible expression of yellow fluorescent protein (YFP; green). (B) Projection of a 3D reconstruction of a human pancreatic islet, captured by confocal microscope and stained for somatostatin (green), insulin (red) and glucagon (white). Nuclei (dapi) are counterstained in blue. Note how the human delta cells are notably more compact compared to the axon-like mouse delta cells. (C) The difference in morphology of mouse and human delta cells and beta cells from the same islet was quantified their circularity, defined as the normalized ratio of the area over the perimeter of the cell outline. Each cell outline was determined in Nikon Elements and circularity was calculated as 4 times π times the perimeter squared: (4*π*Area)/(Perimeter^(2)). A value of one indicates a perfect circle. Mouse delta cells stand out for their elongated morphology, which manifests as a significant reduction in circularity, compared to beta cells, while human delta cells are similarly compact to human beta cells. Numbers in-between parentheses reflect the number of cells quantified from 3D confocal reconstructions of intact islets from two individual subjects for each species.

5.10 The beta cell as a blueprint for the delta cell

The discovery that UCN3 is required for normal GSSS raised the question whether delta cells respond directly to glucose at all, or if GSSS can be fully accounted for by the paracrine actions of UCN3. To develop a working model of the relative contributions of glucose and paracrine signals such as UCN3 on delta cell activity, it is helpful to turn to the beta cells. Beta cells share an immediate precursor with delta cells in pancreas development (70) and the mechanistic basis of their activation has been extensively studied. Beta cell activation is triggered by the uptake of glucose by passive diffusion through glucose transporters, followed by its stepwise catabolism via the TCA cycle and oxidative phosphorylation yielding ATP. The increased ATP/ADP ratio closes ATP-sensitive K^+ leak (K_{ATP})

channels, which causes accumulation of K^+ and depolarization of the beta cell. This triggers opening of voltage-gated Na^+ and L-type Ca^{2+} channels. The resulting Ca^{2+} influx stimulates exocytosis of secretory granules (reviewed by 61).

A number of studies have suggested that beta and delta cells share common mechanisms of activation. Diazoxide, which keeps the K_{ATP} channel complex in the open conformation to prevent depolarization and the L-type calcium channel blocker isradipine, block both insulin and somatostatin secretion when applied to intact islets (10, 78). Importantly, exogenous UCN3 fails to rescue both diazoxide- and isradipine-mediated inhibition of somatostatin secretion (78). This demonstrates that the closure of delta cell K_{ATP} channels and the influx of Ca^{2+} via L-type channels in response to glucose is necessary for normal somatostatin secretion. However, somatostatin release from islets null for *Ucn3* is only modestly (but significantly) stimulated by glucose and can be fully rescued by synthetic UCN3 (78). This proofs that the bulk of 'glucose-stimulated' somatostatin release actually depends on local UCN3. Overall, this favors a model where delta and beta cells use similar mechanisms to trigger hormone release in response to glucose, and further amplify it by G□ s-mediated signaling. Where delta cells differ from beta cells is in the identity of the signals that amplify glucose-stimulated hormone secretion, with locally released UCN3 the principal paracrine signal to stimulate delta cells, while beta cells respond instead to incretins and glucagon (Figure 5.1A).

5.11 The delta cell as a modulating hub that shapes islet cell activity

While UCN3 is the principal paracrine signal to stimulate somatostatin secretion, delta cells respond to a multitude of paracrine, endocrine and neural signals. For example, the potent insulinostatic actions of the hunger hormone ghrelin (17, 18, 54, 76, 84) are mediated indirectly via the stimulation of somatostatin release from delta cells (1, 20). And long-chain free fatty acids, such as palmitate, stimulate insulin secretion not just directly via the stimulation of GPR40 and enhanced beta cell

intracellular metabolic rate (35, 37), but also indirectly by suppressing somatostatin secretion via the inhibitory receptor GPR120 expressed by delta cells (72). Adrenosympathetic inputs (*i.e.* catecholamines) stimulate alpha cells via □1 adrenergic receptors as part of the counterregulatory response to hypoglycemia. Simultaneously, beta and delta cells are inhibited via □2 adrenergic receptors, which suppress insulin secretion and facilitate de-repression of alpha cells from somatostatin-mediated inhibition, respectively (20, 57). Delta cells are also suppressed by cholinergic inputs from autonomic innervation in mouse islets, or from acetylcholine release by human alpha cells (58). Recent transcriptomes from mouse (1, 4) and human (39) delta cells have validated the delta cell-selective expression of these receptors, and suggest furthermore that receptors for leptin (LEPR) and dopamine (DRD2) are expressed by human, but not mouse delta cells. Collectively, these observations cast the delta cell as a central hub within the islet that translates inputs from paracrine and endocrine signals, nutrients, and neurotransmitters into appropriate intra-islet feedback inhibition via somatostatin (Figure 5.1) (39).

5.12 Local feedback inhibition by delta cells determines the set point for plasma glucose

The physiological significance of delta cell paracrine signaling is highlighted by the role of the Ucn3-induced, delta cell-mediated negative feedback loop in postnatal development. Full expression of endogenous UCN3 does not occur until 2-weeks post-partum (P14) and coincides with a notable attenuation of plasma insulin and rise in glucose levels at this young age in mice (6, 79). To establish causality, we generated a doxycycline-inducible beta cell-specific bitransgenic mouse model to induce endogenous levels of UCN3 specifically within insulin-expressing cells with an onset and duration of our choosing (78). We induced UCN3 prematurely by administering doxycycline to pregnant dams

incapable of UCN3 induction from E10.5 onwards. This resulted in a premature increase in plasma glucose in bitransgenic offspring, which reflect the premature onset of UCN3-driven, somatostatin-mediated inhibition of insulin (Figure 5.3A, B). In control littermates this feedback does not set in until full expression of endogenous UCN3 after P14. This experiment established that the onset of local inhibitory feedback by pancreatic delta cells on insulin release determines the homeostatic set point for plasma glucose. Since the induction of UCN3 is restricted to pancreatic beta cells and remains undetectable in blood, we successfully isolated the effect of pancreatic delta cells from the potentially confounding contributions of somatostatin by other sources, such as the enteroendocrine D cells responsible for most of the circulating somatostatin (25, 74).

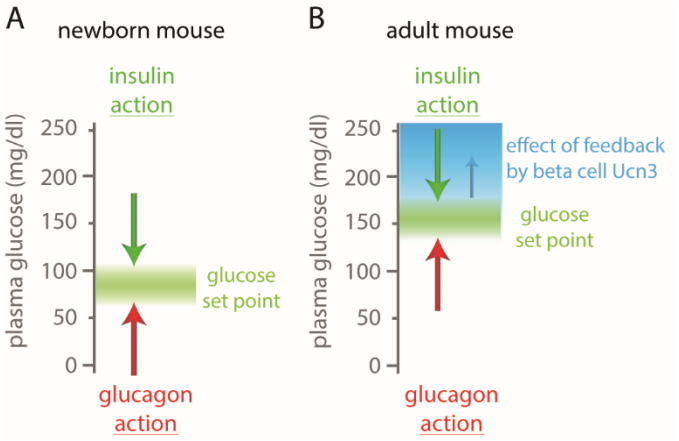

Figure 5.3: (A) In the absence of UCN3 in young neonatal mice, the homeostatic set point for glucose is determined by the balance between insulin and glucagon action. (B) After the onset of UCN3 expression in mouse beta cells, beta cell activation leads to the co-secretion of UCN3 with insulin. This activates feedback inhibition that curbs insulin secretion and effectively reduces insulin action.

5.13 The benefit of feedback inhibition by delta cells

As a field, the focus on restoring beta cell mass and function to increase insulin output and better manage diabetes makes it easy to forget that negative feedback regulation is a fundamental principle in biology to which beta cells are no exception. What then is the benefit of a delta cell-mediated feedback mechanism that inhibits insulin secretion? Unlike incretin hormones which can only amplify insulin secretion during hyperglycemia and are therefore relatively safe from stimulating insulin during hypoglycemia, insulin itself has very real potential to cause dangerous episodes of hypoglycemia. Indeed, insulin-induced hypoglycemia is a major risk factor that contributes to the death of too many patients who manage their diabetes with insulin (15). Somatostatin-mediated feedback control on beta cells is the mechanism by which healthy islets prevent excess insulin release. This feedback control must be robust because even a single hypoglycemic episode can be fatal. Our working model is that the benefit of delta cell-mediated feedback 1) prevents hyperinsulinemia-induced hypoglycemia and 2) ensures stable euglycemia with minimal deviations from the glucose set point.

Insulin secretion under hyperglycemia is pulsatile and driven by beta cell autonomous mechanisms (31, 45). Somatostatin secretion is also pulsatile, synchronized with beta cells, but trails insulin release by 30 seconds to a few minutes (28, 29, 65). While somatostatin secretion is triggered by glucose alone below the glucose threshold of beta cells (Figure 5.1B), the majority of somatostatin release during hyperglycemia depends on UCN3 from beta cells (78), which may account for the delay in somatostatin secretion. A model where somatostatin secretion directly depends on the paracrine actions of beta cell-derived UCN3 ensures: 1) synchronicity of delta and beta cell activity, 2) proportionality between the degree by which plasma glucose and insulin have deviated from their set point and the strength of the ensuing negative feedback, 3) that delta cell-mediated feedback control of insulin secretion is activated with an intrinsic delay. The purpose of negative feedback is not to prevent the initiation of insulin secretion in the face of hyperglycemia; that would lead to diabetes. A delay in somatostatin secretion ensures that the initial insulin secretion in response to hyperglycemia proceeds uninhibited. But thereafter, what we consider to be GSIS is in fact the net result of the simultaneous stimulation of beta cells with glucose and inhibition with somatostatin (Figure 5.4A). We propose that such feedback inhibition on beta cells is instrumental in precisely attenuating insulin secretion *in anticipation of* the return of plasma glucose to its homeostatic set point (Figure 5.4A). This prevents overshooting of insulin, which would cause a hypoglycemic excursion.

Recently, two reports suggested that delta cells are directly coupled to beta cells via gap junctions to explain the synchronicity of pulsatile insulin and somatostatin responses (12, 81), a possibility that had previously been ruled out (47). Indeed, this would lead to instant activation of delta cells upon beta cell activation and could not account for the delay in pulsatile somatostatin release compared to insulin. We have looked at the responses of several thousand delta cells within intact islets and have yet to observe clear evidence of direct gap-junction connections between delta and beta cells (Huising lab, unpublished).

5.14 Loss of UCN3 from beta cells early in diabetes increases glycemic volatility

UCN3 is one of the first beta cell markers to disappear in pre-diabetes (78). The mechanistic basis for this rapid downregulation is not well understood, beyond the observation that treatment with pro-inflammatory cytokines *in vitro* (7) or exposure to a pro-inflammatory environment in the context of the Non-Obese Diabetic (NOD) mouse model of T1D (63) cause a loss of beta cell Ucn3 expression. Treatment with the beta cell toxin streptozotocin similarly causes the downregulation of Ucn3, suggesting that the STZ-induced Nitric Oxide (NO) and Reactive Oxygen Species (ROS) cause oxidative stress (73) that inhibits Ucn3 expression (78). Regardless of the mechanism(s) responsible for the downregulation of Ucn3 in diabetes, the loss of UCN3 deprives delta cells of the principal signal they need to secrete somatostatin in response to hyperglycemia (78), even though delta cells numbers are relatively unaffected in diabetes (30, 52, 64, 71). Indeed, restoration of endogenous levels of Ucn3 in diabetic beta cells using a doxycycline-inducible mouse model secondary to the loss of Ucn3 in T2D aggravated diabetes (78), likely by increasing somatostatin-mediated suppression of insulin. Loss of Ucn3 during diabetes is therefore partially adaptive response that maximizes insulin output in the face of increasing peripheral insulin resistance in T2D (78). However, this comes at the expense of local feedback inhibition of beta cells. Under circumstances where normal Ucn3 and somatostatin-mediated feedback control of beta cells breaks down, GSIS truly becomes dependent on glucose alone. The absence of negative feedback initially allows for excess insulin secretion (Figure 5.4B), with extended insulin action causing plasma glucose to overshoot its set point, activating counterregulation and contributing to glycemic volatility. Indeed, by CGM of *ob/ob* mice we observed markedly increased glycemic volatility in addition to severe hyperglycemia (78). More recently, it was shown that the onset of T1D in NOD mice and T2D in ZDF rats is characterized by a marked increase

in the amplitude of glucose excursions (36, 85). This observation is consistent with the progressive loss of UCN3 – and the feedback control it triggers – prior to the autoimmune-mediated demise of beta cells that causes full-blown hyperglycemia (63).

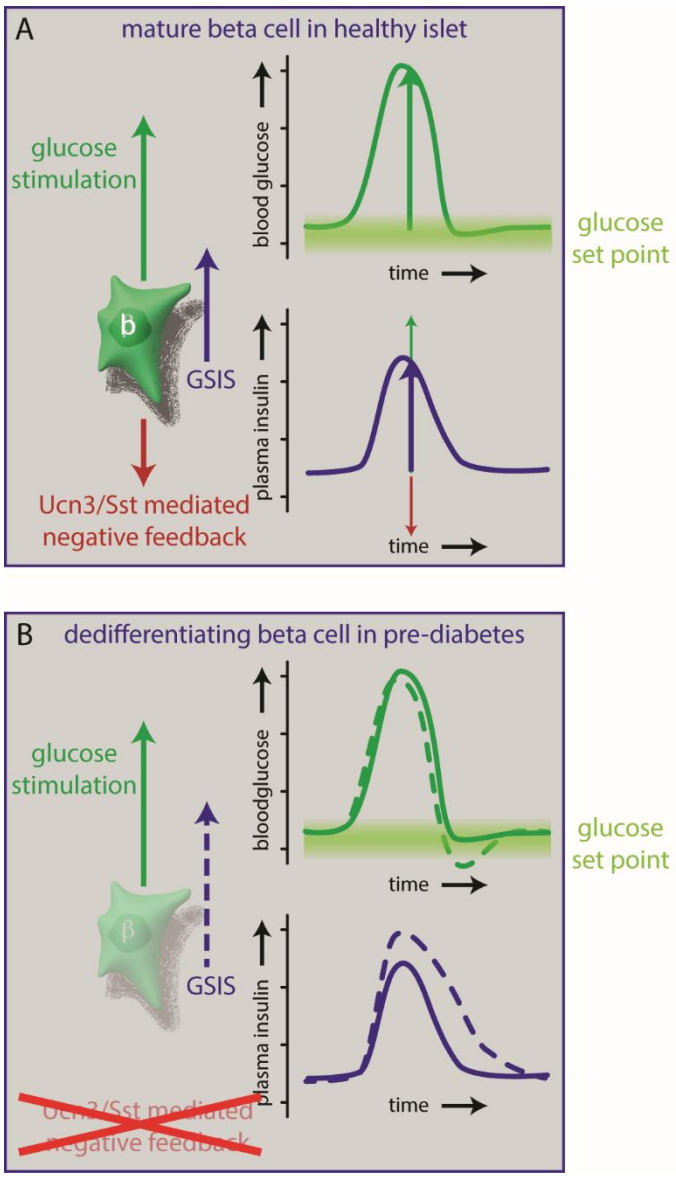

Figure 5.4: (A) Model how tonic feedback inhibition on beta and alpha cells ensures the timely attenuation of insulin (or glucagon) secretion as glucose is restored to its homeostatic equilibrium. (B) When this local feedback breaks down, insulin secretion is des-inhibited. This prolongs insulin action, which causes glucose values to overshoot their glucose set point and contributes to hyperglycemia in diabetes.

5.15 Summary and Conclusions

Pancreatic delta cells are emerging as important contributors that are well-positioned to modulate insulin and glucagon secretion directly at their source. The intra-islet feedback inhibition that delta

cells provide to beta and alpha cells is essential for precise control and coordination of insulin and glucagon secretion. These interactions are necessary for stable glycemic control and determine the homeostatic set point for glucose. In addition to their paracrine activation by UCN3, delta cells receive selective inputs from multiple hormones, neurotransmitters, and nutrients and integrate these into appropriate feedback modulation of insulin and glucagon secretion. Finally, loss of normal delta cell-mediated feedback inhibition occurs early in diabetes and likely contributes significantly to glycemic volatility and other aspects of the pathophysiology of diabetes, including excess glucagon secretion during hyperglycemia. As we better appreciate the physiological contribution of delta cells to glucose homeostasis we would be remiss if we did not consider delta cells and somatostatin as therapeutic targets to realign insulin and glucagon release in diabetes. Although sustained restoration of Ucn3 in T2D aggravated hyperglycemia (78), this observation does not disqualify delta cell-dependent feedback as a target in T2D. It merely indicates that continuous activation of delta cell-dependent feedback in diabetes is no more advisable than the continuous administration of insulin in diabetes. Analogous to insulin, there is a need to align delta cell release of somatostatin with the time its actions are most protective, whether by preventing episodes of hyperinsulinemic hypoglycemia or by curbing excess glucagon secretion in T2D.

5.16 Acknowledgements

This work was supported by grants from the National Institutes of Health (NIDDK110276) and the Juvenile Diabetes Research Foundation (CDA-2-2013-54) to MOH. JLH and GMN were supported by a NIGMS-funded Pharmacology Training Program (T32GM099608). The authors report no conflicts of interest.

5.17 References

1. **Adriaenssens AE, Svendsen B, Lam BY, Yeo GS, Holst JJ, Reimann F, and Gribble FM.** Transcriptomic profiling of pancreatic alpha, beta and delta cell populations identifies delta cells as a principal target for ghrelin in mouse islets. *Diabetologia* 59: 2156-2165, 2016.

2. **Barden N, Alvarado-Urbina G, Cote JP, and Dupont A.** Cyclic AMP-dependent stimulation of somatostatin secretion by isolated rat islets of Langerhans. *Biochemical and biophysical research communications* 71: 840-844, 1976.

3. **Baskin DG.** A Historical Perspective on the Identification of Cell Types in Pancreatic Islets of Langerhans by Staining and Histochemical Techniques. *J Histochem Cytochem* 63: 543-558, 2015.

4. **Benner C, van der Meulen T, Caceres E, Tigyi K, Donaldson CJ, and Huising MO.** The transcriptional landscape of mouse beta cells compared to human beta cells reveals notable species differences in long non-coding RNA and protein-coding gene expression. *BMC Genomics* 15: 620, 2014.

5. **Benninger RK, Hutchens T, Head WS, McCaughey MJ, Zhang M, Le Marchand SJ, Satin LS, and Piston DW.** Intrinsic islet heterogeneity and gap junction coupling determine spatiotemporal Ca(2)(+) wave dynamics. *Biophysical journal* 107: 2723-2733, 2014.

6. **Blum B, Hrvatin SS, Schuetz C, Bonal C, Rezania A, and Melton DA.** Functional beta-cell maturation is marked by an increased glucose threshold and by expression of urocortin 3. *Nat Biotechnol* 30: 261-264, 2012.

7. **Blum B, Roose AN, Barrandon O, Maehr R, Arvanites AC, Davidow LS, Davis JC, Peterson QP, Rubin LL, and Melton DA.** Reversal of beta cell de-differentiation by a small molecule inhibitor of the TGFbeta pathway. *eLife* 3: e02809, 2014.

8. **Bonner-Weir S and Orci L.** New perspectives on the microvasculature of the islets of Langerhans in the rat. *Diabetes* 31: 883-889, 1982.

9. **Braun M.** The somatostatin receptor in human pancreatic beta-cells. *Vitam Horm* 95: 165-193, 2014.

10. **Braun M, Ramracheya R, Amisten S, Bengtsson M, Moritoh Y, Zhang Q, Johnson PR, and Rorsman P.** Somatostatin release, electrical activity, membrane currents and exocytosis in human pancreatic delta cells. *Diabetologia* 52: 1566-1578, 2009.

11. **Brazeau P, Vale W, Burgus R, Ling N, Butcher M, Rivier J, and Guillemin R.** Hypothalamic polypeptide that inhibits the secretion of immunoreactive pituitary growth hormone. *Science* 179: 77-79, 1973.

12. **Briant LJB, Reinbothe TM, Spiliotis I, Miranda C, Rodriguez B, and Rorsman P.** delta-cells and beta-cells are electrically coupled and regulate alpha-cell activity via somatostatin. *J Physiol* 596: 197-215, 2018.

13. **Brown M, Rivier J, and Vale W.** Biological activity of somatostatin and somatostatin analogs on inhibtion of arginine-induced insulin and glucagon release in the rat. *Endocrinology* 98: 336-343, 1976.

14. **Colturi TJ, Unger RH, and Feldman M.** Role of circulating somatostatin in regulation of gastric acid secretion, gastrin release, and islet cell function. Studies in healthy subjects and duodenal ulcer patients. *J Clin Invest* 74: 417-423, 1984.

15. **Cryer PE.** Hypoglycemia-Associated Autonomic Failure in Diabetes: Maladaptive, Adaptive, or Both? *Diabetes* 64: 2322-2323, 2015.

16. **Dean PM and Matthews EK.** Glucose-induced electrical activity in pancreatic islet cells. *J Physiol* 210: 255-264, 1970.

17. **Dezaki K, Damdindorj B, Sone H, Dyachok O, Tengholm A, Gylfe E, Kurashina T, Yoshida M, Kakei M, and Yada T.** Ghrelin attenuates cAMP-PKA signaling to evoke insulinostatic cascade in islet beta-cells. *Diabetes* 60: 2315-2324, 2011.

18. **Dezaki K, Hosoda H, Kakei M, Hashiguchi S, Watanabe M, Kangawa K, and Yada T.** Endogenous ghrelin in pancreatic islets restricts insulin release by attenuating Ca2+ signaling in beta-cells: implication in the glycemic control in rodents. *Diabetes* 53: 3142-3151, 2004.

19. **Diez JA, Arrojo EDR, Zheng X, Stelmashenko OV, Chua M, Rodriguez-Diaz R, Fukuda M, Kohler M, Leibiger I, Tun SBB, Ali Y, Augustine GJ, Barathi VA, and Berggren PO.** Pancreatic Islet Blood Flow Dynamics in Primates. *Cell reports* 20: 1490-1501, 2017.

20. **DiGruccio MR, Mawla AM, Donaldson CJ, Noguchi GM, Vaughan J, Cowing-Zitron C, van der Meulen T, and Huising MO.** Comprehensive alpha, beta and delta cell transcriptomes reveal that ghrelin selectively activates delta cells and promotes somatostatin release from pancreatic islets. *Mol Metab* 5: 449-458, 2016.

21. **Dubois MP.** Immunoreactive somatostatin is present in discrete cells of the endocrine pancreas. *Proc Natl Acad Sci U S A* 72: 1340-1343, 1975.

22. **Franklin I, Gromada J, Gjinovci A, Theander S, and Wollheim CB.** Beta-cell secretory products activate alpha-cell ATP-dependent potassium channels to inhibit glucagon release. *Diabetes* 54: 1808-1815, 2005.

23. **Gopel SO, Kanno T, Barg S, and Rorsman P.** Patch-clamp characterisation of somatostatin-secreting -cells in intact mouse pancreatic islets. *The Journal of physiology* 528: 497-507, 2000.

24. **Gromada J, Franklin I, and Wollheim CB.** Alpha-cells of the endocrine pancreas: 35 years of research but the enigma remains. *Endocrine reviews* 28: 84-116, 2007.

25. **Gutniak M, Grill V, Wiechel KL, and Efendic S.** Basal and meal-induced somatostatin-like immunoreactivity in healthy subjects and in IDDM and totally pancreatectomized patients. Effects of acute blood glucose normalization. *Diabetes* 36: 802-807, 1987.

26. **Hauge-Evans AC, King AJ, Carmignac D, Richardson CC, Robinson IC, Low MJ, Christie MR, Persaud SJ, and Jones PM.** Somatostatin secreted by islet delta-cells fulfills multiple roles as a paracrine regulator of islet function. *Diabetes* 58: 403-411, 2009.

27. **Head WS, Orseth ML, Nunemaker CS, Satin LS, Piston DW, and Benninger RK.** Connexin-36 gap junctions regulate in vivo first- and second-phase insulin secretion dynamics and glucose tolerance in the conscious mouse. *Diabetes* 61: 1700-1707, 2012.

28. **Hellman B, Salehi A, Grapengiesser E, and Gylfe E.** Isolated mouse islets respond to glucose with an initial peak of glucagon release followed by pulses of insulin and somatostatin in antisynchrony with glucagon. *Biochem Biophys Res Commun* 417: 1219-1223, 2012.

29. **Hellman B, Salehi A, Gylfe E, Dansk H, and Grapengiesser E.** Glucose generates coincident insulin and somatostatin pulses and antisynchronous glucagon pulses from human pancreatic islets. *Endocrinology* 150: 5334-5340, 2009.

30. **Henquin JC, Ibrahim MM, and Rahier J.** Insulin, glucagon and somatostatin stores in the pancreas of subjects with type-2 diabetes and their lean and obese non-diabetic controls. *Sci Rep* 7: 11015, 2017.

31. **Hoang DT, Hara M, and Jo J.** Design Principles of Pancreatic Islets: Glucose-Dependent Coordination of Hormone Pulses. *PLoS One* 11: e0152446, 2016.

32. **Hokfelt T, Efendic S, Hellerstrom C, Johansson O, Luft R, and Arimura A.** Cellular localization of somatostatin in endocrine-like cells and neurons of the rat with special references to the A1-cells of the pancreatic islets and to the hypothalamus. *Acta Endocrinol Suppl (Copenh)* 200: 5-41, 1975.

33. **Huising MO, Pilbrow AP, Matsumoto M, van der Meulen T, Park H, Vaughan JM, Lee S, and Vale WW.** Glucocorticoids differentially regulate the expression of CRFR1 and CRFR2alpha in MIN6 insulinoma cells and rodent islets. *Endocrinology* 152: 138-150, 2011.

34. **Ipp E, Dobbs RE, Arimura A, Vale W, Harris V, and Unger RH.** Release of immunoreactive somatostatin from the pancreas in response to glucose, amino acids, pancreozymin-cholecystokinin, and tolbutamide. *J Clin Invest* 60: 760-765, 1977.

35. **Itoh Y, Kawamata Y, Harada M, Kobayashi M, Fujii R, Fukusumi S, Ogi K, Hosoya M, Tanaka Y, Uejima H, Tanaka H, Maruyama M, Satoh R, Okubo S, Kizawa H, Komatsu H, Matsumura F, Noguchi Y, Shinohara T, Hinuma S, Fujisawa Y, and Fujino M.** Free fatty acids regulate insulin secretion from pancreatic beta cells through GPR40. *Nature* 422: 173-176, 2003.

36. **Korstanje R, Ryan JL, Savage HS, Lyons BL, Kane KG, and Sukoff Rizzo SJ.** Continuous Glucose Monitoring in Female NOD Mice Reveals Daily Rhythms and a Negative Correlation With Body Temperature. *Endocrinology* 158: 2707-2712, 2017.

37. **Kristinsson H, Bergsten P, and Sargsyan E.** Free fatty acid receptor 1 (FFAR1/GPR40) signaling affects insulin secretion by enhancing mitochondrial respiration during palmitate exposure. *Biochim Biophys Acta* 1853: 3248-3257, 2015.

38. **Kumar U, Sasi R, Suresh S, Patel A, Thangaraju M, Metrakos P, Patel SC, and Patel YC.** Subtype-selective expression of the five somatostatin receptors (hSSTR1-5) in human pancreatic islet cells: a quantitative double-label immunohistochemical analysis. *Diabetes* 48: 77-85, 1999.

39. **Lawlor N, George J, Bolisetty M, Kursawe R, Sun L, Sivakamasundari V, Kycia I, Robson P, and Stitzel ML.** Single-cell transcriptomes identify human islet cell signatures and reveal cell-type-specific expression changes in type 2 diabetes. *Genome Res* 27: 208-222, 2017.

40. **Li C, Chen P, Vaughan J, Lee KF, and Vale W.** Urocortin 3 regulates glucose-stimulated insulin secretion and energy homeostasis. *Proc Natl Acad Sci USA* 104: 4206-4211, 2007.

41. **Liu YJ, Vieira E, and Gylfe E.** A store-operated mechanism determines the activity of the electrically excitable glucagon-secreting pancreatic alpha-cell. *Cell calcium* 35: 357-365, 2004.

42. **Loud FB, Holst JJ, Egense E, Petersen B, and Christiansen J.** Is somatostatin a humoral regulator of the endocrine pancreas and gastric acid secretion in man? *Gut* 26: 445-449, 1985.

43. **MacDonald PE, De Marinis YZ, Ramracheya R, Salehi A, Ma X, Johnson PR, Cox R, Eliasson L, and Rorsman P.** A K ATP channel-dependent pathway within alpha cells regulates glucagon release from both rodent and human islets of Langerhans. *PLoS Biol* 5: e143, 2007.

44. **Menke A, Casagrande S, Geiss L, and Cowie CC.** Prevalence of and Trends in Diabetes Among Adults in the United States, 1988-2012. *JAMA : the journal of the American Medical Association* 314: 1021-1029, 2015.

45. **Merrins MJ, Poudel C, McKenna JP, Ha J, Sherman A, Bertram R, and Satin LS.** Phase Analysis of Metabolic Oscillations and Membrane Potential in Pancreatic Islet beta-Cells. *Biophysical journal* 110: 691-699, 2016.

46. **Murakami T, Fujita T, Miyake T, Ohtsuka A, Taguchi T, and Kikuta A.** The insulo-acinar portal and insulo-venous drainage systems in the pancreas of the mouse, dog, monkey and certain other animals: a scanning electron microscopic study of corrosion casts. *Arch Histol Cytol* 56: 127-147, 1993.

47. **Nadal A, Quesada I, and Soria B.** Homologous and heterologous asynchronicity between identified alpha-, beta- and delta-cells within intact islets of Langerhans in the mouse. *J Physiol* 517 (Pt 1): 85-93, 1999.

48. **Nyman LR, Ford E, Powers AC, and Piston DW.** Glucose-dependent blood flow dynamics in murine pancreatic islets in vivo. *Am J Physiol Endocrinol Metab* 298: E807-814, 2010.

49. **Ohtani O, Ushiki T, Kanazawa H, and Fujita T.** Microcirculation of the pancreas in the rat and rabbit with special reference to the insulo-acinar portal system and emissary vein of the islet. *Arch Histol Jpn* 49: 45-60, 1986.

50. **Patel YC.** Somatostatin and its receptor family. *Frontiers in neuroendocrinology* 20: 157-198, 1999.

51. **Portela-Gomes GM, Stridsberg M, Grimelius L, Rorstad O, and Janson ET.** Differential expression of the five somatostatin receptor subtypes in human benign and malignant insulinomas - predominance of receptor subtype 4. *Endocr Pathol* 18: 79-85, 2007.

52. **Rahier J, Goebbels RM, and Henquin JC.** Cellular composition of the human diabetic pancreas. *Diabetologia* 24: 366-371, 1983.

53. **Ravier MA and Rutter GA.** Glucose or insulin, but not zinc ions, inhibit glucagon secretion from mouse pancreatic alpha-cells. *Diabetes* 54: 1789-1797, 2005.

54. **Reimer MK, Pacini G, and Ahren B.** Dose-dependent inhibition by ghrelin of insulin secretion in the mouse. *Endocrinology* 144: 916-921, 2003.

55. **Reubi JC, Schaer JC, Wenger S, Hoeger C, Erchegyi J, Waser B, and Rivier J.** SST3-selective potent peptidic somatostatin receptor antagonists. *Proc Natl Acad Sci USA* 97: 13973-13978, 2000.

56. **Rivier J, Gulyas J, Kirby D, Low W, Perrin MH, Kunitake K, DiGruccio M, Vaughan J, Reubi JC, Waser B, Koerber SC, Martinez V, Wang L, Tache Y, and Vale W.** Potent and long-acting corticotropin releasing factor (CRF) receptor 2 selective peptide competitive antagonists. *Journal of medicinal chemistry* 45: 4737-4747, 2002.

57. **Rodriguez-Diaz R and Caicedo A.** Novel approaches to studying the role of innervation in the biology of pancreatic islets. *Endocrinology and metabolism clinics of North America* 42: 39-56, 2013.

58. **Rodriguez-Diaz R, Dando R, Jacques-Silva MC, Fachado A, Molina J, Abdulreda MH, Ricordi C, Roper SD, Berggren PO, and Caicedo A.** Alpha cells secrete acetylcholine as a non-neuronal paracrine signal priming beta cell function in humans. *Nature medicine* 17: 888-892, 2011.

59. **Rodriguez-Diaz R, Molano RD, Weitz JR, Abdulreda MH, Berman DM, Leibiger B, Leibiger IB, Kenyon NS, Ricordi C, Pileggi A, Caicedo A, and Berggren PO.** Paracrine

Interactions within the Pancreatic Islet Determine the Glycemic Set Point. *Cell Metab* 27: 549-558 e544, 2018.

60. **Rorsman P, Berggren PO, Bokvist K, Ericson H, Mohler H, Ostenson CG, and Smith PA.** Glucose-inhibition of glucagon secretion involves activation of GABAA-receptor chloride channels. *Nature* 341: 233-236, 1989.

61. **Rorsman P and Braun M.** Regulation of insulin secretion in human pancreatic islets. *Annu Rev Physiol* 75: 155-179, 2013.

62. **Rorsman P and Huising MO.** The somatostatin-secreting pancreatic delta-cell in health and disease. *Nat Rev Endocrinol* 14: 404-414, 2018.

63. **Rui J, Deng S, Arazi A, Perdigoto AL, Liu Z, and Herold KC.** beta Cells that Resist Immunological Attack Develop during Progression of Autoimmune Diabetes in NOD Mice. *Cell Metab* 25: 727-738, 2017.

64. **Saito K, Yaginuma N, and Takahashi T.** Differential volumetry of A, B and D cells in the pancreatic islets of diabetic and nondiabetic subjects. *Tohoku J Exp Med* 129: 273-283, 1979.

65. **Salehi A, Qader SS, Grapengiesser E, and Hellman B.** Pulses of somatostatin release are slightly delayed compared with insulin and antisynchronous to glucagon. *Regulatory peptides* 144: 43-49, 2007.

66. **Samols E, Marri G, and Marks V.** Interrelationship of glucagon, insulin and glucose. The insulinogenic effect of glucagon. *Diabetes* 15: 855-866, 1966.

67. **Samols E, Marri G, and Marks V.** Promotion of Insulin Secretion by Glucagon. *Lancet* 2: 415-416, 1965.

68. **Samols E and Stagner JI.** Islet somatostatin--microvascular, paracrine, and pulsatile regulation. *Metabolism* 39: 55-60, 1990.

69. **Schauder P, McIntosh C, Arends J, Arnold R, Frerichs H, and Creutzfeldt W.** Somatostatin and insulin release from isolated rat pancreatic islets stimulated by glucose. *FEBS letters* 68: 225-227, 1976.

70. **Sosa-Pineda B, Chowdhury K, Torres M, Oliver G, and Gruss P.** The Pax4 gene is essential for differentiation of insulin-producing beta cells in the mammalian pancreas. *Nature* 386: 399-402, 1997.

71. **Stefan Y, Orci L, Malaisse-Lagae F, Perrelet A, Patel Y, and Unger RH.** Quantitation of endocrine cell content in the pancreas of nondiabetic and diabetic humans. *Diabetes* 31: 694-700, 1982.

72. **Stone VM, Dhayal S, Brocklehurst KJ, Lenaghan C, Sorhede Winzell M, Hammar M, Xu X, Smith DM, and Morgan NG.** GPR120 (FFAR4) is preferentially expressed in pancreatic delta cells and regulates somatostatin secretion from murine islets of Langerhans. *Diabetologia* 57: 1182-1191, 2014.

73. **Szkudelski T.** The mechanism of alloxan and streptozotocin action in B cells of the rat pancreas. *Physiol Res* 50: 537-546, 2001.

74. **Taborsky GJ, Jr. and Ensinck JW.** Contribution of the pancreas to circulating somatostatin-like immunoreactivity in the normal dog. *J Clin Invest* 73: 216-223, 1984.

75. **Taborsky GJ, Jr. and Mundinger TO.** Minireview: The role of the autonomic nervous system in mediating the glucagon response to hypoglycemia. *Endocrinology* 153: 1055-1062, 2012.

76. **Tong J, Prigeon RL, Davis HW, Bidlingmaier M, Kahn SE, Cummings DE, Tschop MH, and D'Alessio D.** Ghrelin suppresses glucose-stimulated insulin secretion and deteriorates glucose tolerance in healthy humans. *Diabetes* 59: 2145-2151, 2010.

77. **Unger RH and Cherrington AD.** Glucagonocentric restructuring of diabetes: a pathophysiologic and therapeutic makeover. *J Clin Invest* 122: 4-12, 2012.

78. **van der Meulen T, Donaldson CJ, Caceres E, Hunter AE, Cowing-Zitron C, Pound LD, Adams MW, Zembrzycki A, Grove KL, and Huising MO.** Urocortin3 mediates somatostatin-dependent negative feedback control of insulin secretion. *Nat Med* 21: 769-776, 2015.

79. **van der Meulen T, Xie R, Kelly OG, Vale WW, Sander M, and Huising MO.** Urocortin 3 marks mature human primary and embryonic stem cell-derived pancreatic alpha and beta cells. *PLoS One* 7: e52181, 2012.

80. **Vieira E, Salehi A, and Gylfe E.** Glucose inhibits glucagon secretion by a direct effect on mouse pancreatic alpha cells. *Diabetologia* 50: 370-379, 2007.

81. **Vierra NC, Dickerson MT, Jordan KL, Dadi PK, Kadare KA, Altman MK, Milian SC, and Jacobson DA.** TALK-1 reduces delta-cell endoplasmic reticulum and cytoplasmic calcium levels limiting somatostatin secretion. *Mol Metab* 9: 84-97, 2018.

82. **Walker JN, Ramracheya R, Zhang Q, Johnson PR, Braun M, and Rorsman P.** Regulation of glucagon secretion by glucose: paracrine, intrinsic or both? *Diabetes Obes Metab* 13 Suppl 1: 95-105, 2011.

83. **Wendt A, Birnir B, Buschard K, Gromada J, Salehi A, Sewing S, Rorsman P, and Braun M.** Glucose inhibition of glucagon secretion from rat alpha-cells is mediated by GABA released from neighboring beta-cells. *Diabetes* 53: 1038-1045, 2004.

84. **Yada T, Damdindorj B, Rita RS, Kurashina T, Ando A, Taguchi M, Koizumi M, Sone H, Nakata M, Kakei M, and Dezaki K.** Ghrelin signalling in beta-cells regulates insulin secretion and blood glucose. *Diabetes Obes Metab* 16 Suppl 1: 111-117, 2014.

85. **Zhang XD, Pechter D, Yang L, Ping X, Yao Z, Zhang R, Shen X, Li NX, Connick J, Nawrocki AR, Chakravarthy M, and Li C.** Decreased complexity of glucose dynamics preceding the onset of diabetes in mice and rats. *PLoS One* 12: e0182810, 2017.

Chapter 6

Transcriptomic comparison of beta and alpha cells in lean and *ob/ob* mice

6.1 Preface

This chapter is being prepared for submission as part of a manuscript to be submitted.

6.1.1 Authorship

Jessica L. Huang*, Alex M. Mawla*, Richard Van, Ariana T. Momen, Justin Huynh, Talitha van der Meulen, Mark O. Huising

*co-first authors

I performed the sample collection and did the library prep. Dr. Alex Mawla did the sequence alignment. Richard Van assisted with mouse measurements. The article has been modified to satisfy the formatting requirements of this dissertation.

6.2 Abstract

Obesity has a high association with insulin resistance and is also a risk factor for Type 2 Diabetes. Despite the strong correlation, not all obese individuals with insulin resistance develop Type 2 Diabetes. This occurs due to beta cell compensation, in which beta cells increase in mass to ramp up

insulin secretion and meet rising insulin demand. In the *ob/ob* mouse model, loss of leptin signaling leads to increased feeding and subsequent obesity. On the C57BL/6 background, these mice become hyperglycemic early in life, but return to normoglycemia shortly after, making them a useful model for studying compensation. Here we provide a phenotypic and transcriptomic comparison of both beta and alpha cells taken from lean and *ob/ob* mice. We demonstrate the possibility that the male *ob/ob* mice have undergone decompensation, as demonstrated by increased glycemia, decreased granularity in their beta cells, and decreased expression of beta cell maturity markers. Conversely, female *ob/ob* mice remain normoglycemic and show no changes in expression of beta cell maturity markers. We also observe that while alpha cells retain their expression of key alpha cell markers, they also appear to have an upregulation in beta cell markers.

6.3 Introduction

Obesity is a growing problem in the U.S. that is strongly associated with insulin resistance and is also a large risk factor for developing Type 2 Diabetes (Kahn *et al.* 2006). However, many obese individuals do not develop diabetes for decades due to compensation, a period of insulin resistance that is balanced by increases in beta cell mass and insulin secretion (Weir & Bonner-Weir 2004). The leptin-deficient *ob/ob* mouse model is commonly used to study obesity. On the C57BL/6 background, *ob/ob* mice are transiently hyperglycemic but quickly return to normoglycemia due to beta cell hyperplasia and hyperinsulinemia (Coleman 1978). For this reason, they are useful for studying beta cell compensation.

The insulin-producing beta cells are located within the islets of Langerhans, which are clusters of hormone-secreting cells that are scattered throughout the pancreas. Neighboring the beta cells are glucagon-producing alpha cells and somatostatin-producing delta cells. The bulk of islet research has focused on beta cells due to their essential role in secreting insulin to lower blood glucose levels. In

response to rising glucose levels, beta cells undergo hyperplasia and hypertrophy to create more beta cell mass and compensate for insulin demand (Weir & Bonner-Weir 2004; Cerf 2013). While beta cells can remain in this state for a long time, in some cases the beta cells can undergo exhaustion and decompensation (Weir *et al.* 2001; Salvi & Abderrahmani 2014). Initially, it was believed that loss of functional beta cell mass in Type 2 Diabetes is primarily due to apoptosis (Butler *et al.* 2003). However, evidence points to beta cells remaining intact in diabetes, and that instead of undergoing apoptosis they undergo dedifferentiation (Talchai *et al.* 2012). Dedifferentiation has been demonstrated to involve loss of beta cell maturity markers such as *Ucn3* (Blum *et al.* 2012; van der Meulen *et al.* 2012, 2015), *Mafa* (Artner *et al.* 2010), or *Slc2a2* (Beamish *et al.* 2016; van der Meulen *et al.* 2017) and an increase in dedifferentiation markers such as *Aldh1a3* (Cinti *et al.* 2016; Kim-Muller *et al.* 2016) and *Gc* (Kuo *et al.* 2019). There are also reports of increased expression of progenitor markers such as *Neurog3* (Talchai *et al.* 2012; Diedisheim *et al.* 2018) or markers of other cell types such as *Gast* (Dahan *et al.* 2017). However, the extent to which each of these occur in different states of insulin resistance and diabetes and the order in which they occur remains unclear.

While much of the attention has been on the effect of obesity and diabetes on beta cells, it is also known that alpha cells also become dysfunctional in diabetes. It has been demonstrated that alpha cells have inappropriate secretion under hyperglycemic conditions, contributing to hyperglycemia (Shah *et al.* 2000). On the other hand, alpha cells also have important paracrine effects on beta cells during hyperglycemia (Svendsen *et al.* 2018; Zhu *et al.* 2019; Liu *et al.* 2021), and these paracrine interactions may be disrupted in Type 2 Diabetes. Thus, investigating transcriptomic changes in alpha cells under conditions of compensation and diabetes is also important.

Here we provide transcriptomes of beta cells and alpha cells that were simultaneously FACS-purified from 8-month-old male and female *ob/ob* mice. We observe that both sexes initially recover from hyperglycemia, but male mice are more prone to becoming hyperglycemic again over time while

female mice remain normoglycemic. Furthermore, our transcriptomic data suggest that this difference in phenotype may be attributed to beta cell decompensation in males. We also observe an increase in beta cell markers in alpha cells in *ob/ob* mice of both sexes. These data may be a useful resource for the study of beta cells and alpha cells in compensation and decompensation.

6.4 Results

6.4.1 Phenotypic comparison between lean and *ob/ob* mice

Both male and female *ob/ob* mice exhibited higher glucose levels relative to lean littermates around 5 weeks of age and began returning to normoglycemia by 15 weeks (Figure 6.1A and 6.1B). Around 33 weeks of age, male *ob/ob* mice once again began displaying hyperglycemia while female mice remained normoglycemic throughout the period of observation. To investigate the potential mechanisms behind the difference in glycemic phenotype, we collected the mice soon after the development of hyperglycemia in the male mice. The expression of the beta cell reporter line *mIns1-H2B-mCherry* (Benner *et al.* 2014) as well as YFP under the control of *Gcg-cre* (Herrera 2000) enabled FACS-purification of beta and alpha cells from each mouse based on mCherry and YFP fluorescence respectively (Figure 6.4). A small population of mCherry+YFP+ cells were observed that may represent alpha cells that transdifferentiated into beta cells; however, we will not be focusing on this population.

Since beta cells undergo hypertrophy in *ob/ob* mice, we examined the forward scatter (FSC) property of the cells, which provides information on the size of the cell. We expected that the FSC would be higher in *ob/ob* mice than in their lean counterparts. However, only beta cells from female *ob/ob* mice had a higher FSC than their lean counterparts, while there was no significant difference in the FSC between male lean and *ob/ob* mice (Figure 6.1C). The effect of sex was significant ($p = 0.002$). In contrast, alpha cells did not exhibit any differences in cell size. Additionally, we examined the side

scatter (SSC), which is a measure of granularity in the cell, with a higher SSC corresponding to higher granularity. As beta cells are known to have larger granules than alpha cells under normal circumstances (Lacy 1961; Dorrell *et al.* 2011; Pfeifer *et al.* 2015), it was not surprising to see that beta cells had a significantly higher SSC profile relative to alpha cells ($p < 0.0001$) (Figure 6.1D). However, while female lean and *ob/ob* mice did not have a significantly different SSC, beta cells from male *ob/ob* mice had a significantly lower SSC than beta cells from the lean controls (sex difference $p < 0.0001$). This suggests that beta cells in male *ob/ob* mice have significantly fewer insulin granules. Interestingly, alpha cells in *ob/ob* mice appeared to exhibit increased granularity regardless of sex, although this did not reach significance. Thus, beta cells become larger in female *ob/ob* mice but less granular in male *ob/ob* mice, while alpha cells do not change in size but potentially become more granular in *ob/ob* mice.

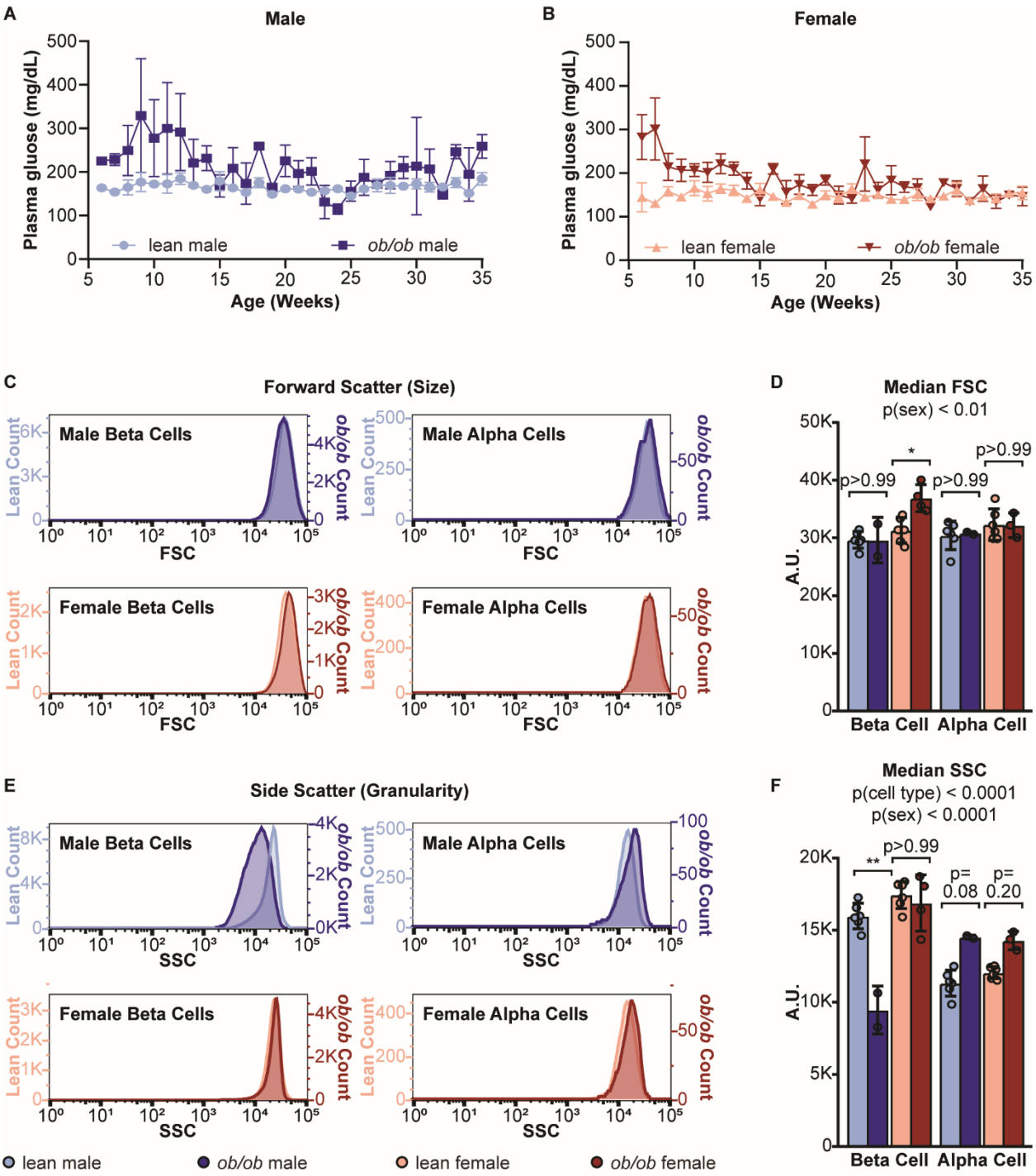

Figure 6.1: Phenotypic comparison of lean and *ob/ob* mice. A and B) Weekly non-fasting glucose measurements of (A) male and (B) female lean and *ob/ob* mice. C) Representative histograms of measured FSC representing cell size, with lean overlaid with respective *ob/ob* counterpart. D) Average FSC median of mCherry+ and YFP+ cells in male and female lean and *ob/ob* mice. E) Representative histograms of measured SSC representing cell granularity, with lean overlaid with respective *ob/ob* counterpart. D) Average SSC median of mCherry+ and YFP+ cells in male and female lean and *ob/ob* mice. Error bars represent SEM. *p < 0.05, **p < 0.01.

6.4.2 Transcriptomic comparison between beta cells from lean and *ob/ob* mice

We first validated our transcriptome data by comparing beta and alpha cells within each sex. As expected, beta cell markers were enriched in the beta cell transcriptome while alpha cell markers were enriched in the alpha cell transcriptome (Supplementary Figure 6.5A and 6.5B). We also quantified the number of mCherry and YFP reads in each sample as an alternative way to assess the purity of the isolation. There were little to no mCherry reads in the alpha cell samples relative to the beta cell ones, although there were a few more reads in the male *ob/ob* YFP+ samples compared to the other YFP samples (Supplementary Figure 6.5C). Likewise, there were few YFP reads in the beta cell samples relative to the alpha cell ones (Supplementary Figure 6.5B).

Next, we compared beta cell transcriptomes from lean and *ob/ob* mice, separated by sex. Differential gene expression analysis revealed that 792 genes that were significantly enriched in beta cells from male lean mice and 1491 genes were significantly enriched in male *ob/ob* mice (FDR < 0.05, log fold change > 0.5) (Figure 6.2A). Fewer genes were differentially expressed in beta cells from female mice, with 349 genes enriched in lean samples and 547 enriched in *ob/ob* samples (FDR < 0.05, log fold change > 0.5) (Figure 6.2B). Upon examining the differentially expressed genes, we found that that several markers of beta cell maturity were significantly downregulated in the beta cells from male *ob/ob* mice, including *Slc2a2*, *Mafa*, and *Ero1lb* (Artner *et al.* 2010; Beamish *et al.* 2016; van der Meulen *et al.* 2017). We also found upregulation of beta cell dedifferentiation genes *Cck*, *Aldh1a3*, and *Gc* (Lavine *et al.* 2010; Kim-Muller *et al.* 2016; Kuo *et al.* 2019). In contrast, there was no significant difference in gene expression of beta cell markers between beta cells from female lean and *ob/ob* mice, but increased expression of dedifferentiated markers was still observed. Both *Neurog3* and *Gast* were only significantly upregulated in beta cells from male *ob/ob* mice.

Analysis of GO terms revealed an enrichment in genes involved in hormone and insulin secretion in male lean mice, while there was an enrichment in genes involved in migration and

adhesion in male *ob/ob* mice (Figure 6.2C). In contrast, the top enriched GO terms in female lean mice involved adhesion and neuron guidance, and in female *ob/ob* mice involved ribosome assembly (Figure 6.2D). The loss of beta cell markers and genes involved in insulin secretion in male *ob/ob* mice but not female *ob/ob* mice suggest beta cell decompensation in the males.

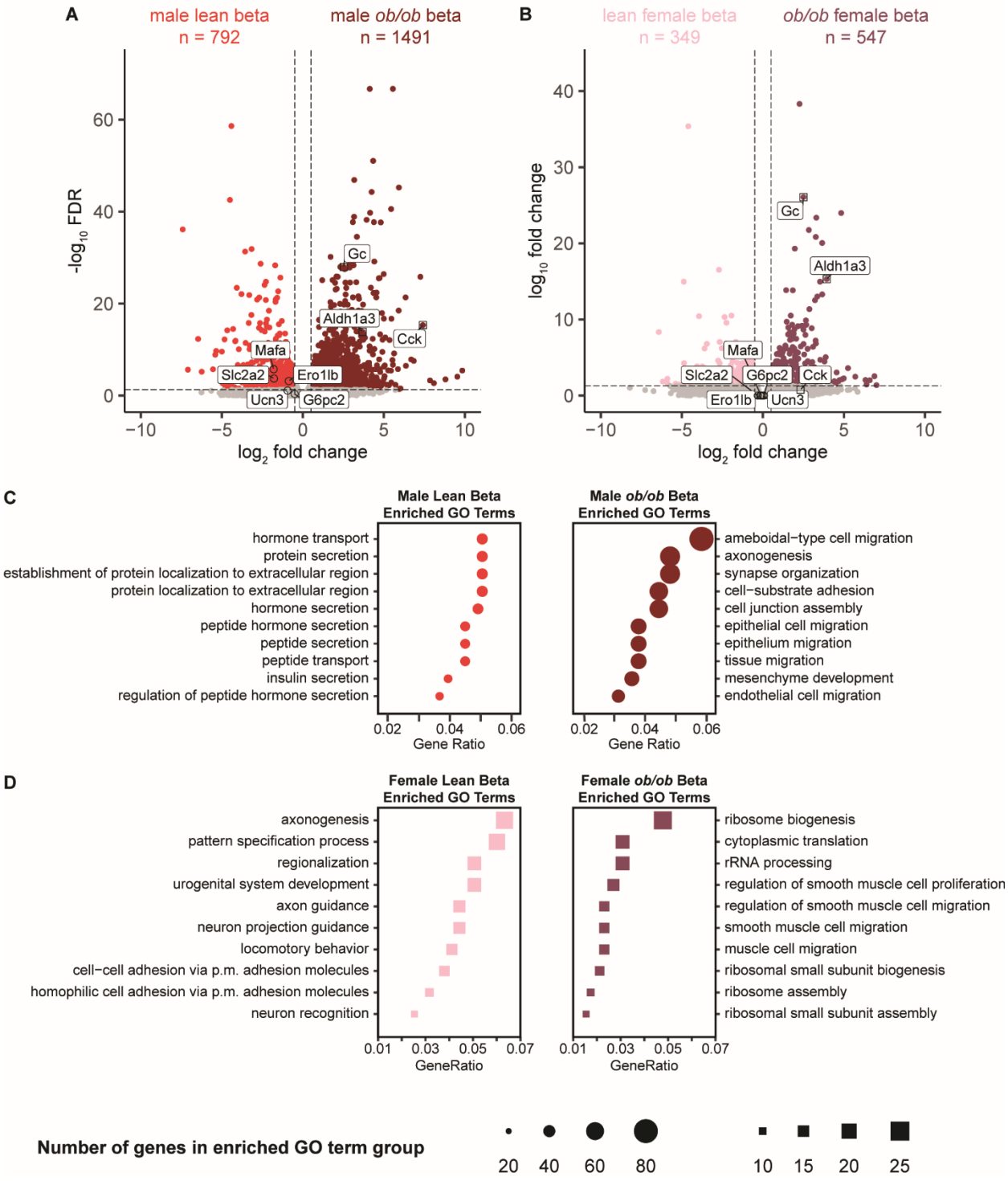

Figure 6.2: Transcriptomic comparison of lean and *ob/ob* beta cells.

Figure 6.2: (continued) A and B) Volcano plots showing number of significantly enriched genes based on FDR < 0.05 and absolute log fold change > 0.5. Comparisons are made between beta cells from A) male and B) female lean and *ob/ob* mice. Selected markers of beta cell maturity (open circles) and dedifferentiation (open squares) are highlighted. C and D) Top 10 enriched GO terms in beta cells from C) male and D) female lean and *ob/ob* mice. Terms are arranged by gene ratio (number of genes differentially regulated relative to total number of genes involved in the biological process). Sizes of the circles or squares denote the total number of genes in a process that were differentially regulated in the sample.

6.4.3 Transcriptomic comparison between alpha cells from lean and *ob/ob* mice

Comparison of alpha cell transcriptomes from lean and *ob/ob* mice revealed that there was more upregulation than downregulation of genes in *ob/ob* samples from both sexes (Figure 6.3A and 6.3B). In contrast to the loss of beta cell markers observed in male *ob/ob* mice, there was no significant difference in expression of alpha cell markers such as *Gcg*, *Arx*, *Mafb*, *Irx1*, or *Irx2* (Benner *et al.* 2014; DiGruccio *et al.* 2016). Surprisingly, there was a significant increase in expression of beta cell markers in alpha cells from both male and female *ob/ob* mice. Since there were few mCherry reads in both lean and *ob/ob* YFP+ samples, and there was little difference between the lean and *ob/ob* groups (Figure 6.5C), it is unlikely that the increase in beta cell genes can be solely attributed to beta cell contamination in the samples.

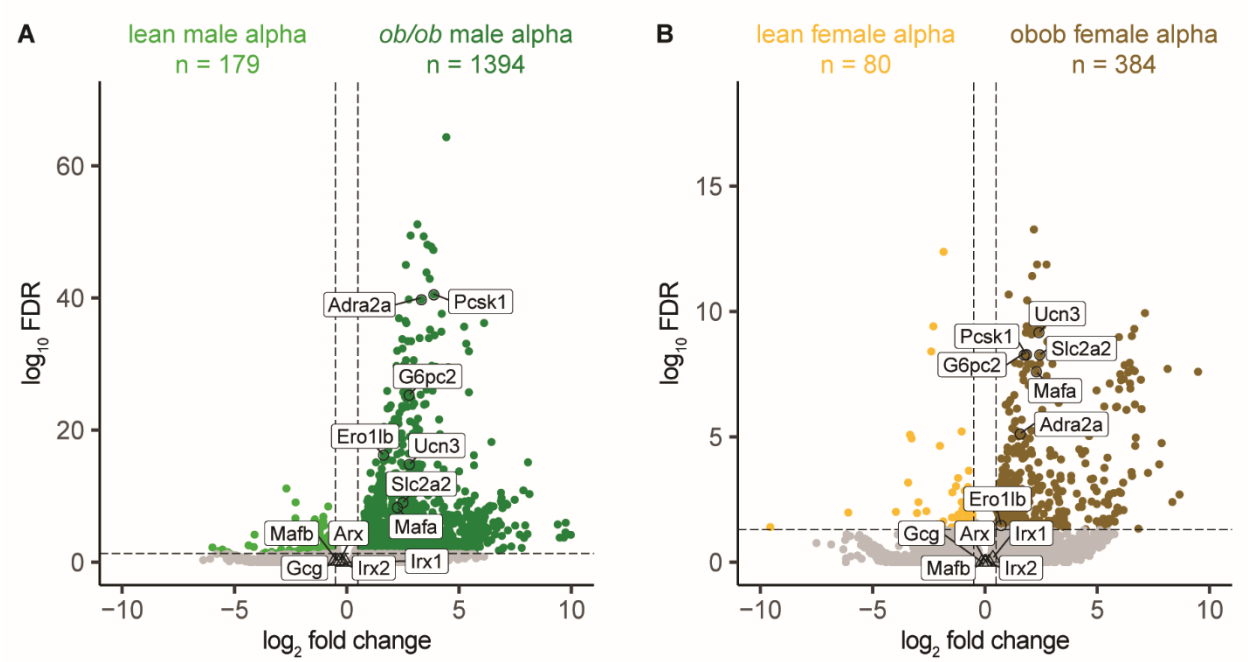

Figure 6.3: Transcriptomic comparison of lean and *ob/ob* alpha cells. A and B) Volcano plots showing number of significantly enriched genes based on FDR < 0.05 and absolute log fold change > 0.5. Comparisons are made between alpha cells from A) male and B) female lean and *ob/ob* mice. Selected markers of alpha cells (open triangles) and beta cells (open circles) are highlighted.

6.5 Discussion

Both beta and alpha cells are known to exhibit changes in function during Type 2 Diabetes. During the period of insulin resistance preceding the onset of diabetes, beta cells are able to compensate for increased insulin demand through hypertrophy and hyperplasia (Weir & Bonner-Weir 2004; Cerf 2013). However, less is known about the behavior of alpha cells during this time. Here we provide transcriptomic data of beta cells and alpha cells from both male and female lean and *ob/ob* mice. We demonstrate that the hyperglycemia and loss of granularity in beta cells observed in male *ob/ob* mice is associated with a loss of beta cell maturity markers and an enrichment in more beta cell dedifferentiation markers. Conversely, female mice retain normoglycemia, and this is associated with

beta cells that retain granularity and fewer changes in the expression of key beta cell genes. In alpha cells, we observe an increase in granularity as well as an increase in expression of beta cell markers.

Over the course of monitoring the mice, we observed that the male *ob/ob* mice began to become hyperglycemic again, while female mice remained normoglycemic. This provided an opportunity for us to study the differences between *ob/ob* mice that presumably have beta cells undergoing decompensation and *ob/ob* mice whose beta cells retain their compensatory ability. FSC and SSC analysis revealed that male *ob/ob* mice have significantly lower granularity, suggesting decompensation, while female *ob/ob* mice exhibit hypertrophy, suggesting continued compensation. Furthermore, transcriptomic analysis revealed that only beta cells from male *ob/ob* mice exhibited a significant downregulation of beta cell maturity markers. GO term analysis confirmed that there was a depletion in genes related to hormone and insulin secretion. The beta cells from female *ob/ob* mice did not demonstrate a significant difference in expression of beta cell markers, but like the male *ob/ob* mice exhibited an increase in several beta cell dedifferentiation markers, including *Aldh1a3* (Kim-Muller *et al.* 2016), *Gc* (Kuo *et al.* 2019), and *Cck* (Lavine *et al.* 2010). This suggests that the upregulation of these dedifferentiation markers precedes loss of maturity markers and full beta cell dysfunction. However, *Neurog3* (Diedisheim *et al.* 2018) and *Gast* (Dahan *et al.* 2017) were only upregulated in male *ob/ob* mice. Therefore, it is possible that these may be considered as late dedifferentiation markers relative to the other dedifferentiation markers. Based on these observations, it is also possible that beta cells in female mice are more protected from decompensation. This may be due to the known protective effects of estrogen (Louet *et al.* 2004).

A recent paper has shown that alpha cell transcriptomes are not as affected as beta cells when subjected to high fat diet-induced obesity and hyperglycemia (Dusaulcy *et al.* 2019). Our data agree that alpha cells do not lose their identity the way beta cells do during decompensation, as alpha cells in both male and female *ob/ob* mice retain expression of alpha cell markers. On the other hand, both

also demonstrate an increase in expression of beta cell markers. Whether this is due to potential beta cell contamination or if a subset of alpha cells truly becomes more beta cell-like will require further investigation. However, we have observed a subset of alpha cells from *ob/ob* mice respond to epinephrine with a decrease in calcium instead of an increase in calcium, in line with increased expression of *Adra2a*, the epinephrine receptor generally found on beta cells, instead of *Adrb1*, the epinephrine receptor generally found on alpha cells (data not published).

In summary, our data informs on differences between compensating and decompensating beta cells in obesity and that in contrast to beta cells, alpha cell dysfunction is not due to loss of alpha cell identity markers.

6.6 Funding and Acknowledgements

This work was supported by the National Institute of Diabetes and Digestive and Kidney Disease (NID DK-110276), the Juvenile Diabetes Research Foundation (CDA-2-2013-54 and 2-SRA-2019-700-S-B), and the American Diabetes Association (#1-19-IBS-078). JLH was supported by a National Institute of General Medical Sciences-funded Pharmacology Training Program (T32 GM-099608). We thank the University of California, Davis Flow Cytometry Core for assisting with the collection of FACS data.

6.7 Materials and Methods

6.7.1 Animals

Mice were maintained in group housing on a 12-hour light/12-hour dark cycle with free access to water and standard rodent chow. Both male and female mice were used for the RNA-seq experiment. Mice heterozygous for the *ob/ob* mutation (+/*ob*) were used to generate both the *ob/ob* mice and lean

(+/+ and +/*ob*) controls. The +/*ob* mice also expressed the transgenes *mIns1*-H2B-mCherry (Jax # 028589) (Benner *et al.* 2014), *Gcg-cre* (Herrera 2000), and *Rosa26*-lsl-YFP (Jax # 006148) (Srinivas *et al.* 2001) to enable the purification of beta and alpha cells. Weekly glucose measurements were obtained from tail vein blood with a glucometer (OneTouch Ultra2; Life Scan, Milpitas, CA). All mouse experiments were approved by the UC Davis Institutional Animals Care and Use Committee and were performed in compliance with the Animal Welfare Act and the Institute for Laboratory Animal Research (ILAR) Guide to the Care and Use of Laboratory Animals.

6.7.2 Islet Isolation and FACS Sorting

Islets were isolated and dissociated as previously described (van der Meulen *et al.* 2017). Islets were not pooled prior to dissociation. Dissociated islet cells were sorted at the UC Davis Flow Cytometry core on a Beckman Coulter MoFlo Astrios EQ using 405, 561, and 640 excitation lines for Dapi, YFP, and mCherry, respectively. Dapi was used to exclude dead cells. Sorted cells were collected directly into Trizol to ensure immediate cell lysis and preservation of RNA integrity.

6.7.3 Nucleic Acid Isolation and Library Prep

RNA was isolated from Trizol-preserved samples by chloroform extraction, assisted by phase lock tubes, and precipitated with isopropanol. Quality of RNA was assessed using the Agilent 2100 Bioanalyzer. Only samples with a RIN value of 8 or higher were used to prepare RNA-seq libraries, with the exception of one sample with a RIN value of 7.4. Indexed sequencing libraries were prepared using the TruSeq RNA sample Prep Kit v2 (Illumina Inc. San Diego, CA) and sequenced at 75 cycles, single read on an Illumina MiSeq platform.

6.7.4 Statistical analysis and bioinformatics

One replicate was removed due to insufficient separation of the YFP+ and mCherry+YFP+ populations during FACS. FACS data was analyzed with mixed-effects model to account for differences between sex, cell type, and genotype. Reads were aligned to mouse genome version mm8 using STAR (Dobin *et al.* 2013). FeatureCounts was used to create counts tables (Liao *et al.* 2014). Differential gene expression analysis was performed using edgeR (Robinson *et al.* 2009). GO term and KEGG pathway analysis were performed using clusterProfiler (Yu *et al.* 2012).

6.8 Supplemental Information

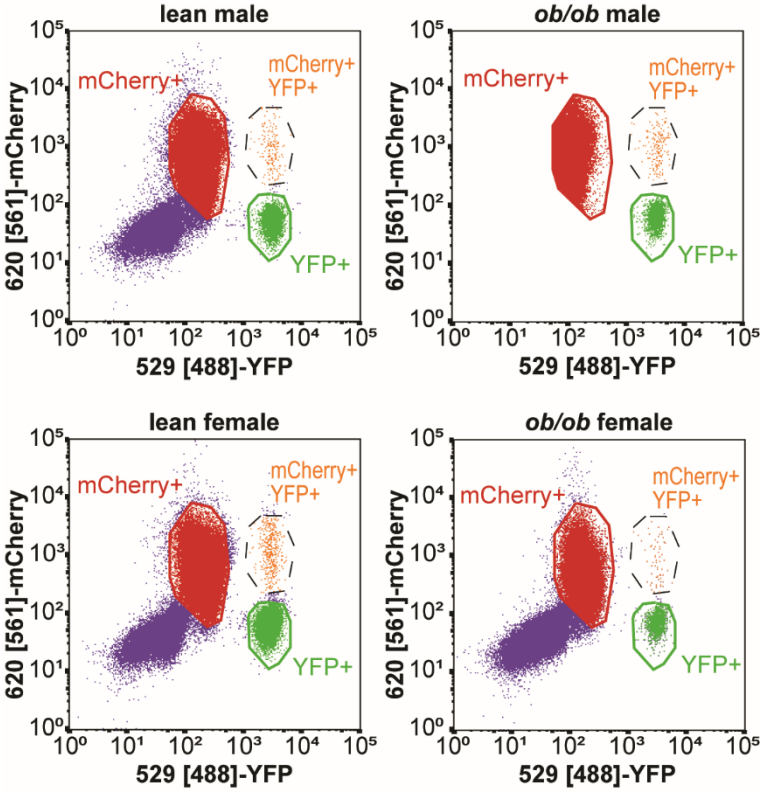

Figure 6.4: S1, related to Figure 6.1. Representative FACS plots from male and female lean and *ob/ob* mice. The mCherry+ population is colored in red, the YFP+ population is colored in green, the mCherry+YFP+ population is colored in orange, and the mCherry-YFP- population are in purple. We focus on the mCherry+ and YFP+ samples from each mouse only.

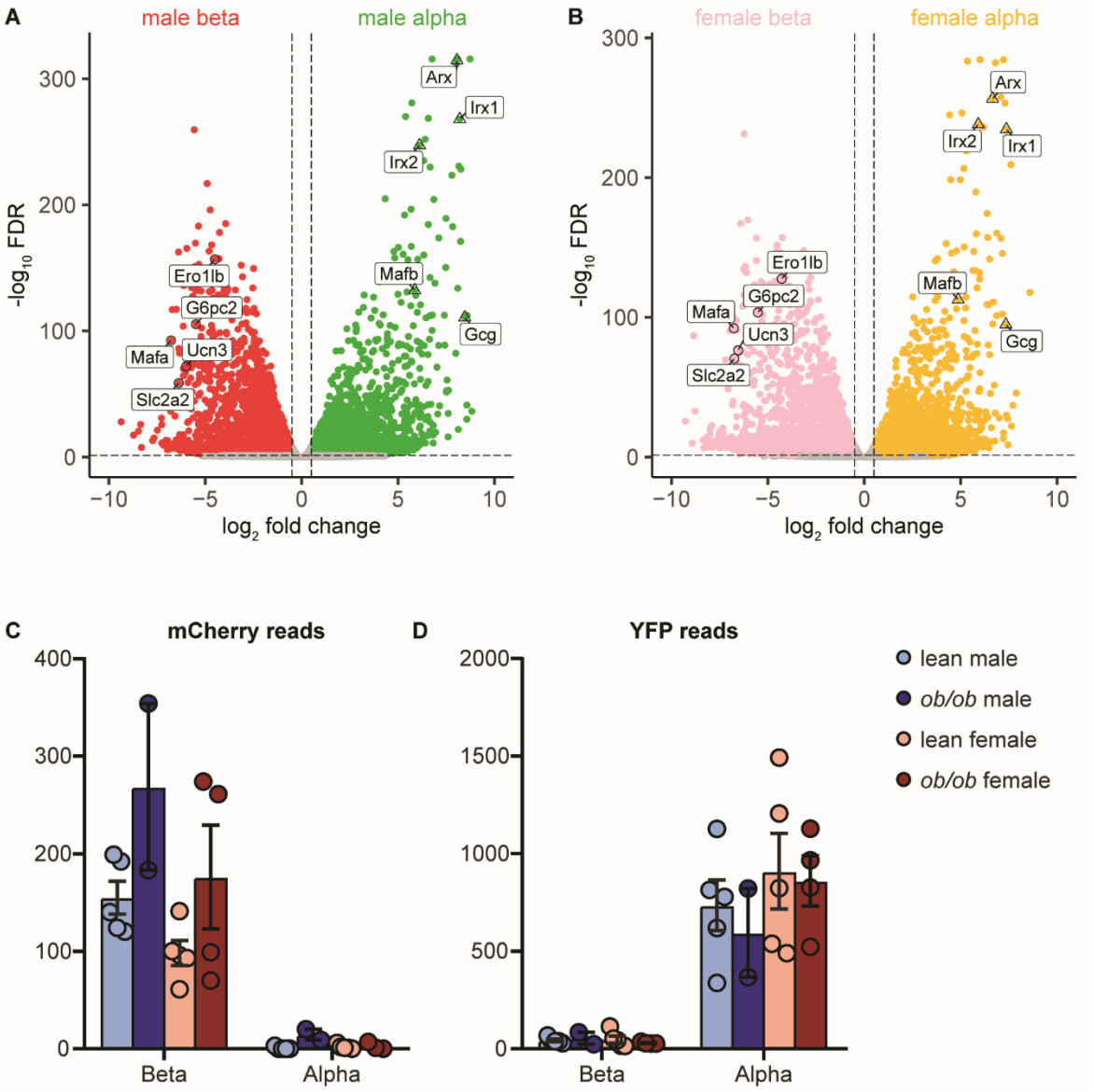

Figure 6.5: S2, related to Figure 6.2. A and B) Volcano plots comparing beta and alpha cells from A) male and B) female lean mice. Beta cell markers are enriched in the beta cell population and alpha cell markers are enriched in the alpha cell population. C) Number of mCherry+ reads in each population. There are little to no mCherry+ reads in alpha cells as expected, except for a small increase in reads in the male *ob/ob* samples. D) Number of YFP+ reads in each population. There are some YFP reads in the beta cells, but the amount in each sample is comparable and much less than the amount seen in alpha cells.

6.9 References

Artner I, Hang Y, Mazur M, Yamamoto T, Guo M, Lindner J, Magnuson MA & Stein R 2010 MafA and MafB regulate genes critical to β-cells in a unique temporal manner. *Diabetes* **59** 2530–2539. (doi:10.2337/db10-0190)

Beamish CA, Strutt BJ, Arany EJ & Hill DJ 2016 Insulin-positive, Glut2-low cells present within mouse pancreas exhibit lineage plasticity and are enriched within extra-islet endocrine cell clusters. *Islets* **8** 65–82. (doi:10.1080/19382014.2016.1162367)

Benner C, van der Meulen T, Cacéres E, Tigyi K, Donaldson CJ & Huising MO 2014 The transcriptional landscape of mouse beta cells compared to human beta cells reveals notable species differences in long non-coding RNA and protein-coding gene expression. *BMC Genomics* **15** 620. (doi:10.1186/1471-2164-15-620)

Blum B, Hrvatin S, Schuetz C, Bonal C, Rezania A & Melton DA 2012 Functional beta-cell maturation is marked by an increased glucose threshold and by expression of urocortin 3. *Nature Biotechnology* **30** 261–264. (doi:10.1038/nbt.2141)

Butler AE, Janson J, Bonner-Weir S, Ritzel R, Rizza RA & Butler PC 2003 Beta-cell deficit and increased beta-Cell apoptosis in humans with type 2 diabetes. *Diabetes* **52** 102–110. (doi:10.2337/diabetes.52.9.2304)

Cerf ME 2013 Beta cell dysfunction and insulin resistance. *Frontiers in Endocrinology* **4** 1–12. (doi:10.3389/fendo.2013.00037)

Cinti F, Bouchi R, Kim-Muller JY, Ohmura Y, Sandoval PR, Masini M, Marselli L, Suleiman M, Ratner LE, Marchetti P *et al.* 2016 Evidence of β-cell dedifferentiation in human type 2 diabetes. *Journal of Clinical Endocrinology and Metabolism* **101** 1044–1054. (doi:10.1210/jc.2015-2860)

Coleman DL 1978 Obese and diabetes: Two mutant genes causing diabetes-obesity syndromes in

mice. *Diabetologia* **14** 141–148. (doi:10.1007/BF00429772)

Dahan T, Ziv O, Horwitz E, Zemmour H, Lavi J, Swisa A, Leibowitz G, Ashcroft FM, Veld PI t., Glaser B *et al.* 2017 Pancreatic β-Cells express the fetal islet hormone gastrin in rodent and human diabetes. *Diabetes* **66** 426–436. (doi:10.2337/db16-0641)

Diedisheim M, Oshima M, Albagli O, Huldt CW, Ahlstedt I, Clausen M, Menon S, Aivazidis A, Andreasson AC, Haynes WG *et al.* 2018 Modeling human pancreatic beta cell dedifferentiation. *Molecular Metabolism* **10** 74–86. (doi:10.1016/j.molmet.2018.02.002)

DiGruccio MR, Mawla AM, Donaldson CJ, Noguchi GM, Vaughan J, Cowing-Zitron C, van der Meulen T & Huising MO 2016 Comprehensive alpha, beta and delta cell transcriptomes reveal that ghrelin selectively activates delta cells and promotes somatostatin release from pancreatic islets. *Molecular Metabolism* **5** 449–458. (doi:10.1016/j.molmet.2016.04.007)

Dobin A, Davis CA, Schlesinger F, Drenkow J, Zaleski C, Jha S, Batut P, Chaisson M & Gingeras TR 2013 STAR: Ultrafast universal RNA-seq aligner. *Bioinformatics* **29** 15–21. (doi:10.1093/bioinformatics/bts635)

Dorrell C, Schug J, Lin CF, Canaday PS, Fox AJ, Smirnova O, Bonnah R, Streeter PR, Stoeckert CJ, Kaestner KH *et al.* 2011 Transcriptomes of the major human pancreatic cell types. *Diabetologia* **54** 2832–2844. (doi:10.1007/s00125-011-2283-5)

Dusaulcy R, Handgraaf S, Visentin F, Howald C, Dermitzakis ET, Philippe J & Gosmain Y 2019 High-fat diet impacts more changes in betacell compared to alpha-cell transcriptome. *PLoS ONE* **14**. (doi:10.1371/journal.pone.0213299)

Herrera PL 2000 Adult insulin- and glucagon-producing cells differentiate from two independent cell lineages. *Development* **127** 2317–2322. (doi:10.1242/dev.127.11.2317)

Kahn SE, Hull RL & Utzschneider KM 2006 Mechanisms linking obesity to insulin resistance and type 2 diabetes. *Nature* **444** 840–846. (doi:10.1038/nature05482)

Kim-Muller JY, Fan J, Kim YJR, Lee SA, Ishida E, Blaner WS & Accili D 2016 Aldehyde dehydrogenase 1a3 defines a subset of failing pancreatic β cells in diabetic mice. *Nature Communications* **7** 1–11. (doi:10.1038/ncomms12631)

Kuo T, Damle M, González BJ, Egli D, Lazar MA & Accili D 2019 Induction of α cell–restricted Gc in dedifferentiating β cells contributes to stress-induced β cell dysfunction. *JCI Insight* **4**. (doi:10.1172/jci.insight.128351)

Lacy PE 1961 Electron microscopy of the beta cell of the pancreas. *The American Journal of Medicine* **31** 851–859. (doi:10.1016/0002-9343(61)90024-9)

Lavine JA, Raess PW, Stapleton DS, Rabaglia ME, Suhonen JI, Schueler KL, Koltes JE, Dawson JA, Yandell BS, Samuelson LC *et al.* 2010 Cholecystokinin is up-regulated in obese mouse islets and expands β-cell mass by increasing β-cell survival. *Endocrinology* **151** 3577–3588. (doi:10.1210/en.2010-0233)

Liao Y, Smyth GK & Shi W 2014 FeatureCounts: An efficient general purpose program for assigning sequence reads to genomic features. *Bioinformatics* **30** 923–930. (doi:10.1093/bioinformatics/btt656)

Liu L, Dattaroy D, Simpson KF, Barella LF, Cui Y, Xiong Y, Jin J, König GM, Kostenis E, Roman JC *et al.* 2021 Gq signaling in α cells is critical for maintaining euglycemia. *JCI Insight* **6** 1–17. (doi:10.1172/jci.insight.152852)

Louet JF, LeMay C & Mauvais-Jarvis F 2004 Antidiabetic actions of estrogen: Insight from human and genetic mouse models. *Current Atherosclerosis Reports* **6** 180–185. (doi:10.1007/s11883-004-0030-9)

van der Meulen T, Xie R, Kelly OG, Vale WW, Sander M & Huising MO 2012 Urocortin 3 Marks Mature Human Primary and Embryonic Stem Cell-Derived Pancreatic Alpha and Beta Cells. *PLoS ONE* **7** 1–12. (doi:10.1371/journal.pone.0052181)

van der Meulen T, Donaldson CJ, Cáceres E, Hunter AE, Cowing-Zitron C, Pound LD, Adams MW, Zembrzycki A, Grove KL & Huising MO 2015 Urocortin3 mediates somatostatin-dependent negative feedback control of insulin secretion. *Nature Medicine* **21** 769–776. (doi:10.1038/nm.3872)

van der Meulen T, Mawla AM, DiGruccio MR, Adams MW, Nies V, Dolleman S, Liu S, Ackermann AM, C??ceres E, Hunter AE *et al.* 2017 Virgin Beta Cells Persist throughout Life at a Neogenic Niche within Pancreatic Islets. *Cell Metabolism* **25** 911-926.e6. (doi:10.1016/j.cmet.2017.03.017)

Pfeifer CR, Shomorony A, Aronova MA, Zhang G, Cai T, Xu H, Notkins AL & Leapman RD 2015 Quantitative analysis of mouse pancreatic islet architecture by serial block-face SEM. *Journal of Structural Biology* **189** 44–52. (doi:10.1016/j.jsb.2014.10.013)

Robinson MD, Mccarthy DJ & Smyth GK 2009 edgeR : a Bioconductor package for differential expression analysis of digital gene expression data. *Bioinformatics* **26** 139–140. (doi:10.1093/bioinformatics/btp616)

Salvi R & Abderrahmani A 2014 Decompensation of beta-cells in diabetes: when pancreatic beta-cells are on ICE(R). *J Diabetes Res* **2014** 768024. (doi:10.1155/2014/768024)

Shah P, Vella A, Basu A, Basu R, Schwenk WF & Rizza RA 2000 Lack of suppression of glucagon contributes to postprandial hyperglycemia in subjects with type 2 diabetees mellitus. *Journal of Clinical Endocrinology and Metabolism* **85** 4053–4059. (doi:10.1210/jc.85.11.4053)

Srinivas S, Watanabe T, Lin CS, William CM, Tanabe Y, Jessell TM & Costantini F 2001 Cre reporter strains produced by targeted insertion of EYFP and ECFP into the ROSA26 locus. *BMC Developmental Biology* **1** 1–8. (doi:10.1186/1471-213X-1-4)

Svendsen B, Larsen O, Gabe MBN, Christiansen CB, Rosenkilde MM, Drucker DJ & Holst JJ 2018 Insulin Secretion Depends on Intra-islet Glucagon Signaling. *Cell Reports* **25** 1127-1134.e2. (doi:10.1016/j.celrep.2018.10.018)

Talchai C, Xuan S, Lin H V., Sussel L & Accili D 2012 Pancreatic β cell dedifferentiation as a mechanism of diabetic β cell failure. *Cell* **150** 1223–1234. (doi:10.1016/j.cell.2012.07.029)

Weir GC & Bonner-Weir S 2004 Five stages of evolving beta-cell dysfunction during progression to diabetes. *Diabetes* **53**. (doi:10.2337/diabetes.53.suppl_3.S16)

Weir GC, Laybutt DR, Kaneto H, Bonner-weir S & Sharma A 2001 Beta Cell Adaptation and Decompensation During the Progression of Diabetes. **50**. (doi:10.2337/diabetes.50.2007.S154)

Yu G, Wang LG, Han Y & He QY 2012 ClusterProfiler: An R package for comparing biological themes among gene clusters. *OMICS A Journal of Integrative Biology* **16** 284–287. (doi:10.1089/omi.2011.0118)

Zhu L, Dattaroy D, Pham J, Wang L, Barella LF, Cui Y, Wilkins KJ, Roth BL, Hochgeschwender U, Matschinsky FM *et al.* 2019 Intraislet glucagon signaling is critical for maintaining glucose homeostasis. *JCI Insight* **4**. (doi:10.1172/jci.insight.127994)

Chapter 7

Conclusions and Future Work

7.1 Abstract

In this dissertation, I address the contribution of delta cells to the regulation of both beta and alpha cells, with a focus on delta and beta cell interaction to determine the glycemic set point. I also investigate changes in beta cell maturity and alpha cell function. The work performed for this dissertation includes bulk RNA-seq analysis, immunofluorescence, hormone secretion assays, and live cell imaging of intact islets over time. Together with *in vivo* mouse experiments, these provide a picture that tie together cellular mechanisms with physiology. This chapter will summarize the key findings of the previous chapters and then discuss potential future directions.

7.2 Summary of Work

Chapter 1 is an introduction to the pancreatic islet and the roles of the insulin-producing beta cells, glucagon-producing alpha cells, and somatostatin (SST)-producing delta cells. We focus primarily on the delta cells, which act as a central regulator in the islet by taking in different inputs and secreting SST to modulate beta and alpha cell activity. Towards the end, we also draw comparisons between delta cells and other SST-expressing cells in the body, focusing on the D cells in the gastrointestinal system and SST+ neurons in the hypothalamus.

Chapter 2 establishes the contribution of Urocortin 3 (UCN3) to beta cell maturation. UCN3 has previously been demonstrated to be expressed in all mature beta cells, and the onset of its expression coincides with the point at which beta cells achieve functional maturity (Blum *et al.* 2012; van der Meulen *et al.* 2012, 2015). While this establishes UCN3 as a marker of beta cell maturity, it brings up the question of whether UCN3 expression is required for beta cells to achieve maturity.

We demonstrate here that UCN3 is not essential for beta cell maturation. Using *Ucn3*-null mice, we find that there are no differences in gene expression in other markers of beta cell maturity and validate that these markers remain intact by immunofluorescent staining. Furthermore, we observe no increases in the expression of beta cell dedifferentiation markers, establishing that UCN3 expression is also not required for beta cells to retain functional maturity. We then investigated whether virgin beta cells remain in the absence of UCN3. Virgin beta cells resemble immature beta cells found during development, but are present in adults. Our lab has previously identified them based on the absence of UCN3 expression and furthermore observed that they are localized to the periphery of the islet (van der Meulen *et al.* 2017). Since virgin beta cells also lack other markers of beta cell maturity, we used these other markers to demonstrate that virgin beta cells remain in the absence of UCN3 and continue to localize to the periphery. We then go on to demonstrate that beta cells have a normal calcium response to glucose in the absence of UCN3, demonstrating that UCN3 expression is not required for beta cells to display their characteristic pulsatile and synchronous response to glucose. Together, these data establish that UCN3 expression is not required for beta cells to achieve functional maturity.

Chapter 3 characterizes the transcriptomic changes in beta and alpha cells after exposure to exogenous SST and blocking SST signaling using antagonists for the SST receptors found on alpha and beta cells, SSTR2 (alpha) and SSTR3 (beta and alpha). Although SST inhibition of beta and alpha

cells through $G_{\alpha i}$-mediated inhibition of cAMP production is well-known, there have been no studies investigating the effects of SST on gene expression.

To this end, we incubated intact isolated islets with SST, SSTR2 and SSTR3 antagonists, or SST and the SSTR2 and SSTR3 antagonists combined, then sorted beta and alpha cells from each group by FACS. Upon analyzing transcriptomic data from beta cells, we discovered several genes involves in actin regulation were upregulated in the presence of exogenous SST, while these same genes were downregulated when endogenous SST signaling was blocked using the SSTR antagonists. We found similar changes in the alpha cells. Since remodeling of the actin cytoskeleton is an important component of exocytosis and has been demonstrated to be necessary for insulin secretion (Kalwat & Thurmond 2013; Arous & Halban 2015; Naumann *et al.* 2018), this suggests a novel mechanism of SST inhibiting both beta and alpha cell secretion through regulation of actin dynamics.

Chapter 4 investigates the contribution of delta cells to establishing the glycemic set point, which has not previously been studied. Previous experiments have demonstrated that grafting islets from donor species into mice changes the set point in mice to match that of the donor species (Carroll *et al.* 1992; Rodriguez-Diaz *et al.* 2018). Thus, islets are sufficient for determining the glycemic set point. It has been proposed that the glycemic set point is established by the crossover point between beta and alpha cell response (Pagliara *et al.* 1974). Furthermore, experiments blocking glucagon signaling within human islets transplanted into mice have suggested that the paracrine contributions of alpha to beta cells plays an important role in establishing the glycemic set point. However, given the established paracrine role of delta cells, it is likely that they contribute to the determination of the glycemic set point as well. Furthermore, our lab has demonstrated that the onset of UCN3 and subsequent SST signaling leads directly to an increase in the glucose set point in mice.

We began with studying *Sst*-Cre homozygous mice, which are effectively *Sst*-null mice, and observe that these mice exhibit lower glucose levels relative to *Sst*-Cre heterozygous mice. Since these mice are born without SST expression, we next turned to the *Sst*-Cre x lsl-DTR model, which allowed us to completely ablate delta cells at a time of our choosing. We observed that delta cell ablation led to a sustained decrease in the glycemic set point as well as an increase in glucose tolerance. Measuring plasma insulin *in vivo* as well as secreted insulin from islets *in vitro* demonstrated that in the absence of delta cells, there is an increase in glucose-stimulated insulin secretion. Using live cell calcium imaging of intact islets, we demonstrated that in the absence of delta cells, there is a decrease in the glucose threshold that is necessary for insulin secretion that matches the decrease in glucose levels observed in delta cell-ablated mice. Altogether, these data suggest that delta cells and SST contribute to the glycemic set point through their interaction with the neighboring beta cells.

Chapter 5 provides a review on the importance of delta cells to glucose control. We first briefly review the history of delta cells, then discuss the different paracrine interactions between the islet and how the delta cells contribute. In particular, we focus on the communication between beta and delta cells, in which beta cells secrete UCN3 under high glucose to stimulate SST, leaading to negative feedback inhibition of beta cells. We then draw comparisons between the beta and delta cell, as they are close in lineage and have similar machinery. Finally, we discuss how the feedback inhibition provided to the islet by delta cell-derived SST allows for better glucose control, and how this control is lost in diabetes due to the loss of UCN3.

Chapter 6 investigates changes in beta and alpha cell transcriptomes during obesity. In particular, we observe that male *ob/ob* mice may more readily undergo beta cell compensation compared to female mice, leading to development of hyperglycemic later on in life. We demonstrate that beta cells from

male *ob/ob* mice have decreased granularity, decreased expression of beta cell markers, and increased expression of beta cell dedifferentiation markers, while beta cells from female mice exhibit hypertrophy and do not exhibit loss of beta cell markers, but do have increased expression of a subset of beta cell dedifferentiation markers. These data suggest that some dedifferentiation markers may appear prior to the loss of beta cell markers, while others appear around the same time or after loss of maturity. We further observe that alpha cells in *ob/ob* mice of both sex display increased granularity and increased expression of beta cell genes, suggesting that some alpha cells may become more beta cell-like. While these data will need to be validated, we have unpublished observations that a subset of alpha cells are inhibited by epinephrine like beta cells are, instead of stimulated as is usually the case.

7.3 Future Directions

7.3.1 Regulation of actin dynamics in beta and alpha cells by SST

Our transcriptomic data on beta and alpha cells in the presence of SST or SSTR antagonists demonstrate differential expression of genes involved in actin regulation. This brings up the exciting possibility that in addition to the known mechanisms of decreasing cAMP production and decreasing cell excitation through G-coupled inwardly-rectifying potassium channels (Kailey *et al.* 2012), SST may also inhibit exocytosis in both beta and alpha cells through regulation of actin cytoskeleton remodeling. The effect of SST on actin cytoskeleton remodeling can potentially be visualized using the LifeAct mouse line, in which F-actin is labeled by GFP (Riedl *et al.* 2010). SSTR-specific agonists can also be applied to investigate the differential response of beta and alpha cells.

7.3.2 Alpha cell contribution to beta cell activity in the absence of delta cells

In Chapter 4, we demonstrate that the glycemic set point in mice decreases in the absence of SST and delta cells. Furthermore, beta cells respond at a lower glucose threshold in the absence of delta cells, suggesting that the glycemic set point is primarily established by the glucose threshold of beta cells, which can be modulated by paracrine SST signaling from delta cells. On the other hand, alpha cell ablation does not have an effect on basal glycemia. While alpha cells have important systemic and paracrine contributions to glucose homeostasis, this suggests that alpha cells do not contribute to the glucose threshold in beta cells. It is possible that the paracrine contribution of alpha cells is more important above the beta cell glucose threshold. Indeed, the GCGR as well as GLP1R are both $G_{\alpha s}$-coupled receptors that act to amplify insulin secretion through increasing cAMP production. Therefore, more experiments will have to be conducted to examine the contribution of alpha cells to the enhancement of insulin secretion in the absence of delta cells. For example, antagonists against GCGR and GLP1R can be applied individually or in combination. If glucagon from alpha cells contributes to the increase in insulin secretion in the absence of delta cells, this would be expected to at least partially prevent the increase in insulin secretion. On the other hand, the glucose threshold for response would be expected to remain lower in the absence of delta cells regardless of paracrine glucagon signaling. This data can potentially also be used to create more accurate models of paracrine interactions within the islet.

7.3.3 Effect of delta cell ablation during diabetes

While delta cell ablation decreases the glycemic set point in non-diabetic mice, it remains unknown how the absence of delta cells would affect the development of diabetes. In Type 1 Diabetes, beta cells are absent due to autoimmune attack. The absence of beta cells would presumably lead to decreased delta cell activity under high glucose. Thus, removal of delta cells in a Type 1 Diabetes

model would likely not lead to a decrease in glucose levels as there would be little to no beta cells left to secrete more insulin. It is possible that there may be a brief decrease if delta cells are ablated at a point when some beta cells remain. However, what is more likely is that removal of delta cells would lead to increased alpha cell activity, exacerbating hyperglycemia. This possibility may be investigated using the non-obese diabetic (NOD) mouse model, in which immune infiltration of pancreatic islets leads to reduced insulin content, or through streptozotocin-mediated destruction of beta cells.

On the other hand, in Type 2 Diabetes beta cells remain intact but are unable to secrete sufficient insulin to keep up with insulin demand. Beta cells attempt to compensate this through mechanisms such as downregulation of UCN3, which would reduce SST feedback and allow for increased insulin secretion. It is possible that ablation of delta cells and complete removal of local SST signaling would allow for even more insulin secretion to help restore normoglycemia. However, there is evidence that beta cells undergo exhaustion while trying to keep up with the increased insulin demand in Type 2 Diabetes (Salvi & Abderrahmani 2014), and removal of inhibition by delta cells may instead exacerbate the progression of Type 2 Diabetes. This can be investigated by ablating delta cells in *ob/ob* mice or mice on a high fat diet. Investigating the effects of removing delta cells in models of diabetes will establish their contribution to the development of diabetes and inform on potential treatments targeting delta cells to modulate islet activity.

7.3.4 Contribution of delta cells to the glycemic set point in humans

The glycemic set point in humans is around 90 mg/dL (Gerich 1993), which is lower than 120-140 mg/dL set point generally observed in mice (Ewing & Tauber 1964; Blum *et al.* 2012; Rodriguez-Diaz *et al.* 2018). The set point is driven by the islet, as demonstrated by studies in which islets from different donor species were grafted into mice, leading to establishment of a glycemic set point that matches the set point observed in the donor species (Carroll *et al.* 1992; Rodriguez-Diaz *et al.* 2018). It has been

suggested that the glycemic set point established by human islets is determined by paracrine interactions between the beta and the alpha cell (Rodriguez-Diaz *et al.* 2018). However, multiple alpha cell ablation experiments have demonstrated that in mice, the alpha cells do not contribute to the glycemic set point (Thorel *et al.* 2011; Pedersen *et al.* 2013). On the other hand, we have demonstrated that delta cell ablation in mice leads to a decrease in the glycemic set point. It is therefore likely that there is a paracrine contribution of delta cells to the establishment of the glycemic set point in humans as well.

While ablating delta cells in human islets is more difficult, there are a few potential ways to investigate the contribution of human delta cells to the glycemic set point. There are currently no known specific markers for human delta cells, but our lab has previously successfully purified human beta and alpha cells for transcriptomic analysis using the cell surface markers HPi2 and HPα1 (Benner *et al.* 2014). Thus, it may be possible to sort out human beta and alpha cells, reaggregate them, then transplant them into mice and observe whether the re-established glycemic set point differs from the set point that is established by transplanting intact human islets. The caveat is that this would also remove the rarer cell types found in the islet. Another possibility is to transplant the islets and block SST signaling from human islets using antagonists specific to the SSTRs expressed in the human islet. The contribution of human delta cells to the glucose threshold for response in human beta cells can also be studied by transducing the islets with GCaMP6, with delta cells removed or SST signaling blocked by antagonists.

7.4. Conclusions

Taken together, the findings in this dissertation highlight the importance of paracrine interactions within the pancreatic islet. While beta cells are critical for the secretion of insulin to lower glycemia, the contributions of the other cells cannot be discounted. There is increasing appreciation for alpha

cells and their paracrine contributions to the potentiation of insulin secretion. However, the delta cells remain understudied. The secretion of SST from delta cells is an important paracrine regulator within the islet, and how it is capable of differentially regulating beta and alpha cells remains to be seen. Furthermore, there remain gaps in our understanding of how SST can potentially inhibit exocytosis through mechanisms in addition to decreased cAMP production. While this dissertation demonstrates the contribution of delta cells to the glycemic set point, it also remains to be seen how this effect may change under diseased states, or how it may be different in humans. Overall, greater understanding of the interactions between the cells of the islet and appreciation of their contributions can lead to the development of better treatments for diabetes, in which more than simply the beta cell is affected.

7.5 References

Arous C & Halban PA 2015 The skeleton in the closet: actin cytoskeletal remodeling in β-cell function. *American Journal of Physiology - Endocrinology And Metabolism* **309** E611–E620. (doi:10.1152/ajpendo.00268.2015)

Benner C, van der Meulen T, Cacéres E, Tigyi K, Donaldson CJ & Huising MO 2014 The transcriptional landscape of mouse beta cells compared to human beta cells reveals notable species differences in long non-coding RNA and protein-coding gene expression. *BMC Genomics* **15** 620. (doi:10.1186/1471-2164-15-620)

Blum B, Hrvatin S, Schuetz C, Bonal C, Rezania A & Melton DA 2012 Functional beta-cell maturation is marked by an increased glucose threshold and by expression of urocortin 3. *Nature Biotechnology* **30** 261–264. (doi:10.1038/nbt.2141)

Carroll PB, Zeng Y, Alejandro R, Starzl TE & Ricordi C 1992 Glucose homeostasis is regulated by donor islets in xenografts. *Transplantation Proceedings* **24** 2980–2981.

Ewing KL & Tauber OE 1964 Blood chemistry changes in mice fed high levels of polyoxyethylene

sorbitan derivatives. *Toxicology and Applied Pharmacology* **6** 442–446. (doi:10.1016/S0041-008X(64)80010-7)

Gerich JE 1993 *Control of Glycaemia*. (doi:10.1016/S0950-351X(05)80207-1)

Kailey B, van de Bunt M, Cheley S, Johnson PR, MacDonald PE, Gloyn AL, Rorsman P & Braun M 2012 SSTR2 is the functionally dominant somatostatin receptor in human pancreatic β- and α-cells. *AJP: Endocrinology and Metabolism* **303** E1107–E1116. (doi:10.1152/ajpendo.00207.2012)

Kalwat MA & Thurmond DC 2013 Signaling mechanisms of glucose-induced F-actin remodeling in pancreatic islet β cells. *Experimental and Molecular Medicine* **45** e37-12. (doi:10.1038/emm.2013.73)

van der Meulen T, Xie R, Kelly OG, Vale WW, Sander M & Huising MO 2012 Urocortin 3 Marks Mature Human Primary and Embryonic Stem Cell-Derived Pancreatic Alpha and Beta Cells. *PLoS ONE* **7** 1–12. (doi:10.1371/journal.pone.0052181)

van der Meulen T, Donaldson CJ, Cáceres E, Hunter AE, Cowing-Zitron C, Pound LD, Adams MW, Zembrzycki A, Grove KL & Huising MO 2015 Urocortin3 mediates somatostatin-dependent negative feedback control of insulin secretion. *Nature Medicine* **21** 769–776. (doi:10.1038/nm.3872)

van der Meulen T, Mawla AM, DiGruccio MR, Adams MW, Nies V, Dolleman S, Liu S, Ackermann AM, C??ceres E, Hunter AE *et al.* 2017 Virgin Beta Cells Persist throughout Life at a Neogenic Niche within Pancreatic Islets. *Cell Metabolism* **25** 911-926.e6. (doi:10.1016/j.cmet.2017.03.017)

Naumann H, Rathjen T, Poy MN & Spagnoli FM 2018 The RhoGAP Stard13 controls insulin secretion through F-actin remodeling. *Molecular Metabolism* **8** 96–105. (doi:10.1016/j.molmet.2017.12.013)

Pagliara AS, Stillings SN, Hover B, Martin DM & Matschinsky FM 1974 Glucose modulation of amino acid induced glucagon and insulin release in the isolated perfused rat pancreas. *Journal of*

Clinical Investigation **54** 819–832. (doi:10.1172/JCI107822)

Pedersen J, Ugleholdt RK, Jørgensen SM, Windeløv JA, Grunddal K V, Schwartz TW, Füchtbauer EM, Poulsen SS, Holst PJ & Holst JJ 2013 Glucose metabolism is altered after loss of L cells and α-cells but not influenced by loss of K cells. *American Journal of Physiology - Endocrinology and Metabolism* **304** 60–73. (doi:10.1152/ajpendo.00547.2011)

Riedl J, Flynn KC, Raducanu A, Gärtner F, Beck G, Bösl M, Bradke F, Massberg S, Aszodi A, Sixt M *et al.* 2010 Lifeact mice for studying F-actin dynamics. *Nature Methods* **7** 168–169. (doi:10.1038/nmeth0310-168)

Rodriguez-Diaz R, Molano RD, Weitz JR, Abdulreda MH, Berman DM, Leibiger B, Leibiger IB, Kenyon NS, Ricordi C, Pileggi A *et al.* 2018 Paracrine Interactions within the Pancreatic Islet Determine the Glycemic Set Point. *Cell Metabolism* **27** 549-558.e4. (doi:10.1016/j.cmet.2018.01.015)

Salvi R & Abderrahmani A 2014 Decompensation of beta-cells in diabetes: when pancreatic beta-cells are on ICE(R). *J Diabetes Res* **2014** 768024. (doi:10.1155/2014/768024)

Thorel F, Damond N, Chera S, Wiederkehr A, Thorens B, Meda P, Wollheim CB & Herrera PL 2011 Normal glucagon signaling and β-cell function after near-total α-cell ablation in adult mice. *Diabetes* **60** 2872–2882. (doi:10.2337/db11-0876)